The Roles of Heat Shock Factor during Diapause and Stress Tolerance in the Crustacean *Artemia franciscana*

By

Jiabo Tan

Submitted in partial fulfillment of the requirements

for the degree of Doctor of Philosophy

at

Dalhousie University

Halifax, Nova Scotia

August 2018

Dedicated to my parents Tan Qigui and Sui Wenwen: Their supports are the most important power for me

Table of Contents

List of Tables

List of Figures

Abstract

Encysted embryos of the crustacean *Artemia franciscana* enter diapause, a developmental state of greatly reduced metabolic activity and enhanced stress tolerance that allows survival under adverse environmental conditions. Diapausing *A. franciscana* are characterized by the synthesis of molecular chaperones such as the small heat shock proteins (sHSPs), p26, ArHsp21 and ArHsp22, and the ferritin homologue, artemin. A full-length cDNA encoding the *A. franciscana* transcription factor, heat shock factor 1 (Hsf1), was cloned and sequenced, revealing a deduced protein of 65.3 kDa which contained a conserved DNA binding domain. *Hsf1* cDNA was employed as template to make double stranded RNA (dsRNA) used for RNA interference (RNAi) and thus to determine the role of Hsf1 in the regulation of gene expression during diapause. qRT-PCR and immunoprobing of western blots with an antibody raised to Hsf1 from *A. franciscana* respectively demonstrated the knockdown of *hsf1* mRNA and Hsf1 in nauplii and cysts released from females receiving dsRNA. Nauplii lacking Hsf1 appeared normal but they died prematurely upon culturing. Hsf1 knockdown cysts were less stress resistant than cysts containing Hsf1, demonstrating a role for this transcription factor in the stress tolerance of diapausing *A. franciscana*. Immunoprobing of western blots showed that cysts released from females receiving *hsf1* dsRNA lacked p26, an important diapause-specific sHsp in *A. franciscana* cysts. The knockdown of other sHsps and artemin, which have less influence on the stress tolerance of diapause cysts, also occurred but was more variable in extent. qRT-PCR and immunoprobing of western blots with an antibody raised to Hsf1 from *A. franciscana* demonstrates *hsf1* mRNA and Hsf1 appeared earlier and was more abundant in oviparous versus ovoviviparous embryos. Examination of immunofluoresencently stained samples demonstrates Hsf1 localized earlier to nuclei from oviparous embryos. The results support the conclusion that Hsf1, perhaps in concert with other transcription factors, regulates expression of diapause-specific genes required for stress resistance and diapause in *A. franciscana* and that Hsf1 is important during *A. franciscana* development especially for the oviparous embryos.

LIST OF ABBREVIATIONS AND SYMBOLS USED

Ago	argonaute
ATP	adenosine 5’-triphosphate
AU	arbitrary units
BSA	bovine serum albumin
bp	base pairs
Ct	cycle threshold
DAPI	4',6-diamidino-2-phenylindole
DBD	DNA binding domain
dsRNA	double-stranded RNA
ECL	enhanced chemiluminescence
EDTA	ethylenediaminetetraacetic acid
EGTA	ethylene glycol-bis (β-aminoethyl ether)-N, N, N', N'-tetraacetic acid
FITC	fluorescein isothiocyanate
GFP	green fluorescent protein
HSE	heat shock element
HSF	heat shock factor
HR	heptad repeats
HRP	horse radish peroxidase
HST	high salt/Tween
IgG	immunoglobulin G

IPTG	isopropyl β-D-1-thiogalactopyranoside
kDa	kiloDaltons
mRNA	messenger RNA
ORF	open reading frame
PBS	Phosphate-buffered saline
PBSAT	BSA in PBS with Triton-X 100
PCR	polymerase chain reaction
qRT-PCR	quantitative reverse transcription PCR
RD	Regulatory domain
RISC	RNA-induced silencing complex
RNA	ribonucleic acid
RNAi	RNA interference
SDS	sodium dodecylsulfate
TAD	trans-activation domain
TBE	Tris, boric acid, EDTA
TBS	Tris-buffered saline
TBS-T	Tris-buffered saline Tween
TE	Tris, EDTA
Tris	tris-(hydroxymethyl)amino methane
Tween	polyoxyethylenesorbitan monolaurate
UV	ultraviolet
X-gal	5-bromo-4-chloro-3-indolyl-β-D-galactopyranosid

Acknowledgements

I express my sincere gratitude to my supervisor, Dr. Thomas H. MacRae for his guidance on the way of research, his support and encouragement during the hard times and his wisdom on both life and science. With great patience, he helped me a lot on scientific English writing and communication. Without his help, my pursuit of a Ph. D at Dalhousie would not have been possible. His rigorous attitude on science and optimistic attitude on life will always benefit my future life and career.

Secondly, I thank my committee members for their invaluable supports, Dr. Sophia Stone for her support of my research and life in the department, Dr. John Wright for his insightful questions, Dr. Neil Ross for his endless trouble shooting with patience and Dr. Patrice Côté for his guidance and feedback on my research. I also thank Dr. Bill Pohajdak for his advice and help of my research.

Additionally, I thank all my great lab mates. Guojian Jiang helped me settle down in Canada and introduced me to the lab. Jantina Toxopeus taught me the necessary lab protocols. Nathan Rowarth offered help throughout my research and gave me knowledge on local culture. Hajer Malitan, Louise Tunnah, Afnan Fatani, Sheethal Panchakshari, Azzah Alotaibi and Dung Nguyen cooperated on lab work and showed me the charm of various cultures. Allison King and Heather Robbins offered a lot of help. I could not have finished my work without them. I can't forget to thank Charlotte Ryder-Burbidge, Alicia Roy and Yayra Gbotsyo for their assistance, friendship and the joys we had together.

Dr. Ping Li helped with picture processing. Ms. Laura Tatar helped with cell culture and immunofluoresence. Dr. Stephen Whitefield taught me how to use confocal microscope. I express my thanks to them for their kind support.

To my roommates and friends Xu Zhiqiang, Lian Delin and Lu Longfei, I thank them for the good times we had together and for their company through my down points. My parents are always supportive of my decisions and I thank them for their understanding.

I express my thanks to the Chinese Scholarship Council and the Chinese Embassy in Canada. I can't be here without their help. I thank Nova Scotia graduate student funding and Dr. Patrick Lett for financial assistance.

Chapter 1 introduction

1.1 The extremophile crustacean, *Artemia franciscana*

Artemia is a crustacean commonly known as the brine shrimp. The adults are usually about 1 cm long with females longer than males. It takes about 3 weeks for swimming nauplii to develop into sexually mature adults and 5 days for fertilized females to release cysts or swimming nauplii (King and MacRae, 2012). Mature females are a darker color than males and possess a pair of egg sacs on the lower half of the body. Males are distinguished by a pair of claspers on the anterior end.

Artemia inhabit hypersaline environments and they exist in high chloride, sulphate or carbonate waters (Triantaphyllidis et al., 1998). Additionally, encysted *Artemia* embryos survive 4 years of continuous anoxia when fully hydrated as well as other stresses such as temperature extremes, desiccation, anoxia and radiation (Clegg, 1997). This environmental resilience enables *Artemia* to have a wide geographical distribution and they are found on all continents except Antarctica (Triantaphyllidis et al., 1998) at altitudes from sea level to 4400 m in Zhangchaka Lake, Tibet, China (Xin et al., 1994). *A. franciscana* is the dominant species in North America (Triantaphyllidis et al., 1998).

The life history of *Artemia* plays an important role in its ability to tolerate extreme environments. After fertilization, embryos may undergo either oviparous development and are released from females as encysted embryos, or ovoviviparous development resulting in the release of swimming nauplii. After release from females,

cysts enter diapause, a form of metabolic dormancy characterized by high stress tolerance, low metabolism and arrested development (Fig. 1) (Clegg et al., 1996; MacRae, 2005). *A. franciscana* diapause is terminated by desiccation and freezing or a brief treatment of cysts with H_2O_2 (Robbins et al., 2010; Veeramani and Baskaralingam, 2011). Upon diapause termination and hatching of cysts, first instar nauplii are released and undergo several molts to become adults (Fig.1) (Clegg, 2005). *Artemia* cysts possess a number of adaptations that favour survival during diapause when they encounter stressors. The rigid, semi-permeable shells of cysts protect the embryos from mechanical damage as well as UV radiation and high temperature (Tanguay et al., 2004; MacRae, 2016; Dai et al., 2011; Ma et al., 2013). Other adaptations include high trehalose concentration (Clegg and Evans, 1962; Clegg, 1967), late embryogenesis abundant (LEA) proteins (Sharon et al., 2009; Warner et al., 2010; Toxopeus et al., 2014; Moore et al., 2016), and the abundant, diapause-specific, ATP-independent molecular chaperones, p26, a small heat shock protein (sHsp) (Liang and MacRae, 1999; Clegg, 2011; King and MacRae, 2012; King et al., 2013) and artemin, a ferritin homologue (Chen et al., 2003; Chen et al., 2007; Clegg, 2011; King et al., 2014).

The relatively short life history and ready availability of cysts and nauplii makes *A. franciscana* an ideal animal model to examine stress tolerance and development. The study of *A. franciscana* offers knowledge on the development and stress tolerance of other crustaceans and arthropods like insects which could facilitate the production of arthropods for commercial purposes and pest control, especially of insects that

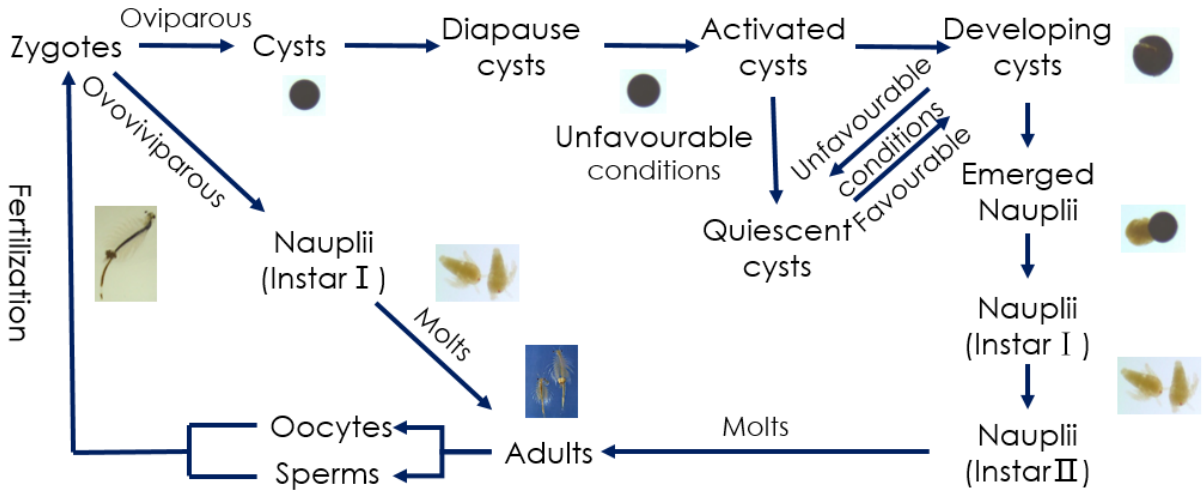

Fig. 1. *A. franciscana* life history. Females release free swimming nauplii via the ovoviviparous pathway which then undergo a series of molts before reaching adulthood. Alternatively, females release encysted gastrulae via the oviparous pathway which enter diapause. Once diapause is terminated, cysts develop into nauplii if conditions are favorable. If conditions are not favorable activated cysts are maintained in post-diapause quiescence until introduction to an environment conducive to development (adapted from Liang and MacRae, 1999).

destroy crops.

1.2 Heat shock factor (HSF)

1.2.1 HSF, structure and function

First isolated from *Saccharomyces cerevisiae* (Sorger and Pelham, 1988) and *Drosophila melanogaster* (Clos et al., 1990), Hsf is a protein of about 50-90 kDa in mass and it binds to the upstream sequence of genes, mostly heat shock protein (*hsp*) genes and starts their transcription (Neudegger et al., 2016). Under normal conditions, Hsf is held in an inactive momomeric form by interacting with Hsp90 and forming a Hsf-Hsp90-p23-immunophilin complex (Voellmy, 2004; Anckar and Sistønen, 2011; Luo et al., 2010). Hsp70 and Hsp40 help with the introduction of Hsp90 into the complex (Voellmy, 2004). When triggered by stress, HSF monomers are released from the complex, hyperphosphated and trimerize into active transcription factors. The interactions between HSF and Hsps are important during stress tolerance. HSF is also heat sensitive by itself, as revealed by several *in vitro* tests showing that purified Hsf acquires DNA binding activity upon heat shock (Nakai, 2016). Hsf trimers then bind to a short sequence of DNA known as heat shock element (HSE) upstream of the target gene and initiate transcription (Hashikawa 2007; Jaeger et. al., 2014; Yamamoto et. al., 2009). HSEs consist of three inverted repeats “nGAAn” where “n” can be any nucleotide. Sometimes, HSE sequences may vary from this canonical structure and consist of four repeats instead of three, or possess more than one gap between “nGAAn” repeats (Abane and Mezger, 2010; Yamamoto et al., 2009). The ability to

bind non-classical HSEs explains the diverse array of genomic loci to which Hsf binds and the large number of genes regulated by HSF.

From the amino-terminus to the carboxyl-terminus of HSF, there is a DNA binding domain (DBD), a hydrophobic repeat (HR) regions (HR-A & B domain), a regulatory domain and a HR-C domain (Fig. 2) (Pirkkala et. al., 2001; Miozzo et al., 2015). The DBD, which is the core of HSF, is composed of a helix-turn-helix motif and enables HSF binding to HSEs in the promoter area of genes (Fig. 2) (Neudegger et al., 2016). HR-A & HR-B are α-helices composed of a repeating pattern of heptad repeats containing hydrophobic amino acids such as leucine (L), isoleucine (I), and valine (V) and they function in HSF trimerization via coiled-coil interactions (Neudegger et al., 2016). The regulatory domain controls HSF activity before and after trimerization. Post-translational modifications such as phosphorylation, acetylation and SUMOylation occur on the regulatory domain of HSF (Kline and Morimoto, 1997; Hietakangas et al., 2003; Westerheide et al., 2009; Raychaudhuri et al., 2014). HR-C, found in HSF1 and HSF2 in humans and HSF3 in birds and mammals but not in other organisms, maintains HSF as monomers by suppressing trimerization through intramolecular coiled-coil interactions with HR-A/B when there is no trigger for activity (Anckar and Sistønen, 2007; Åkerfelt et. al., 2010; Sakurai and Enoki, 2010; Neudegger et al., 2016). A temperature-dependent stabilization of HR-A and unfolding of HR-C enables HSF1 to “sense” temperature change and react to thermal stress (Gomez-Pastor et al., 2018).

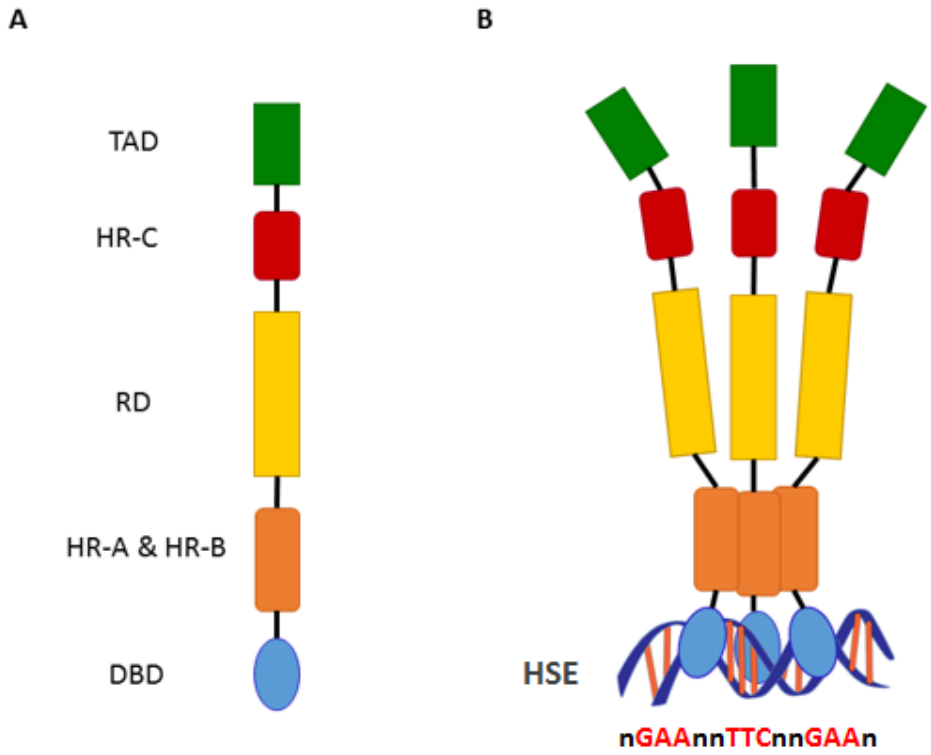

Fig. 2. HSF monomer and trimer. (A) Domains of a typical HSF. DBD, DNA binding domain, blue; HR-A & HR-B domain, orange; RD, regulatory domain, yellow; HR-C, red. TAD, transactivation domain, green. (B) HSF trimer binds to a heat shock element (HSE). Modified from Miozzo et al (2015).

HSF initiates transcription of target genes by releasing paused RNA polymerase II (Pol-II). Classical *hsp* genes accumulate paused Pol-II 20-50 bp downstream from the transcription start site (TSS). The transcription factor GAGA-associated factor (GAF) is bound to the promoter of *hsp* genes prior to heat shock and assists with the formation and maintenance of the paused Pol-II. Upon heat shock, HSF binds to HSEs and recruits co-activators, such as P-TEFb. The complex of HSF and co-activators changes the chromatin structure and leads to the release of Pol-II from the paused complex to initiate elongation (Duarte et al., 2016; Nakai, 2016).

1.2.2 HSF family.

HSFs are found in organisms ranging from *S. cerevisiae* to *Homo sapiens*. Vertebrates have as many as 6 different HSFs, including HSF1, HSF2, HSF3, HSF4, HSFX and HSFY (Fig. 3) (Abane and Mezger, 2010; Fujimoto and Nakai, 2010; Fujimoto et al., 2010). Humans apparently have a HSF5 which has only been confirmed at the transcript level, while lacking HSF3 which is found in chicken and mouse (Fig. 3) (Fujimoto and Nakai, 2010; Fujimoto et al., 2010). Some plants have large families of HSFs with more than 20 members (Vasquez et. al., 2015). For example, *Arabidopsis thaliana* has 21 *hsf* genes and they are divided into 3 different classes whereas the soybean *Glycine max* has 52 *hsf* genes, the largest number for all species examined so far (Scharf et al., 2012). Arthropods have only 1 type of HSF, termed Hsf1 (Abane and Mezger, 2010), which has all the functional domains mentioned above and shares high identity in the DBD and HR-A/B domains with

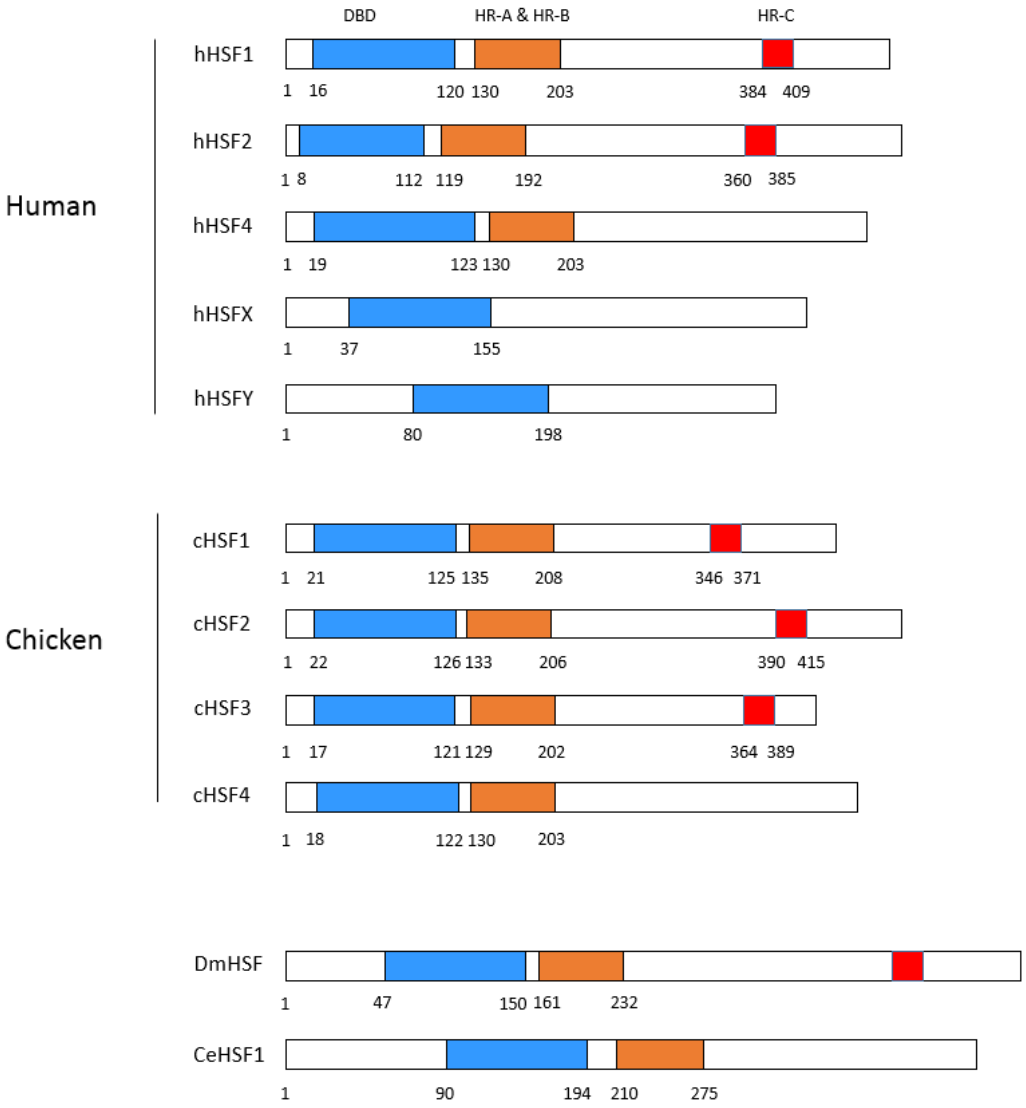

Fig.3. Members of the HSF superfamily. The diagram represents HSFs from human, chicken and two invertebrate species. h, human; c, chicken; Dm, *Drosophila melanogaster*; Ce, *Caenorhabditis elegans*. The numbers are the position of amino acids starting from the amino-terminal. (Modified from Fujimoto and Nakai; 2010)

vertebrate HSF1 (Yan et al., 2014). HSF1 to HSF4 possess conserved DBD and HR-A & HR-B domains, but HSFX and HSFY do not have all these domains (Fig. 3). *hsf*X and *hsf*Y are sex related genes located on sex chromosomes and they possess only the conserved DBD domain (Abane and Mezger, 2010; Kichine et al., 2012).

Different HSFs have different roles in animals. HSF1 is a master regulator of genes involved in the stress response and development in vertebrates and invertebrates and it plays an important role in maintaining protein homeostasis (Tanabe et al., 1998; Nakai, 2016). HSF3 is necessary for induction of the heat shock response in chickens, especially when the temperature is high and avian HSF3 functions similarly to HSF1 while also directly influencing HSF1 activity (McMillan et al., 1998; Tanabe et al., 1998). Mouse HSF3 induces the expression of non-classical heat shock genes such as membrane glycoprotein prominin-2 (PROM2) during heat shock (Fargeas et al., 2003; Fujimoto et al., 2010). Although not induced during classical stress response, HSF2 and HSF4 are important in embryogenesis and early animal development. For example, HSF2 knockout female mice have defects in oogenesis (Edelmann et al., 1999) and males display gametogenesis defects and misguided neuronal migration (Chang et al., 2006). HSF2 is associated with heart chamber formation in mouse (Eriksson et al., 2000). HSF4 is a key protein in the development of mammalian lens cells, preventing protein crystallization and aggregation in lens fiber cells and protecting normal lens structure and function (Shi et al., 2009). Dysfunctional HSF4 is associated in humans with dominant hereditary cataracts (Bu et al., 2002). HSFX and HSFY, the sex chromosome located HSFs

found in humans, are critical for human spermatogenesis and malfunction of these sex-related HSFs is involved in azoopermia and oligospermia in mammals (Kichine et al., 2012; Stahl et al., 2011; Shinka et al., 2004).

1.3 HSF, HSPs and stress tolerance

1.3.1 Introduction to HSPs

Hsps, known as molecular chaperones or stress proteins, are divided into six major families based on their molecular mass, sequence, structure and function, and these include Hsp110, Hsp90, Hsp70, Hsp60, Hsp40 and the small heat shock proteins (sHsps) (MacRae, 2000; Bakthisaran, 2015). Hsps play important roles in cell integrity during normal growth and stress and their roles include the folding of nascent proteins, translocation of proteins through membranes, and refolding and/or degradation of misfolded proteins (Ciocca et al., 2013; Hartl et al., 2011). Hsp90, Hsp70 and Hsp60 are ATP-dependent proteins which means their interactions with substrates are driven by ATP binding and hydrolysis, followed by exchange of ADP for ATP (Zuehlke et al., 2018; Craig, 2018). Hsp90 is characterized by ATP and geldanamycin binding domains, and a C-terminal MEEVD motif found only in cytoplastic Hsp90 (Li et al., 2012). Hsp90 is one of the most abundant proteins in cells, accounting for 1-2% of total soluble protein in most tissues even in normal conditions (Li et al., 2012). Hsp90 functions as a homodimer and dimerization is essential for its function *in vivo* (Zuehlke et al., 2018). Hsp70 is characterized by two conservative domains: the amino-terminal ATPase domain and the carboxyl-terminal

peptide-binding domain (Baringou et al., 2016). The Hsp70 family consists of several members, such as constitutively expressed heat shock cognate protein 70 (Hsc70), heat-inducible heat shock protein 70 (Hsp70) and glucose-regulated protein GRP78 (Li et al., 2009). The J-domain protein Hsp40 is an important co-chaperone of Hsp70 which is characterized by a conservative histidine, proline, and aspartic acid (HPD) motif. (Jiang et al., 2016).

sHsps are Hsps composed of monomers varying from about 12–40 kDa in molecular mass and most assemble into dynamic oligomers, either for storage in the cell or for function (King and MacRae, 2013; Sun and MacRae, 2005; Carra et al., 2017). sHsps monomers possess a conserved α-crystallin domain of about 90 amino acid residues located toward the carboxyl-terminus and it signifies membership within the sHsps chaperone family (Sun and MacRae,2005; van Montfort et al. 2001). The α-crystallin domain is preceded by a poorly conserved amino-terminal domain which influences higher-order oligomerization, subunit dynamics and chaperoning and followed by a flexible carboxyl-terminal extension of variable length and sequence which stabilizes oligomers while mediating sHsp solubility and chaperoning (Sun and MacRae, 2005; MacRae, 2000; Friedrich et al., 2004). sHsps are phylogenetically widespread and function within subcellular compartments where they bind and protect proteins (Sun and MacRae, 2005).

1.3.2 HSF and Hsps during stress tolerance

HSF is essential to stress defense because it activates the expression of *hsp* genes,

the corner-stone of stress tolerance in all organisms. Coping with stress is accompanied by over-expression of Hsps (Ciocca et al., 2013). All classes of Hsps are induced by stress, but responses vary with the type of stress and from one animal to another. Hsp70 folds nascent peptides and refolds unfolded proteins upon stress (Craig, 2018). From a practical perspective, Hsp70 is often used as a stress marker in crustaceans (Baringou et al., 2016). Hsp60 promotes the correct folding and assembly into oligomeric structures of other polypeptide chains (Stanley and Fenton, 2000). Hsp90 facilitates protein maturation, aggregation-prone protein stabilization and refolding or degradation of misfolded proteins while keeping proteins in active conformations (Zuehlke et al., 2018). Cytoplasmic Hsp90 is involved in cell regulatory pathways by activating protein kinases, transcriptional factors, cell cycle regulators and steroid hormone receptors (Schopf et al., 2017; Li et al., 2012; Li et al., 2009). Hsp90 is a key repressor of HSF and the stress response starts with HSF activation by release from Hsp90. Activated HSF initiates the transcription of *hsp90* mRNA and the extra Hsp90 synthesized during heat shock binds to and inactivates HSF, thereby reducing the transcription of *hsp* genes (Zou et al., 1998). Hsp90 is up-regulated in many tissues during stress and as one example, it is induced by heat shock in gill, heart, hepatopancreas, stomach, intestine, eyestalk, pleapod, thoracic ganglia and hemocyte of the black tiger shrimp, *Penaeus monodon* (Rungrassamee et al., 2010).

Hsps cooperate with each other during stress. As an example, Hsp70 interacts with co-chaperones such as Hsp40 and nucleotide exchange factors (NEFs) in an

ATP-dependent cycle, thereby maintaining correct folding of nascent proteins and assisting in refolding and/or destruction of aberrant proteins (Baringou et al., 2016). Hsp70 and Hsp90 cooperate via the actions of co-chaperones such as HOP (Hsp70/Hsp90 organizing protein). HOP facilitates chaperoning by Hsp90 upon binding to both molecular chaperones and regulating the transfer of substrate from Hsp70 to Hsp90 (Ruckova et al., 2012; Yamamoto et al., 2014). A HSE resides in the promotor region of the *HOP* gene, indicating that HSF regulates this gene (Ruckova et al., 2012).

The sHsps bind to and prevent the irreversible denaturation of proteins in an ATP-independent manner, and in animals such as insects they respond differently to dissimilar stresses. Five *sHSP* genes are induced by heat shock in *Bombyx mori* fifth instar larvae but *sHSP 21.4* is not induced. (Sakano et al., 2006). Reducing Hsf in nuclei by knocking down karyopherin alpha 3 (KPNA3) which transports Hsf into nuclei in *B. mori* decreases the recovery of *HSP19.9*, *HSP20.4* and *HSP25.4* mRNA 24 hours after heat shock (Li et al., 2016). The expression of *Cshsp19.8* and *Cshsp21.2b* is induced by extreme temperature in larvae of the rice stem borer, *Chilo suppressalis* and *Cshsp21.5* is only induced by cold (Lu et al., 2014). Induction of *Drosophila Hsp23*, *Hsp22*, *Hsp26* and *Hsp27* by cold is less intense than by heat shock due to the differential activation of Hsf (King and MacRae, 2015; Colinet et al., 2010). ArHsp22 appears in *A. franciscana* adults with the highest amount at 6 hr of recovery (Qiu and MacRae, 2008b). Moveover, sHsps are especially critical for some arthropods during diapause, which enables increased stress tolerance and enhanced

survival in adverse environments (Li et al., 2009). p26 has a role in diapause stress resistance as only 6% of *A. franciscana* cysts lacking p26 hatch after diapause breakage by desiccation and freezing, compared with 58% of cysts containing p26 hatch (King and MacRae, 2012).

1.3.3 HSF regulates the transcription of non-HSP genes

Hsf binding sites are found in almost all *hsp* promotors in the genes of *Drosophila* 3rd stage larvae that respond to heat shock (Gonsalves et al., 2011), suggesting an essential role for Hsf in their expression. In *Drosophila*, the *hsp* promotors account for only about 8.7% of all the effective Hsf binding sites in genes activated after heat shock (Gonsalves et al., 2011). Of the 188 genes regulated by Hsf during heat shock in *Drosophila* embryos, only 17 are molecular chaperones. Others include proteins involved in basic metabolism, protein modification and degradation, cell cycle and apoptosis (Birch-Machin et al., 2005). As many as 654 different transcripts are up-regulated by Hsf upon heat shock in *C. elegans*. Of the top 15 up-regulated transcripts, 9 are the products of *hsp* genes while another 6 are not (Brunquell et al., 2016). How HSF regulates non-HSPs during stress is not clear but the findings in *C. elegans* and *Drosophila* show that HSF controls a much wider range of genes than previously anticipated (Brunquell et al., 2016; Åkerfelt et al., 2007; Gonsalves et al., 2011). As examples, Hsf binds to the promoter of non-HSP genes, including *TOM34*, *TAF7*, and *GSTD*, after heat shock in *Drosophila* (Gonsalves et al., 2011). Hsf also promotes the initiation of *CUP1* transcription, a metallothionein

encoding gene, upon heat shock in *S. cerevisiae* (Lin and Lis, 1999). Mouse HSF3 activates non-heat shock protein genes such as *PDZK3* and *PROM2* during thermal stress (Fujimoto et al., 2010) and HSF1 regulates the apoptosis related genes, *Hsph1*, *Hspa1*, *Dnaja1* and *Phlda1*, in mouse upon heat shock (Kus-Liskiewicz et al., 2013).

1.4 HSF and chaperones during diapause

1.4.1 Diapause

Diapause is a physiological process of developmental delay regulated by complex patterns of gene expression and it is characterized by reduced metabolism, sequestration of nutrient reserves, a halt or slowing of development, a decline of water content, and increased tolerance to environmental stresses. During diapause, animals tolerant adverse environmental conditions (MacRae, 2010; Koštál, 2006) and dormant animals in diapause will only break diapause when triggered by environmental signals (Koštál, 2006; Robbins et al., 2010).

Diapause can be divided into three stages, namely pre-diapause induction and initiation, maintenance and termination (Koštál, 2006). Diapause in arthropods is triggered by environmental signals like photoperiod, temperature changes and pheromones generated by food depletion and crowding, but arthropods may enter diapause without an environmental trigger as an obligate part of their life history (Saunders et al., 1989; Koštál, 2006; MacRae, 2010; Reznik and Voinovich, 2016). The termination of diapause generally occurs when there is a good chance that organisms will experience favorable growth conditions and in some species

diapause-terminating conditions are strict. For instance, larvae of the fly *Chymomyza costata* only terminate diapause under low temperature conditions (Koštál et al., 2000). Diapause of many organisms may be precociously terminated, by artificial stimuli such as mechanical shaking, electrical or temperature shocks, injury, infection, or treatment with solvents and other chemicals (Clegg et al., 1996). After the termination of diapause, animals may either resume development, or enter quiescence where they remain dormant while unfavorable environmental conditions persist but resume development when circumstances improve (MacRae, 2005).

1.4.2 HSF regulates HSPs during diapause

HSF regulates *hsp* gene expression during embryonic diapause and in one example, Hsf binds to the HSEs of the *Hsp70* gene and enhances its expression in diapause-destined embryos of *B. mori*, suggesting that Hsf is essential for diapause entry (Kihara et al., 2011). Furthermore, Hsf may affect entrance into and maintenance of diapause via mechanisms that involve proteins other than HSPs. For example, several genes involved in lipid synthesis and transport are up-regulated by Hsf independent of heat shock in *C. elegans* (Brunquell et al., 2016) and some animals like *Calanus finmarchicus* increase their lipids before diapause (Tarrant et al., 2008). Therefore, Hsf may assist in lipid production and transport during diapause.

Despite nearly a 90% reduction in metabolism during diapause, two Hsp70s and six sHsps increase significantly in brains of the pupae of the flesh fly *S. crassipalpis* during diapause (Li et al., 2007). Additionally, as shown by subtractive hybridization,

the mRNA encoding *TCP-1*, a member of the Hsp60 family, is up-regulated during *S. crassipalpis* diapause (Rinehart et al., 2007). These Hsps are thought to be essential to the longterm survival of diapausing fly pupae at low temperature. In other cases of increased HSPs during diapause, *hsp70* mRNA rises significantly compared to *hsc70* mRNA in diapausing pre-pupae of the solitary bee *Megacbilero tundata* (Wang et al., 2007) and Hsp70A and Hsp22 are elevated in the marine copepod *C. finmarchicus* during deep diapause (Aruda et al., 2011), indicating a role for Hsp70 and sHsps during diapause.

The up-regulation of HSPs just described indicates that the accumulation of these proteins is necessary for successful diapause in arthropods (Li et al., 2007; Rinehart et al., 2007) and that their synthesis, resulting in augmentation of HSPs in diapausing animals, increases early in diapause, thereby promoting stress tolerance and survival. Undoubtedly, the increased synthesis of Hsps enhances the ability of cells to save substrate proteins from irreversible denaturation.

During diapause in pupae of *S. crassipalpis*, *hsp90* mRNA is down-regulated two-fold and only returns to pre-diapause levels 12 hours post diapause termination. The increase in HSP90 upon diapause termination coincides with the breakage of G0/G1 cell cycle arrest and an increase in transcripts encoding proliferating cell nuclear antigen (PCNA), indicating a role for Hsp90 in the reinitiation of development (Rinehart and Denlinger, 2000). Hsp70 increases 222-fold in eggs of the neritic calanoid copepod *Acartia tonsa* (Dana) during recovery from diapause, a change that is apparently not due simply to enhanced metabolism which increases

only 2.51 times (Nilsson et al., 2014). It has been proposed that the increased Hsp90 and Hsp70 offset the developmental delay associated with diapause and thereby promote development after diapause (Aruda et al., 2011).

Hsps in some arthropods do not change during diapause. The amount of Hsp70 remains constant during the induction of larval diapause in the blow fly *Lucilia sericata* (Tachibana et al., 2005). Additionally, Hsp70 is not modified during adult diapause of the mosquito *Culex pipiens* (Rinehart et al., 2006) nor does Hsp90 respond to the adult diapause program in *Drosophila triauraria* (Goto and Kimura, 2004). Proteomic analysis showed that Hsp90, Hsp20.8, Hsp20.4 and Hsp70 are not significantly different between diapause and non-diapause eggs of *B. mori* (Sasibhushan et al., 2012). Hsps may not change during diapause because they are important for embryo development while maintaining basic metabolism and immune defenses (Sasibhushan et al., 2012).

1.4.3 sHSPs and artemin during diapause of *A. franciscana*

The sHSPs p26, ArHsp21 and ArHsp22 are restricted to diapause-destined embryos *A. franciscana* (Qiu and MacRae, 2008 a, b; Liang and MacRae, 1999), indicating a role in diapause. p26 accounts for about 7% of all soluble proteins in encysted embryos of *A. franciscana* and knockdown of p26 leads to termination of diapause in the absence of an external cue (King and MacRae, 2012). p26 is required for optimal development of diapause-destined embryos of *A. franciscana* and knockdown of p26 extends the time required to cyst release from females after

fertilization. p26, ArHsp21 and ArHsp22 exist largely at day 4 and day 5 in oviparous embryos and are found in cysts entering diapause, indicating these sHSPs are involved in the maintenance of diapause (Liang and MacRae, 1999; Qiu and MacRae, 2008 a, b; King and MacRae, 2012). sHSPs have different roles during diapause in different animals. For example, *SnoHsp20.8* is down-regulated in the corn stalk borer, *Sesamia nonagrioides*, as it enters diapause and then up-regulated as diapause ends, while the *SnoHsp19.5* gene is expressed consistently (Gkouvitsas et al., 2008). *Hsp23* and *hsp24* are upregulated in the diapausing blow fly *Callipbora vicina*, suggesting a role in diapause maintenance, perhaps preserving proteins essential for diapause termination and post-diapause development (Fremdt et al., 2014).

Artemin is a ferritin homologue exhibiting chaperone activity and artemin monomers form oligomers containing 24 monomers (Chen et al., 2007). Artemin comprises approximately 7% of the post-ribosomal protein in diapause cysts, suggesting a role in diapause maintenance (King et al., 2014). The knockdown of artemin extends the time required for the complete release of a brood of cysts from females, suggesting that it assists in diapause-destined embryo development (King et al., 2014).

1.5 RNA interference (RNAi) as a tool to study protein function

RNAi is a technology that targets specific mRNA transcripts and degrades them to generate an organism with reduced amounts of a particular protein. Such organisms missing a protein exhibit a loss-of-function phenotype that makes it possible to study

the function of the protein *in vivo* (Siomi and Siomi, 2009). RNAi was first discovered in an attempt to down-regulate gene expression wherein dsRNA was found to be more potent in silencing genes than sense or antisense RNA alone (Fire et al., 1998). RNA-induced silencing complex (RISC), a ribonucleoprotein complex, is minimally composed of a small single-stranded RNA known as guide RNA of about 20–31 nucleotides and Argonaute (Ago) which is an effector protein. A dsRNA-binding domain (dsRBP) and dicer, a large endoribonuclease containing a helicase domain and an internally dimerized pair of Rnase III (Wilson and Doudna, 2013), form RISC-loading proteins with Ago and generate diced dsRNA which is loaded onto Ago. Ago leads RISC to the target with other associated machinery by the loaded guide RNA. The RISC then silences the sequence specific complementary target mRNA by endonucleolytic cleavage or translational repression (Fig. 4) (Ghildiyal and Zamore, 2009; Wilson and Doudna, 2013). There are three principal RNAi pathways, respectively involving microRNA (miRNA), small interfering RNA (siRNA) and Piwi-interacting RNA (piRNA) (Wilson and Doudna, 2013). siRNA was employed in this research by introducing exogenous dsRNA specifically targeting *hsf*. dsRNA used for RNAi is trimmed down to a dsRNA duplex of the appropriate size for loading onto Ago by the Dicer enzyme. Dicing, loading and ejection of the exogenous dsRNA is accomplished by dsRNA-binding proteins (dsRBPs) and dsRBPs direct mature dsRNA to Ago. siRNA-loaded RISC is an endonuclease that recognizes targets with perfect or nearly perfect base complementarity, thus favoring silencing through slicing of the target (Ipsaro and Joshua-Tor, 2015).

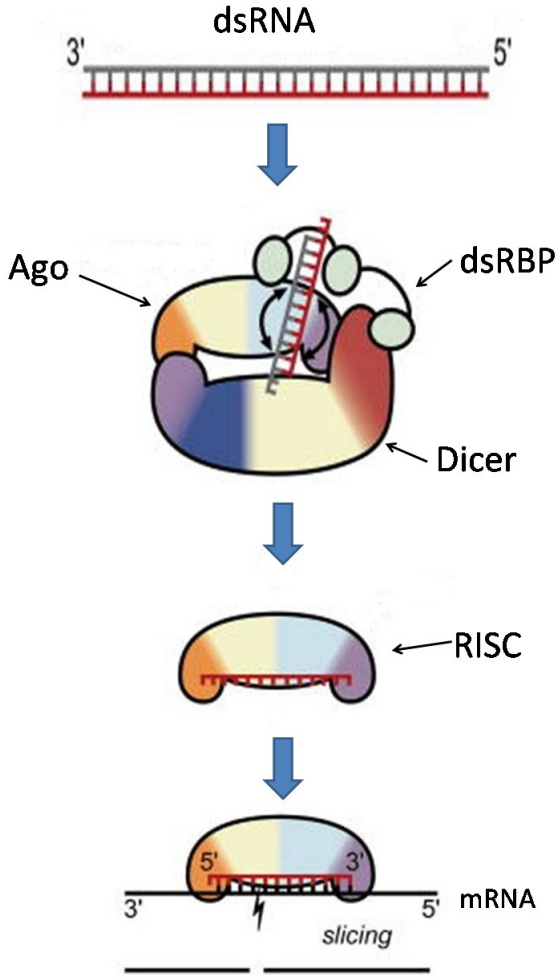

Fig. 4. Mechanism of RNA inference with dsRNA. Dicer and dsRBP digest and present dsRNA to Ago. Ago forms RISC with guide RNA and cut target mRNA. dsRBP, dsRNA-binding proteins; Ago, Argonaute; RISC, RNA-induced silencing complex. Modified from Wilson and Doudna (2013).

RNAi has been used previously to study HSF function. For example, RNAi knockdown of HSF1 enhances the pro-inflammatory transcription factors NF-κB and AP-1 in rat aorta and human intestinal smooth muscle (HISM) cells (Chen and Currie, 2006). The loss of Hsf1 suppresses Hsp27 in both unstressed and heat shocked HISM cells (Chen and Currie, 2006). Knockdown of HSF1 in Hela cells by RNAi dramatically increases their sensitivity to hyperthermochemotherapy, causing apoptosis in more than 95% of cancer cells (Ghildiyal and Zamore, 2009). However, there are no reports of the knockdown of Hsf1 in crustaceans and *hsf* cDNA has only been reported in a few species of crustacean (Yan et al., 2014).

Summary

The objective of the research described herein was to determine the role of Hsf1 in the stress tolerance of diapausing *A. franciscana*. *Hsf1* cDNA was cloned from *A. franciscana* and the deduced amino acid sequence was analyzed to determine Hsf1 structure. RNAi was then employed to study the function of Hsf1 *in vivo*. The knockdown of Hsf1 was confirmed by qRT-PCR and immunoprobing of western blots and its loss led to reduced stress tolerance of diapausing cysts. The loss of Hsf1 was accompanied by reductions in the amounts of p26, ArHsp21, ArHsp22 and artemin in cysts indicating that Hsf1 regulates the expression of their genes. Hsf1 was also knocked down in ovoviviparously developing embryos revealing that it influenced stress tolerance and longevity of nauplii. That both cysts and nauplii released by females possessed Hsf1, but only cysts produced p26, ArHsp21, ArHsp22 and artemin,

may result from differences in the amounts and localizations of Hsf1 in the respective life forms. The results of the study provide a foundation for future studies of the function of Hsf1 during diapause and stress tolerance of all arthropods, many of economic and social importance.

Chapter 2 Materials and Methods

2.1 Culture of *A. franciscana*

A. franciscana cysts from the Great Salt Lake (INVE Aquaculture Inc., Ogden, UT, USA) were hydrated overnight at 4^{o}C in distilled water, collected by filtration, washed with cold distilled water followed by filtered and autoclaved sea water from Halifax Harbour, hereafter called sea water, and incubated in sea water with vigorous shaking at room temperature. Nauplii were harvested and grown in sea water at room temperature with gentle aeration. Animals were fed daily with *Isochrysis sp*. (clone synonym *T-Iso*) obtained from the Provasoli-Guillard National Centre for Culture of Marine Phytoplankton (West Boothbay Harbor, ME, USA).

Once it was possible to differentiate males and females, they were captured individually and incubated in sea water at room temperature in containers housing either males or females. Algae and aeration were supplied as described above. Male and female *A. franciscana* were mated in 5 cm diameter Petri dishes containing sea water at room temperature. Females with a shell gland were identified as cyst releasing (Liang and MacRae, 1999). Nauplii and cysts were collected and used in experiments as they were released from females. Cysts were incubated in sea water for 6 to 8 days before harvesting if they were required to be in diapause. Dead or abnormal animals were discarded.

2.2 Cloning of *A. franciscana hsf1* cDNA and bioinformatics analysis

2.2.1 *Hsf1* full length cDNA.

Five male *A. franciscana* adults were heat shocked at 38°C for 20 min in seawater, washed twice with ion-free water and homogenized in 1 ml TRIzol® (Invitrogen, Burlington, ON, Canada). RNA was recovered with the RiboPure™ RNA Purification Kit (Invitrogen) following manufacturer's instruction. The $A_{260:280}$ ratio of RNA samples was determined with a nanophotometer P360 (Implen, Westlake village, CA, USA). First strand cDNA was synthesized using RNA as template with the SuperScript® III First-Strand Synthesis System (ThermoFisher Scientific, Waltham, Massachusetts, USA) following manufacturer's instructions. Briefly, RNA samples were denatured at 65℃ and annealed to Oligo$(dT)_{20}$ primers on ice. First strand cDNA was synthesized by SuperScript® III reverse transcriptase at 50℃. RNA was then digested with *E. coli* RNase H.

Degenerate primers (Table 1) synthesized by Integrated DNA Technologies (IDT) for the cloning of a partial *A. franciscana hsf1* cDNA were designed by aligning Hsf1 protein sequences from arthropods deposited with the National Center for Biotechnology Information (NCBI). A partial cDNA encoding *A. franciscana* Hsf1 was amplified in 50 µl PCR mixtures containing 5 µl 10 x Taq buffer, 2 µl 25 mM $MgCl_2$, 2 µl dNTP mixture at 10 mM each, 2 µl of each primer at 10 µM, 2 µl first strand cDNA, 34.8 µl H_2O and 0.2 µl Taq polymerase at 5 U/µl (Thermofisher Scientific). Amplification was for 5 min at 95°C, followed by 35 cycles of 95°C for 30 s, 49°C for 30 s, 72°C for 1 min and then 6 min at 72°C. PCR products were resolved in 1.2% agarose gels in 1 x TBE buffer (90 mM Tris, 90 mM boric acid, 1 mM EDTA, pH 8.5) at 95 V and stained with 0.01% SYBR® Safe (Thermofisher Scientific) prior to visualization with a DNR Bio-Imaging Systems MF-ChemiBIS 3.2 gel documentation system (Montreal Biotech, Montreal, QC, Canada). The Frogga Bio 1 kb DNA Ladder (Frogga Bio, North York, ON, Canada) was used as size marker. DNA of the

appropriate size were excised from the gel and purified with a QIAEX II Gel Extraction Kit (Qiagen, Toronto, ON, Canada) following manufacturer's instructions. Purified DNA fragments were ligated into the pCR™2.1-TOPO® vector (Thermofisher Scientific) and used to transform TOP10 F' competent *Escherichia coli* (ThermoFisher Scientific). Vectors were harvested with GenElute™ Plasmid Miniprep Kit (Sigma-Aldrich, Oakville, Canada) following manufacturer's instructions. cDNA in harvested vectors containing putative *hsf1* cDNA was sequenced at the Center for Applied Genomics DNA Sequencing Facility (TCAG) (Toronto Sick Kids Hospital, Toronto, ON, Canada).

Primers (Table1) for 5'- and 3'-RACE were designed based on the partial sequence of *A. franciscana hsf1* cDNA obtained with the degenerative primers. RNA was extracted from cysts and first strand cDNA was prepared as described above. cDNA was then purified and ligated to adaptors provided by the FirstChoice® RLM-RACE Kit (Ambion Applied Biosystems, Austin, TX, USA) and used as template to amplify the 5' and 3' regions of *hsf1* cDNA by nested PCR following manufacturer's instructions. Outer PCR was at 95°C for 5 min followed by 35 cycles of 95°C for 30 s, 53°C for 30 s 72°C for 1 min, then 6 min at 72°C. Inner PCR was at 95°C for 5 min followed by 30 cycles of 95°C for 30 s, 60.5°C for 30 s, 72°C for 1 min and then 6 min at 72°C. PCR products were resolved in 1.2% agarose gels in 1 x TBE buffer at 95 V and stained with 0.01% SYBR® Safe (Invitrogen) prior to visualization with a DNR Bio-Imaging Systems MF-ChemiBIS 3.2 gel documentation system (Montreal Biotech). PCR products of the appropriate size were excised from the gel and purified with a QIAEX II Gel Extraction Kit (Qiagen), ligated into

pCR™2.1-TOPO® vector (Thermofisher Scientific) and used to transform TOP10 F' competent *E. coli* (ThermoFisher Scientific). Putative *hsf1* cDNA fragments were sequenced at TCAG. A second *hsf1* cDNA was cloned from hydrated cysts as described above and shown to have the same sequence as the initial *hsf1* cDNA clone.

2.2.2 Bioinformatics

The deduced amino acid sequence of *A. franciscana* Hsf1 was translated from the cDNA sequence using online software open reading frame finder (https://www.ncbi.nlm.nih.gov/orffinder/). Sequence secondary structure was deduced with STRAP tool box (http://www.bioinformatics.org/strap/Scripting.html) for protein analysis. The amino acid sequence of *A. franciscana* Hsf1 was then aligned using Clustal Omega (https://www.ebi.ac.uk/Tools/msa/clustalo/) with the amino acid sequence of Hsf1s from several other organisms available at NCBI. The alignment was presented with DNAman (Lynnon Corporation, San Ramon, CA, USA). The identity of HSF1 amino acid sequences were calculated with Sequence Identity And Similarity (SIAS) (http://imed.med.ucm.es/Tools/sias.html). The domains of Hsf1 were deduced with blast (https://blast.ncbi.nlm.nih.gov/Blast.cgi).

2.3 Injection of *A. franciscana* females with double stranded RNA (dsRNA)

2.3.1 dsRNA preparation

RNA prepared from hydrated *A. franciscana* cysts using TRIzol® (Invitrogen) and the RiboPure™ RNA Purification Kit (Invitrogen) was used as described above to

Table 1. Primers used for cloning *hsf1* cDNA by RACE and for Hsf1 synthesis in *E. coli*.

Primer Name	Forward Primer (5'- 3')	Reverse Primer (5'- 3')	Tm (^{o}C)
Partial HSF1 A	TAYTTYAARCAY AAYAATATGG	TYYTGRATYTGY TGCTGCTT	49
Partial HSF1 B	TAYTTYAARCAY AAYAATATGG	GCTTCRTTYTC YTTTTTCAT	49
5'-RACE outer	GCTGATGGCGAT GAATGAACACTG*	TCCTCCGATTGT CTTGTACCA	54
5'-RACE inner	CGCGGATCCGAA CACTGCGTTTGC TGGCTTTGATG*	CCTTGCTCAACC GATGATACCTTC CGAAACCC	60
3'-RACE outer	CGGTTGAGCAAG GAAGCCTTC	GCGAGCACAGAA TTAATACGACT*	53
3'-RACE inner	AACGAAAGCTGC CATCTGGTACAA GACAATC	CGCGGATCCGAA TTAATACGACTC ACTCACTATAGG*	60
HSF1 (E)	CGGGGATCCCGT ATTGTGTAGTTG AGCCTG	CCGGAATTCCGA ATTAATACGACT CACTATAGG	60

PCR reaction conditions are described in Materials and Methods. All primers were synthesized by Integrated DNA Technologies (IDT), Coralville, IA, USA. Tm (^{o}C), annealing temperature; *, primers provided in the FirstChoice® RLM-RACE Kit; E, protein expression primers.

make first strand cDNA which was employed for amplification of *hsf1* cDNA with specific primers that had a T7 promotor added to 5' ends (Table 1). Touchdown RCR was at 95°C for 5 min, 3 cycles of 95°C for 30 s, 49°C for 30 s and 72°C for 1 min, followed by 3 cycles with the annealing temperature starting at 50°C and successively increased 1°C after each cycle. Subsequently, 30 cycles at 95°C for 30 s, 60°C for 30 s and 72°C for 1 min, followed by 6 min at 72°C were performed. PCR products were resolved in 1.2% agarose gels in 1 x TBE buffer at 95 V, stained with 0.01% SYBR® Safe DNA Gel Stain (ThermoFisher Scientific) and visualized with a DNR Bio-Imaging Systems MF-ChemiBIS 3.2 gel documentation system. *Hsf1* dsRNA was synthesized using the PCR products as template with the MEGAscript® RNAi Kit (Ambion Applied Biosystems, Austin, TX, USA). GFP PCR templates were amplified from the vector pEGFP-N1 (Clonetech, Mountain View, CA, USA) using the above reaction conditions and *GFP* dsRNA was produced with the same procedure as for *hsf1* dsRNA (King and MacRae, 2013). dsRNAs were resolved in agarose gels and visualized as described above to ensure that a single dsRNA of the appropriate size was obtained for each sample.

2.3.2 Injection of *A. franciscana* females with dsRNA

The concentration of dsRNA was determined by measuring the A_{260} of each sample in a nanophotometer P360 (Implen). dsRNA was mixed with 0.5% phenol red in Dulbecco's phosphate buffered saline (DPBS) (Sigma-Aldrich) to achieve the final concentration of 0.32 µg/µl. Glass micropipettes (Sutter Instrument Co., Novato, CA, USA) were pulled with a P-97 Flaming/Brown Micropipette Puller (Sutter Instrument Co., Novato, CA, USA) using program 25 (Appendix B) to make glass needles for injection. The ends of needles were cut at a 45° angle using a razor blade under an

Olympus SZ61 stereomicroscope (Olympus, Markham, Ontario, Canada). Each female was injected with 250 nl of dsRNA solution with a Nanoject II microinjector (Drummond Scientific Co., Broomall, PA, USA) under an Olympus SZ61stereomicroscope (Olympus). Females destined to produce cysts were identified by the presence of a shell gland whereas those destined to produce nauplii lacked a shell gland (Liang and MacRae, 1999). Before injection, females were immobilized on 3% agarose precooled to 4℃ and seawater was removed with Kimwipes. Females were incubated in sea water for 1 day after injection and those losing phenol red after 2 h were discarded as were females exhibiting abnormal behaviour and morphology 24 h post-injection. Surviving females were incubated separately in 5.5 cm diameter Petri dishes with a single male for mating.

2.3.3 Cyst and nauplius release time and female viability

Harvested cysts and nauplii were either used immediately or placed in 1.5 ml microtubes, frozen in liquid nitrogen and stored at -80℃. Most females produced 2 broods of cysts but some yielded up to 5 broods before dying. The first broods of cysts were used in experiments. The time it takes from fertilization to the release of cysts or nauplii was recorded. The time from injection to the death of females was recorded.

2.4 Knockdown of *hsf1* and molecular chaperone mRNA

2.4.1 Knockdown on *hsf1* and molecular chaperone mRNA in *A. franciscana* cysts

RNA was extracted from 80 cysts by homogenization with a micropestle (Fisher

Scientific) in a 1.5 ml Eppendorf tube with 300 µl TRIzol® (Invitrogen) using the RiboPure™ RNA Purification Kit (Invitrogen). First strand cDNA was generated with the SuperScript® III First-Strand Synthesis Kit for RT-PCR (Thermofisher Scientific) using 0.1 µg of RNA as template and oligo$(dT)_{20}$ primers as described above. The first strand cDNA was then amplified using Hsf1 and α-tubulin forward and reverse primers from IDT (Table1). Amplification was for 5 min at 95°C, followed by 35 cycles of 95°C for 30 s, 55°C for 30 s, 72°C for 1 min and 6 min at 72°C. All RNA preparations were incubated without reverse transcriptase to ensure the absence of genomic DNA.

The RT-PCR products were resolved in 1.2% agarose gels in 1 x TBE buffer at 95 V and stained with 0.01% SYBR® Safe (Invitrogen) prior to visualization with a DNR Bio-Imaging Systems MF-ChemiBIS 3.2 gel documentation system (Montreal Biotech).

qRT-PCR was conducted with a QuantiTect® SYBR Green PCR Kit (Qiagen, Mississauga, ON, Canada) in a Rotor-Gene RG-3000 system (Corbett Research, Sydney, NSW, Australia) using 1 µl cDNA and primer pairs specific for HSF1, p26, ArHsp21, ArHsp22, artemin and tubulin at 10 µmol/L (Table 2). Copy numbers of *hsf1*, *p26*, *ArHsp21*, *ArHsp22* and artemin mRNAs were determined from a standard curve of Ct values and normalized against α-tubulin mRNA (King et al., 2013). Primer fidelity was assessed by melting curve analysis.

2.4.2 Knockdown on *hsf1* mRNA in *A. franciscana* nauplii

Nauplii released from females were collected in 1.5 ml Eppendorf tubes with each tube containing at least 80 nauplii and washed twice with distilled water. RNA was extracted from nauplii as described above. First strand cDNA was generated with the SuperScript® III First-Strand Synthesis Kit for qRT-PCR (Invitrogen) using 0.1 µg of RNA as template and oligo dT_{20} primers. The resulting cDNA was then used for RT-PCR with primers for Hsf1 and tubulin using the same procedure and annealing temperature as described for cysts. The PCR products were resolved in 1.2% agarose gels and visualized with a DNR Bio-Imaging Systems MF-ChemiBIS 3.2 gel documentation system (Montreal Biotech) as described above. cDNA was used for qRT-PCR with primers for Hsf1 and tubulin using the same procedure and annealing temperature as described for cysts.

2.5 Knockdown of Hsf1 and molecular chaperones

2.5.1 Hsf1 polyclonal antibody

An antibody was made to Hsf1 by Abbiotec (San diego, CA, USA) using peptide "525-TLNTPVHAPEAPLFSSRKKK-544" from the deduced amino acid sequence. Antibodies were tested using proteins extracted from *E. coli* transformed with the pRSET A expression plasmid (ThermoFisher Scientific) either with or without a partial *hsf1* cDNA. *hsf1* cDNA for transformation of *E. coli* was cloned from hydrated canned cysts as described above. PCR was performed using a forward primer containing a BamHI restriction site and a reverse primer with an EcoRI site (Table 1). Touchdown PCR was at 95°C for 5 min, 3 cycles of 95°C for 30 s, 49°C for

Table 2. Primers used for quantification of mRNAs by RT-PCR and qRT-PCR.

Protein Encoded by mRNA	Forward Primer (5'- 3')	Reverse Primer (5'- 3')	Tm (^{o}C)
HSF1	GTCCTCCTTGCT TTCGCTATTT	TGTCGGCTTCTT GGTCTGATTC	53
p26	GCACTTAACCCA TGGTACGG	CATCAGATCGCT CGTCATCT	53
ArHsp21	ATCGCTTTTGCT TCTCGG	TTCTGCTCGCAC TTTCCA	52
ArHsp22	GACCCCTTTGCT GACTTA	ATCTGGACGCTC TTTATG	49
Artemin	AGATGCCTTTTC CCATTGTG	CTTGTGAACCGA TGCAGTGT	52
Tubulin	CTGCATGCTGTA CAGAGGAGATGT	CTCCTTCAAGAG AGTCCATGCCAA	53
HSF(R)	TATGTATGGGTT TCGGAAGG	GACGCTTATCTA CTGAATCTTGTT	55
Tubulin(R)	ACCTATGCGCCT GTCATCTC	TGCCAACCTCCT CGTAATCT	58

PCR reaction conditions were described in Materials and Methods. All primers were synthesized by Integrated DNA Technologies (IDT), Coralville, IA, USA. Tm (^{o}C), annealing temperature. R, Primers used for RT-PCR only.

30 s and 72°C for 1 min, followed by 3 cycles with the annealing temperature starting at 50°C and successively increased 1°C after each cycle. Subsequently, 30 cycles at 95°C for 30 s, 60°C for 30 s and 72°C for 1 min, followed by 6 min at 72°C were performed. PCR products were resolved in 1.2% agarose gels in 1 x TBE buffer at 95 V, stained with 0.01% SYBR® Safe DNA Gel Stain (Invitrogen) and visualized with a DNR Bio-Imaging Systems MF-ChemiBIS 3.2 gel documentation system.

PCR products were purified with QIAquick PCR purification kit (Qiagen) and the plasmid pRSET A were then digested separately at 37℃ with BamHI and EcoRI for 20 h. The digested cDNA and plasmid pRSET A were purified with QIAquick PCR purification kit (Qiagen) and quantified with a nanophotometer P360 (IMPLEN) prior to mixing in a 3 to 1 ratio and ligating. Ligations were performed at 22℃ with T4 ligation enzyme (ThermoFisher Scientific) for 1.5 h.

pRSET A plasmids with and without *hsf1* DNA fragments were transformed into TOP10 F' competent *E. coli*. Colonies with plasmids containing target DNA were white when grown on LB (Appendix C) agar covered by X-gal and these colonies were picked and grown in 5 ml LB broth with 50 μg/ml ampicilin and 1 mM isopropyl β-D-1-thiogalactopyranoside (IPTG) at 27 ℃ overnight. Cells were collected by centrifugation, resuspended in 200μl PIPES buffer (100 mM Pipes, 1 mM $MgCl_2$, 1 mM EGTA, pH 6.5) with 1% Halt™ protease inhibitor cocktail (ThermoFisher Scientific) and homogenized with a Branson sonifier 150 (Emerson Electric, St. Louis, Missouri, USA). Cell homogenates were mixed with 2 x treatment buffer (125 mM Tris, 140 mM SDS, 20% (v/v) glycerol, 10% (v/v) β-mercaptoethanol,

0.1% (w/v) bromophenol blue, pH6.8) at a 1: 1 ratio, placed in a boiling water bath for 5 min and then centrifuged at 10000 x g for 1 min at 23^{o}C. Protein samples were resolved in 12.5% SDS polyacrylamide gels and either stained with Coomassie blue or blotted at 100 mA overnight at room temperature in transfer buffer (25 mM Tris, 200 mM glycine in 20% (v/v) methanol) to nitrocellulose membranes (Bio-Rad, Mississauga, ON, Canada). The BLUelf pre-stained protein ladder (FroggaBio) was used as marker.

To detect antibody-reactive proteins, nitrocellulose membranes were incubated at room temperature in TBS (10 mM Tris, 140 mM NaCl, pH7.4) containing 5% low fat milk for 1 h and then exposed to Hsf1 antibody in TBS. The membranes were washed for 1, 2, 3 and 4 min with TBST (TBS containing 0.1% Tween20) followed by 1, 2, 3 and 4 min in HST (10 mM Tris, 1 M NaCl, 0.5% (v/v) Tween-20, pH 7.4). After washing, membranes were incubated for 20 min in HRP-conjugated goat anti-rabbit IgG antibody (Sigma-Aldrich) in TBS. The membranes were washed as described above and immunoreactive proteins were visualized with the Pierce^{TM} ECL western blotting substrate (ThermoFisher Scientific) in a DNR Bio-Imaging Systems MF –ChemiBIS 3.2 gel documentation system.

Protein extracts were prepared from hydrated commercially obtained cysts and instar 1 nauplii in PIPES buffer with 1% Halt^{TM} protease inhibitor cocktail (ThermoFisher Scientific), centrifuged at 2000 x g and mixed with 2 x treatment buffer at a 1: 1 ratio prior to placing in a boiling water bath for 5 min and centrifuging at 10000 x g for 1 min at 23^{o}C. Protein samples were resolved in 12.5% SDS

polyacrylamide gels and blotted to nitrocellulose membranes (Bio-Rad) as described above. The blot was stained with 2% ponceau S solution (0.1% (w/v) ponceau S, 5% (v/v) acetic acid) to confirm the existence of protein and then washed with TBS for 3 min before blocking in TBS containing 5% low fat milk. As a control for specificity, Hsf1 antibody was also mixed with peptide antigen (Abbiotec) and then used for probing of blots.

2.5.2 Determination of cyst viability and protein concentration

The metabolic activity of cysts was tested after their release from females injected with either *GFP* or *hsf1* dsRNA to determine if they were viable (King and MacRae, 2012). Briefly, 10 cysts from females receiving either *hsf1* or *GFP* dsRNA were collected and incubated immediately after release in Costar 90 well UV plates (Corning Inc., Corning, NY, USA) with 100 µl of test solution containing 1000 U penicillin, 100 µg/ml streptomycin sulfate and 0.03% (w/v) phenol red at pH 8.5. Control wells contained either test solution only or test solution with 10 cysts heated in a boiling water bath for 10 min. The absorbance of test solution at 553 nm (A_{553}) was determined with a SPECTRAmax PLUS microplate reader (Molecular Devices, Sunnyvale, CA, USA) at 24 h intervals after adding cysts to wells. Test solution excluding cysts was transferred to fresh wells for measurement. After absorbance measurement, residue test solution was removed with autoclaved Q-tips from the wells containing cysts and 100 µl fresh test solution was added for the next 24 h incubation (King and MacRae, 2012).

Protein in extracts from 50 cysts released from females injected with either *GFP* or *hsf1* dsRNA was quantified by the Bradford assay using the Pierce™ Coomassie Protein Assay Kit (ThermoFisher Scientific). Absorbance of samples was measured at A595 nm with a SPECTRAmax PLUS384 microplate reader (Molecular Device, Sunnyvale, CA, USA).

2.5.3 Knockdown of Hsf1 and the loss of chaperone proteins in *A. franciscana* cysts

Fifty cysts released from females injected with either *hsf1* or *GFP* dsRNA were collected by centrifugation for 1 min at 10000 x g, washed twice with distilled water, homogenized in 2 x treatment buffer, placed in a boiling water bath for 5 min and then centrifuged at 10000 x g for 1 min at 23°C. Protein samples were resolved in 12.5% SDS polyacrylamide gels and either stained with Coomassie blue or blotted at 100 Ma overnight at room temperature in transfer buffer to nitrocellulose membranes (Bio-Rad). The BLUelf pre-stained protein ladder (FroggaBio) was used as marker. The membranes were then washed, exposed separately in TBS to polyclonal antibodies raised in rabbits against Hsf1, p26 (Liang and MacRae, 1999), ArHsp21 (Qiu and MacRae, 2008a), ArHsp22 (Qiu and MacRae, 2008b), artemin (Chen et al., 2007) and tyrosinated α-tubulin (Xiang and MacRae, 1995). Immunoreactive proteins were visualized as described above. Experiments were done in triplicate. The immunoreactive bands on the blots were quantified with Image Studio Software (LI-COR Technology, Lincoln, NE, USA) and the ratio of Hsf1 to tyrosinated α-tubulin was determined.

2.5.4 Knockdown of Hsf1 in *A. franciscana* nauplii

Eighty nauplii released from females injected with either *GFP* or *hsf1* dsRNA were collected in 1.5 ml Eppendorf tubes, sea water was removed and nauplii were washed twice with distilled water. Nauplii were homogenized in 2 x treatment buffer, placed in a boiling water bath for 5 min and then centrifuged at 10000 x g for 1 min at 23^{o}C. Protein samples were resolved in 12.5% SDS polyacrylamide gels and either stained with Coomassie blue or blotted at 100 Ma overnight at room temperature in transfer buffer to nitrocellulose membranes (Bio-Rad). The BLUelf pre-stained protein ladder (FroggaBio) was used as marker.

The membranes were then washed, probed with polyclonal antibodies raised in rabbits against Hsf1 and tyrosinated α-tubulin and visualized as described above. The experiment was done in triplicate. The immunoreactive proteins on the blots were quantified with Image Studio Software (LI-COR technology) as described above.

2.6 Stress tolerance of cysts from *A. franciscana* females injected with dsRNA

Cysts released from *A. franciscana* females injected with either *hsf1* or *GFP* dsRNA were collected separately and incubated in sea water for 5 to 6 days to allow entry into diapause. To terminate diapause and concurrently test stress tolerance, the cysts were dried in a desiccator over DryRite (DryRite, Nashville, TN, USA) for 4 weeks and stored at -80°C for 3 months (King and MacRae, 2012). The viability of stressed cysts was determined by incubation in seawater at room temperature to allow hatching after which swimming nauplii were counted and removed. Experiments were

terminated 5 days after the last nauplius hatched. Eighty to 100 cysts were used for each experiment. The experiment was performed 3 times and chi-square independence of factors tests was performed to evaluate the difference in hatching between cysts from females injected with either *GFP* or *hsf1* dsRNA.

2.7 Viability of nauplii from *A. franciscana* females injected with dsRNA.

Nauplii released from females injected with either *hsf1* or *GFP* dsRNA were harvested and incubated in separate Petri dishes containing seawater at room temperature. The number of surviving nauplii was determined each day for 5 days after release from females, with non-motile nauplii considered to be dead and removed from Petri dishes. Data were collected from nauplii released from 4 females injected with *GFP* dsRNA and 4 females injected with *hsf1* dsRNA. A two-tailed student's t-test ($\alpha = 0.05$) was performed to evaluate the differences in viability.

2.8 Quantification of *hsf1* mRNA and Hsf1 during embryo development of *A. franciscana*

Oocysts were collected from *A. franciscana* females prior to fertilization and developing embryos were collected at 2 and 4 days after fertilization. Cysts and nauplii were also harvested immediately after release from females. For collection of oocytes and embryos, females were immobilized on a cold slide under an SZ61 stereomicroscope (Olympus). Egg sacs were then excised and harvested embryos were put in 2 ml tubes before freezing in liquid nitrogen. RNA and protein were prepared from each sample as described above for knockdown cysts and nauplii.

qRT-PCR was performed and data were analyzed as described above. Protein samples were resolved in SDS polyacrylamide gels, transferred to nitrocellulose membranes (Bio-Rad) and probed with antibody to Hsf1 and tyrosinated α-tubulin followed by HRP-conjugated anti-rabbit IgG antibody as described above. Immunoreactive protein bands were quantified with Image Studio Software (LI-COR Technology). Protein band luminance in boxes of the same size was measured using the non-luminescent membrane around box as blank.

2.9 Localization of Hsf1 in developing *A. franciscana* embryos

Immunofluorescent staining was employed to detect Hsf1 in *A. franciscana* essentially as described by Liang et al. (1997). Oocytes destined to become cysts and nauplii, ovoviviparously and oviparously developing embryos at 2 and 4 days post fertilization and freshly released cysts and nauplii, were collected, gently crushed and fixed immediately with methanol for 5-10 min at -20℃, and spread on poly-L-lysine coated slides (Sigma-Aldrich). Slides were washed in ice-cold PBS (137 mM NaCl, 2.7 mM KCl, 10 mM Na_2HPO_4, 1.8 mM KH_2PO_4, pH7.4) 3 times for 10 min and incubated in 2 changes of PBSAT (0.5% (w/v) BSA, 0.75% (w/v) Triton X-100 in PBS) for 2 - 3 h. The samples were then incubated at room temperature for 1 h in antibody to Hsf1 diluted 1:200 in PBSAT, followed by overnight 4℃. After 3 washes in PBSAT, samples were then incubated at room temperature for 2 h in FITC-conjugated goat anti-rabbit IgG antibody (Abcam Inc, Toronto, ON, Canada) diluted 1:200 in PBSAT. After washing in PBS 3 times for 10 min followed by a 5

min wash in distilled water, samples were incubated in 0.5% (w/v) DAPI (ThermalFisher Scientific) for 2 min. Samples were rinsed in distilled water, mounted in a drop of Vectashield (Vector Laboratories, Burlingame, CA), covered with a coverslip and sealed with nail polish. The slides were examined with a Zeiss laser scanning confocal microscope LSM 710 (Olympus Canada Inc, Toronto, ON, Canada). As a control for specificity, Hsf1 antibody mixed with peptide antigen (Abbiotec) and PBSAT without Hsf1 antibody were used for probing slides with oviparously developing embryos at 2 days post-fertilization.

2.10 Statistics

A one-tailed student's t-test ($\alpha = 0.05$) was used to assess the difference between means for mRNA and protein prepared from HSF1 and GFP knockdown cysts and nauplii. The difference between knockdown and control means for viability of females and release time for cysts and nauplii was assessed using a two-tailed student's t-test ($\alpha = 0.05$). The viability of cysts after diapause termination was compared using chi-square independence of factors tests as was the viability of nauplii after release from females. One-way ANOVA Dunnett t tests were performed for mRNA and protein at different stages of embryo development. Analysis were carried out using Microsoft Excel 2013. All data were plotted as mean +/- SD unless otherwise stated.

Chapter 3 Results

3.1 *A. franciscana hsf1* cDNA and sequence analysis

A full length *hsf1* cDNA of 1818 nucleotides was obtained from adult males of *A. franciscana* (Fig.5A) and an identical cDNA was cloned from *A. franciscana* cysts with different primers ensuring that no artifacts were introduced by PCR. The *A. franciscana hsf1* cDNA contained a 5'-untranslated region (UTR) of 78 nucleotides and a 3'-UTR of 115 nucleotides with a poly(A) tail preceded by a typical polyadenylation signal and a 3'-UTR instability motif. The ORF of 1632 base pairs (bps) encoded a polypeptide of 544 amino acid residues. The polypeptide had a predicted molecular mass of 65.3 kDa and a theoretical pI of 4.74. The *hsf1* cDNA sequence of *A. franciscana* was deposited in GenBank with the accession number KY985304.

The deduced amino acid sequence of *A. franciscana* Hsf1 contained a conserved DNA binding domain (DBD) and the heptad repeat HR-A & HR-B and HR-C domains (Fig. 5A, B). The DBD is underlined by blue (N15-K115). The HR-A & HR-B domains are underlined by orange (F129-Q198). The HR-C domain is from the 410th amino acid residue to the 428th amino acid residue as underlined by red (D410-L428). There are also two non-conserved domains in *A. franciscana* Hsf1, the regulatory domain (RD) underlined by yellow (E214-N409) and the trans-activation domain (TAD) underlined by green (P429-K544) (Fig. 5A).

Fig. 5. Hsf1 sequence and domain structure. A. *hsf1* cDNA and deduced amino acid sequence. DNA binding domain, blue underline; oligomerization domain, orange underline; regulatory domain, yellow underline; heptad repeat (HR-C) domain, red underline; transactivation domain, green underline. 3'-UTR instability motif, purple box. B. Schematic representation of Hsf1 domains in order from the amino to carboxyl terminal are DNA binding, DBD; oligomerization, HR-A & HR-B; regulatory (RD); heptad repeat, HR-C; trans-activation (TAD). The peptide 525-TLNTPVHAPEAPLFSSRKKK-544 was used as antigen to make an antibody to *A. franciscana* Hsf1 (shaded grey). *, stop codon. Nucleotide and amino acid residue positions are indicated on the left side of the figure. B. Schematic representation of the domain structure of Hsf1 from *A. franciscana.*

A

```
   1 aaaagattacgcgattttcatataattagcctattgcgtgatttattgcgttaattgattaaaaagacATGCATGCAGTTGGTGAAGAAA
   1                                                                   M  H  A  V  G  E  E  N
  91 ATGGAAGTCCTACCTTTTCAAATGTGCCTGCATTCCTGGCAAAGCTTTGGAAGCTTGTTGAAGACCTGGAAGCAGATGACCTGATATGCT
   9  G  S  P  T  F  S  N  V  P  A  F  L  A  K  L  W  K  L  V  E  D  L  E  A  D  D  L  I  C  W
 181 GGAGTGATAGTGGCGCAAGTTTCTACATAAGAAATCAAGCCTTGTTTGCCAGACAACTGTTGCCCCTCTATTACAAGCATAATAATATGG
  39  S  D  S  G  A  S  F  Y  I  R  N  Q  A  L  F  A  R  Q  L  L  P  L  Y  Y  K  H  N  N  M  A
 271 CTAGCTTCATCAGACAGCTTAATATGTATGGGTTTCGGAAGGTATCATCGGTTGAGCAAGGAAGCCTTCGTGTGGACAAGGATGAGATGG
  69  S  F  I  R  Q  L  N  M  Y  G  F  R  K  V  S  S  V  E  Q  G  S  L  R  V  D  K  D  E  M  E
 361 AATTTCAACATAATTATTTCCTAAGAGGTCGCGAGTATCTTCTAGAAAATATTAAACGAAAGCTGCCATCTGGTACAAGACAATCGGAGG
  99  F  Q  H  N  Y  F  L  R  G  R  E  Y  L  L  E  N  I  K  R  K  L  P  S  G  T  R  Q  S  E  D
 451 ATTTCGATAAAGTTCGTCCAGATTTTGCACAAAAGGTGTTAACGGATGTAAGAATTTTAAAGGGGAAACAAGATTCAGTAGATAAGCGTC
 129  F  D  K  V  R  P  D  F  A  Q  K  V  L  T  D  V  R  I  L  K  G  K  Q  D  S  V  D  K  R  L
 541 TAGCTGGCATGAAAAGAGAAAATGAAGTTCTCTGGAGAGAAGTGGCATCTCTTAGGCAGAAACATTTCAAGCAGCAGCAAATTGTAAACA
 159  A  G  M  K  R  E  N  E  V  L  W  R  E  V  A  S  L  R  Q  K  H  F  K  Q  Q  Q  I  V  N  K
 631 AGTTGATACAATTTCTCGTTACCCTGGTCCAAAGGAAGGACATATCAACAAAAAGAAGGTATCCACTTGCTATACAGGAATCGGAGAAAG
 189  L  I  Q  F  L  V  T  L  V  Q  R  K  D  I  S  T  K  R  R  Y  P  L  A  I  Q  E  S  E  K  D
 721 ATGATCTCTTTTCTCCATCTGGAAGTAAGCAAAGGCGGAAATTCAACGACAAAGGACCCATAATACACGATTTGACGAATGATATGATAC
 219  D  L  F  S  P  S  G  S  K  Q  R  R  K  F  N  D  K  G  P  I  I  H  D  L  T  N  D  M  I  Q
 811 AAGAAGCGTCTAAGCTGTCTAGCGCTGAATCTCTTGAGAATCCTGCACAAATACCTATTAGAATTGAATCTGATGATCAAGATGAAGTCA
 249  E  A  S  K  L  S  S  A  E  S  L  E  N  P  A  Q  I  P  I  R  I  E  S  D  D  Q  D  E  V  T
 901 CTCTTGAGCCGTATTGTGTAGTTGAGCCTGTATTGACGGATGAACAAGAGAACTCGGCTGCTGCAAATGGAGATTATGCTATTACCATTG
 279  L  E  P  Y  C  V  V  E  P  V  L  T  D  E  Q  E  N  S  A  A  A  N  G  D  Y  A  I  T  I  G
 991 GCTATCAAATTGGTGATGACCCTGTAGAAATAATAAGCGAAAGACCAGTATCAGCCCATTCATCGGCAGAGAGTAACCCCAGAAGCCCCT
 309  Y  Q  I  G  D  D  P  V  E  I  I  S  E  R  P  V  S  A  H  S  S  A  E  S  N  P  R  S  P  S
1081 CTGTGGAGCTGATGACGGTAAATCCAAAGACATTGACAAAACCAACTGATGTCGTGAATGACGAAGAAAGTGGGGCATTCATTGATGAGT
 339  V  E  L  M  T  V  N  P  K  T  L  T  K  P  T  D  V  V  N  D  E  E  S  G  A  F  I  D  E  S
1171 CACTCATAATACCTACTTTAGAAGAGCCGGTATCACTTCTTCAAGGCAAATTTTCAGGAAAACATCAAAAGATTGACGACAAAACGGTTG
 369  L  I  I  P  T  L  E  E  P  V  S  L  L  Q  G  K  F  S  G  K  H  Q  K  I  D  D  K  T  V  A
1261 CTATTGCCTCGGACTCACTGCCTATGAACAGGAATGATTTGGACAATCATTTAGAAAACTTCGATGTTGAATTGGAAGGTCTGAAGGATT
 399  I  A  S  D  S  L  P  M  N  R  N  D  L  D  N  H  L  E  N  F  D  V  E  L  E  G  L  K  D  L
1351 TGATGACATTGCAAAATGGAGGAACTTTCGATGTGTCCTCCTTGCTTTCGCTATTTGACACTGATGATTCATTGCATTCAGCTTTGCCGA
 429  M  T  L  Q  N  G  G  T  F  D  V  S  S  L  L  S  L  F  D  T  D  D  S  L  H  S  A  L  P  M
1441 TGCCAATGCCATCTGCAAGTCAATCAAGTAACTCGAAAACCGGCAATGAAGTAATAACTTACAACCCTGTCTTGGACCTTGGATACGACG
 459  P  M  P  S  A  S  Q  S  S  N  S  K  T  G  N  E  V  I  T  Y  N  P  V  L  D  L  G  Y  D  D
1531 ATCACAGCTTTTTCAGATYTGAATCAGACCAAGAAGCCGACAGCAGTTTTCTACTCGAAAGTGATTACCTAATTGACGTTAACTCCCCGG
 489  H  S  F  F  R  S  E  S  D  Q  E  A  D  S  S  F  L  L  E  S  D  Y  L  I  D  V  N  S  P  E
1621 AGGATCAGTTAATAAATTCGACTCTAAATACCCCTGTACATGCACCTGAGGCTCCTCTGTTTTCGTCGCGGAAAAAGAAGTAAtctgtgc
 519  D  Q  L  I  N  S  T  L  N  T  P  V  H  A  P  E  A  P  L  F  S  S  R  K  K  K  *
1711 ctatttgctgtattgaggggcattctagtctggtacagaagggttgccacccatattgatttatcactattttagtgaatttttatgcct
1801 aaacgaaaaaaaaaaaaa
```

B

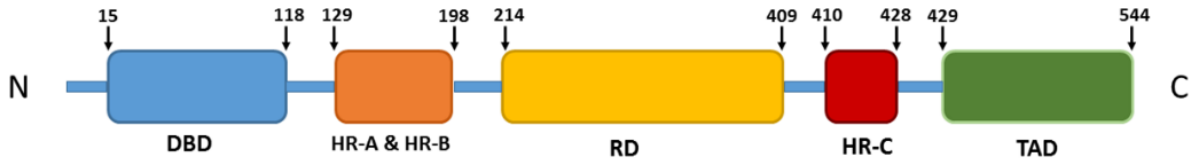

As predicted by using the Strap tool box and blast software, the Hsf1 DBD has a typical helix-turn-helix structure whereas α-helices of the HR-A & HR-B domains consist of a repeating pattern of seven amino acids with hydrophobic amino acids such as leucine (L), isoleucine (I), and valine (V) at the first and fourth positions (Fig. 6). HR-C has a similar structure (Fig. 6). Hsf1 amino acid sequences from 5 arthropods, 4 vertebrates, 2 molluscs and 1 nematode were aligned with *A. franciscana* Hsf1. The DBD and HR-A & HR-B domains were similar in sequence but similarity in the carboxyl regions of the Hsf1s examined was less evident (Fig. 7). The identity between *A. franciscana* Hsf1 and Hsf1 from each of the species considered were calculated (Table 3). *A. franciscana* Hsf1 has the largest identity with Hsf1 from *Xenopus laevis*, and the least to Hsf1 from *Caenhorhabditis elegans*.

3.2 Knockdown of *hsf1* mRNA and Hsf1

3.2.1 Preparation of dsRNA and injection of *A. franciscana*

GFP and *hsf1* cDNA used as templates for production of dsRNA and dsRNA prepared for injection into females migrated in agarose gels at the expected sizes (Fig. 8A). dsRNAs generated from *GFP* and *hsf1* cDNA were respectively 309 bp and 335 bp in length. *GFP* dsRNA is not complementary to *hsf1* mRNAs, nor to any other *A. franciscana* mRNAs (Zhao et al., 2012).

Fig. 6. Secondary structure of *A. franciscana* Hsf1. The putative secondary structure of Hsf1 with the main domains. DNA binding domain, blue underline; oligomerization domain; orange underline; heptad repeat (HR-C) domain, red underline. α-helix, pink; β-sheet, yellow.

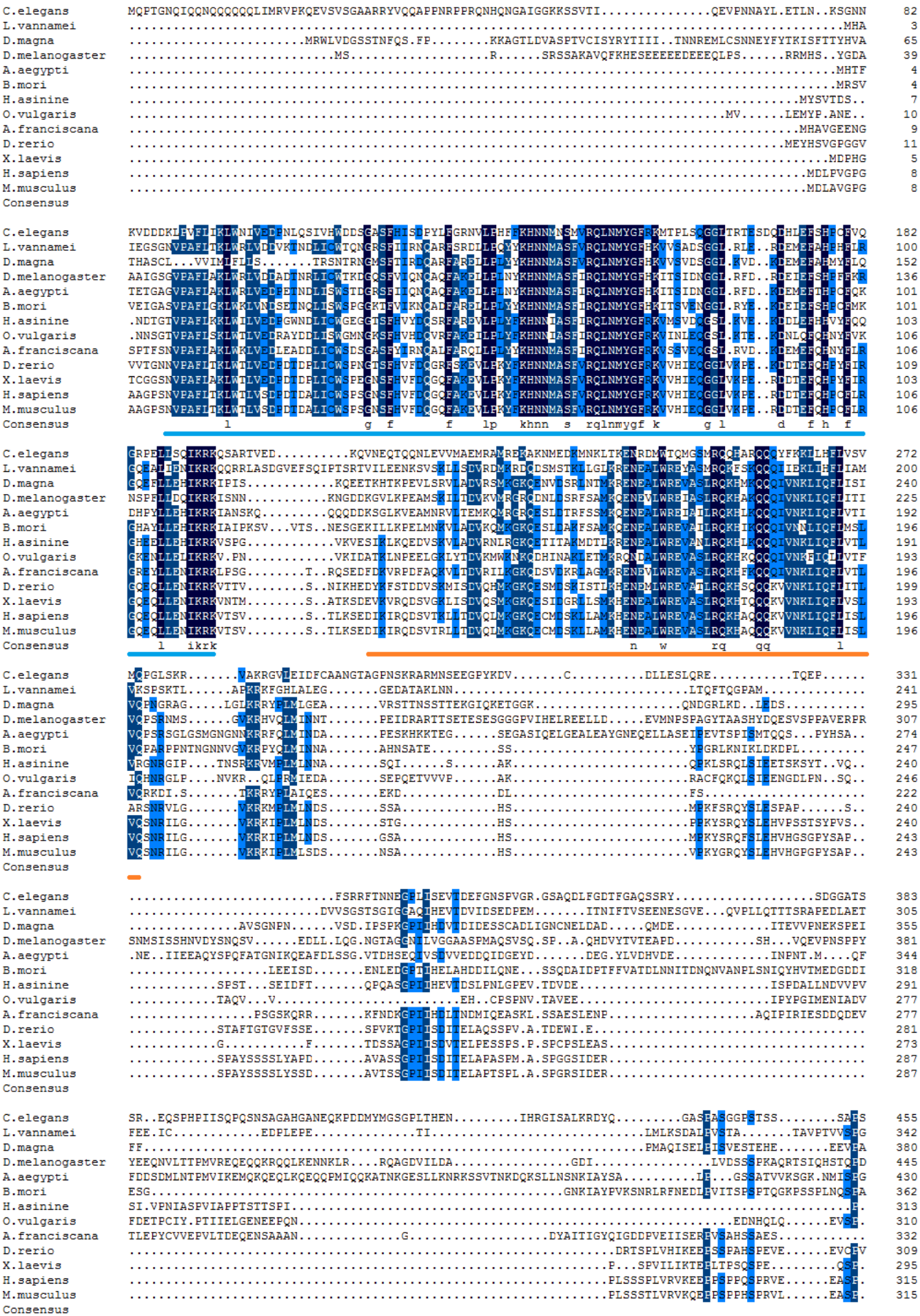
C.elegans
L.vannamei
D.magna
D.melanogaster
A.aegypti
B.mori
H.asinine
O.vulgaris
A.franciscana
D.rerio
X.laevis
H.sapiens
M.musculus
Consensus

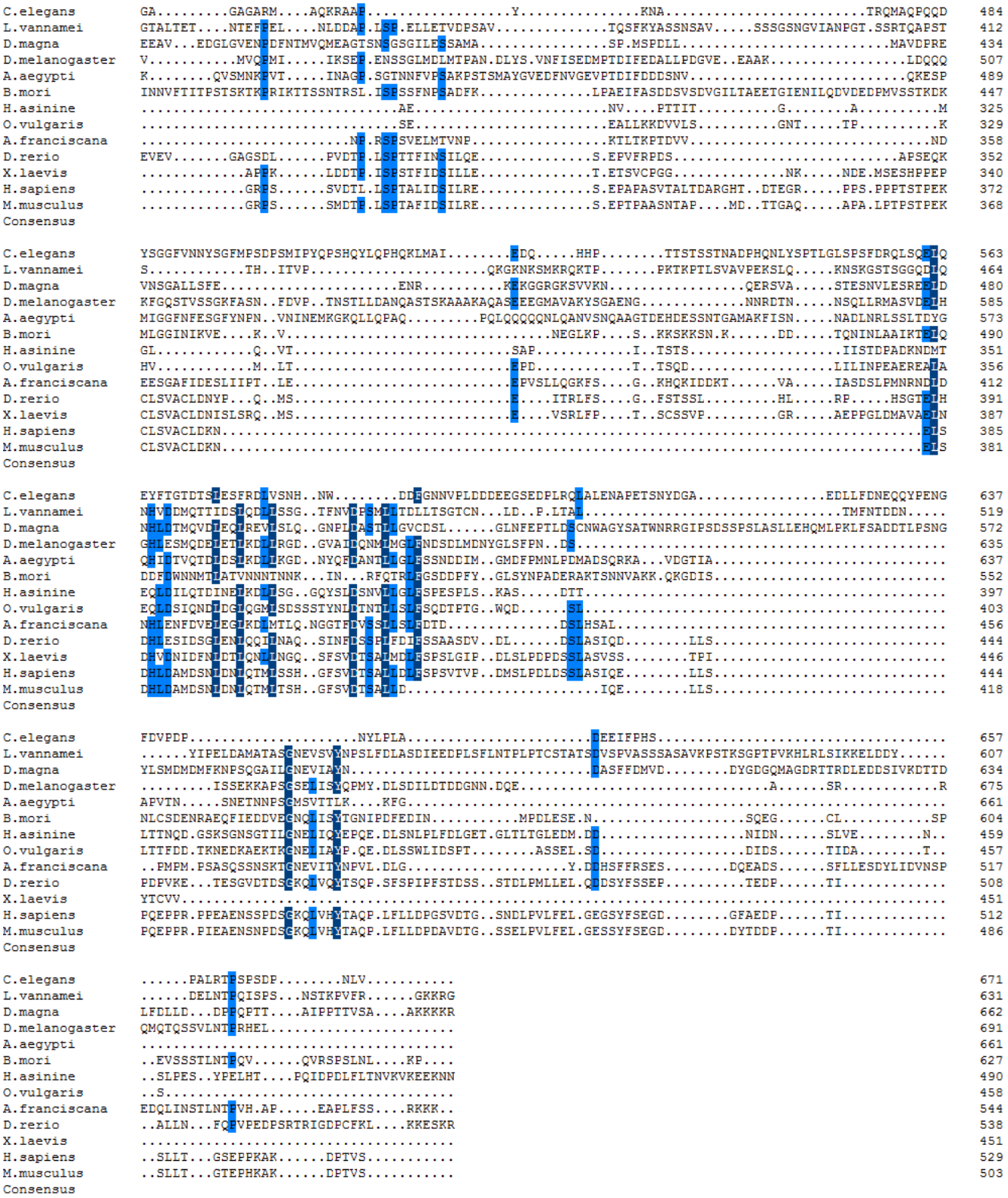

Fig. 7. Multiple sequence alignment of Hsf1s. The amino acid sequence of Hsf1 from *A. franciscana* was aligned with Hsf1s from the species listed in Table 3. Identical amino acid residues are indicated by black, 75% identity in a row of amino acid residues by dark blue and 50% identity in a row of amino acid residues by light blue. The *A. franciscana* DBD is marked with blue underline and HR-A & HR-B with orange underline.

Table 3. Hsf1 from *A. franciscana* shares sequence identity with Hsf1 from other organisms.

Organism	Phylum	Class	Species	%Identity	Accession #
Caenhorhabditis elegans	Nematoda	Chromadorea	Roundworm	22.97	NP_493031.1
Litopenaeus vannamei	Arthropoda	Molacostraca	Shrimp	32.35	AHI13794.1
Daphnia magna	Arthropoda	Branchiopoda	Wafer flea	35.11	JAM73014.1
Drosophila melanogaster	Arthropoda	Insecta	Fruit fly	31.25	NP_476575.1
Adedes aegypti	Arthropoda	Insecta	Mosquito	30.33	JAN95553.1
Bombyx mori	Arthropoda	Insecta	Silkworm	30.88	BAK26396.1
Haliotis asinina	Mollusca	Gastropoda	Abalone	34.28	ABR15461.1
Octopus vulgaris	Mollusca	Cephalopoda	Octopus	34.06	AGZ63438.1
Danio rerio	Chordata	Actinopterygii	Zebrafish	32.89	NP_571675.1
Xenopus laevis	Chordata	Amphibia	Toad	37.91	NP_00108403
Homo sapiens	Chordata	Mammalia	Human	31.94	NP_005517.1
Mus musculus	Chordata	Mammalia	Mouse	33.2	NP_032322.1

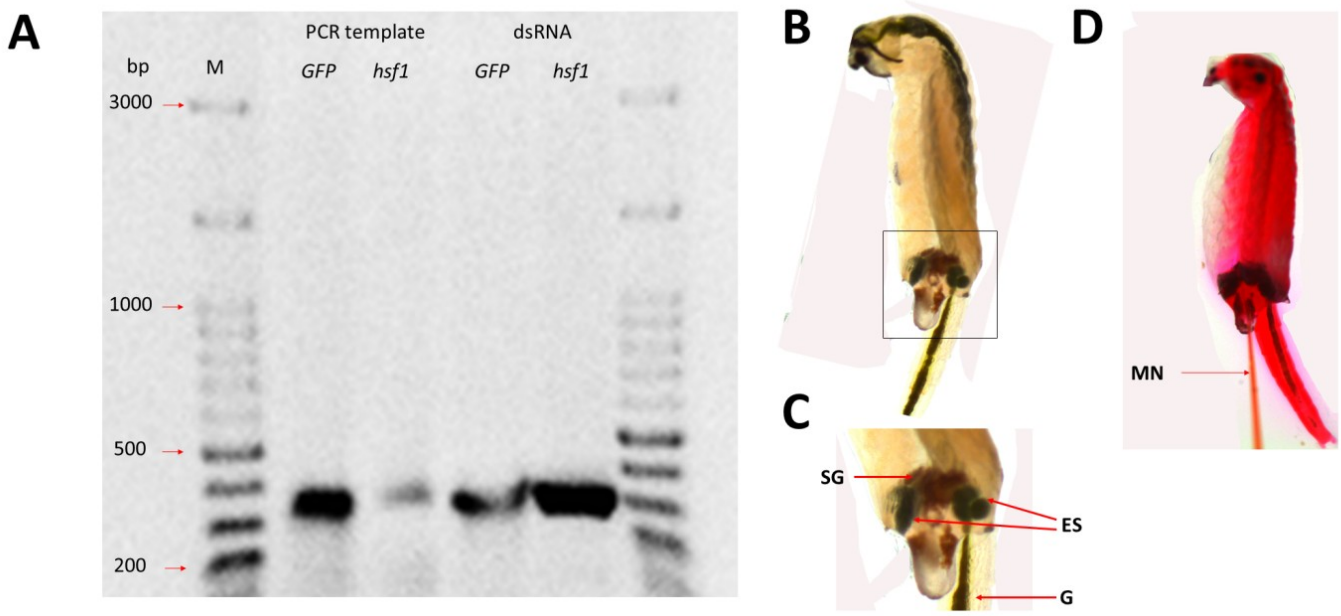

Fig. 8. Synthesis of dsRNA and injection of *A. franciscana*. A. *GFP* and *hsf1* cDNA, dsRNAs, and Frogga Bio 1kb DNA Ladder (Frogga Bio) were resolved in agarose gels. The first and sixth lanes are the DNA Ladder. The second and third lanes are the cDNAs used respectively as templates for production of *GFP* and *hsf1* dsRNAs. The fourth and fifth lanes are respectively *GFP* and *hsf1* dsRNAs. M, size marker; bp, base pairs. B. Unfertilized female *A. franciscana* with the shell gland and egg sacs boxed. C. An enlarged version of the box in B. D. female after injection. B, C and D are the same animal. SG, shell gland. ES, egg sac. G, gut. MN, microneedle.

Females were unfertilized if they possessed separated egg sacs (Fig. 8B, C). Injection of egg sacs with dsRNA containing phenol red stained the entire female, demonstrating that the dsRNA migrated throughout the animal (Fig. 8D). Females injected with dsRNA retained phenol red and were pink 2 h after injection but the color disappeared by the next day.

3.2.2 Knockdown of *hsf1* mRNA

cDNA amplified by RT-PCR with either tubulin or Hsf1 primers (Table 2) from both *GFP* and *hsf1* mRNA knockdown cysts yielded a single band of varying intensity after agarose gel electrophoresis, with more mRNA in cysts arising from females injected with *GFP* dsRNA (Fig. 9A). The amount of tubulin mRNA in cysts from females injected with *hsf1* dsRNA versus *GFP* dsRNA was similar. qRT-PCR results presented as the ratio of *hsf1* versus tubulin mRNA revealed that *hsf1* mRNA was reduced by 64.3% in cysts released by females receiving *hsf1* dsRNA versus *GFP* dsRNA (Fig. 9B)

3.2.3 Antibody specificity

To test specificity, equivalent amounts of protein from *E. coli* transformed with expression plasmids either containing or not containing *hsf1* cDNA were resolved in SDS polyacrylamide gels, transferred to nitrocellulose and probed with antibody raised to an Hsf1 peptide. The antibody recognized a protein in the extract from

Fig. 9. Knockdown of *hsf1* mRNA in *A. franciscana* cysts. A. RNA was prepared from cysts released by females receiving either *hsf1* (F) or *GFP* (G) dsRNA. cDNA was amplified by RT-PCR using either Hsf1 or α-tubulin primers and resolved in agarose gels. M, DNA size marker. B. The amount of *hsf1* mRNA in *A. franciscana* cysts released from females receiving *GFP* (1) and *hsf1* (2) dsRNA was determined by qPCR using tyrosinated α-tubulin as internal standard. The experiment was done 3 times using samples from 3 different females and error bars show standard deviation. The asterisk indicates that the amount of *hsf1* mRNA in cysts from females receiving *hsf1* dsRNA was statistically different ($p < 0.05$) from the amount of *hsf1* mRNA in cysts from females receiving *GFP* dsRNA.

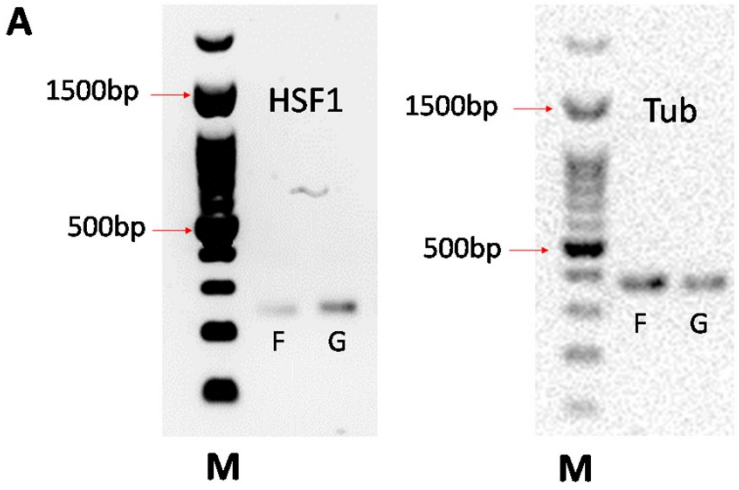
A
1500bp
500bp
HSF1
F
G
M
1500bp
500bp
Tub
F
G
M

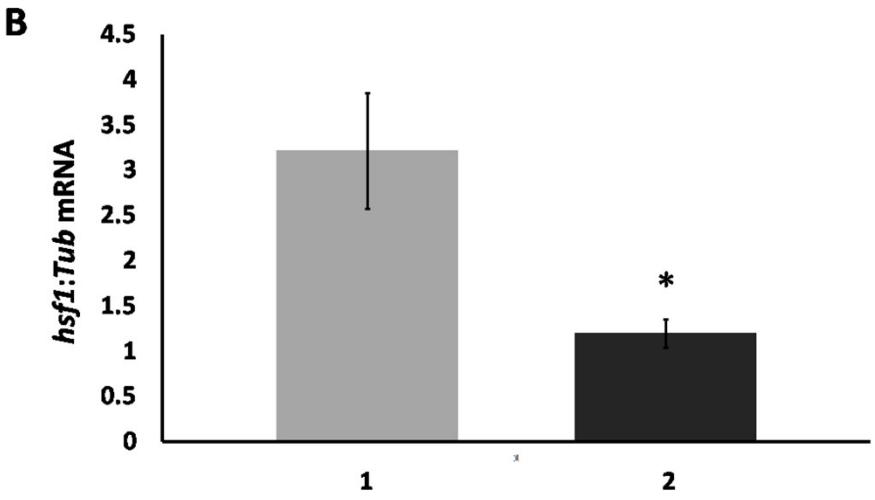
B
hsf1:Tub mRNA
4.5
4
3.5
3
2.5
2
1.5
1
0.5
0
*
1
2

E. coli transformed with the plasmid containing *hsf1* cDNA but not in the extract with the empty plasmid (Fig. 10A).

Protein extracts prepared from hydrated cysts and instar 1 nauplii were resolved in SDS polyacrylamide gels, transferred to nitrocellulose membrane and stained with 2% ponceau S (Fig. 10B). Probing of blots with antibody to Hsf1 yielded a strong immune-reactive band in extracts from cysts and nauplii and this band disappeared when the antibody was mixed before application to the blot with the peptide against which the antibody to Hsf1 was raised (Fig. 10C).

3.2.4 Knockdown of Hsf1 in *A. franciscana* cysts

As revealed by immunoprobing of western blots, cysts released from females injected with *hsf1* dsRNA but not *GFP* dsRNA underwent a decrease of 75.6% in Hsf1 while tubulin was unaffected (Fig. 11A, B).

3.3 Hsf1 knockdown reduced the stress tolerance of diapausing cysts

Cysts released from females injected with either *hsf1* or *GFP* dsRNA were desiccated and frozen to terminate diapause after which they were incubated in sea water at room temperature for hatching, the indicator of post-stress viability used in this study. Approximately 60% of cysts from females injected with *GFP* dsRNA and thus containing Hsf1 hatched upon incubation in sea water, as compared to 6% of cysts from females injected with *hsf1* dsRNA (Fig. 12A).

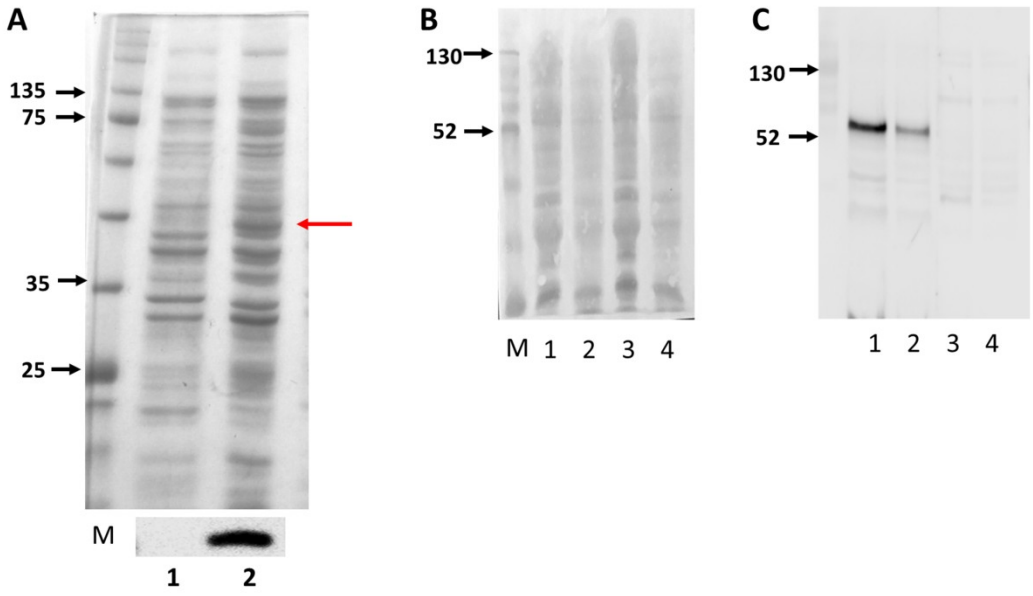

Fig. 10. Antibody specificity. A. Protein extracts from *E. coli* transformed with expression plasmids either lacking (lane 1) or containing (lane 2) *hsf1* cDNA were resolved in SDS polyacrylamide gels and stained with Coomassie blue (upper) or blotted to nitrocellulose yielding 1 protein that reacted with antibody to Hsf1 (lower). Red arrow indicates the putative band of Hsf1. B. Fifteen µl of protein extracts from hydrated cysts (lanes 1, 3) and instar 1 nauplii (lanes 2, 4) containing 23 µg of protein were resolved in SDS polyacrylamide gel, transferred to nitrocellulose and stained with ponceau S. C. Nitrocellulose membrane from B probed with antibody to Hsf1 before (lanes 1, 2) and after (lanes 3, 4) mixing with the peptide antigen against which the antibody to Hsf1 was raised. M, size marker.

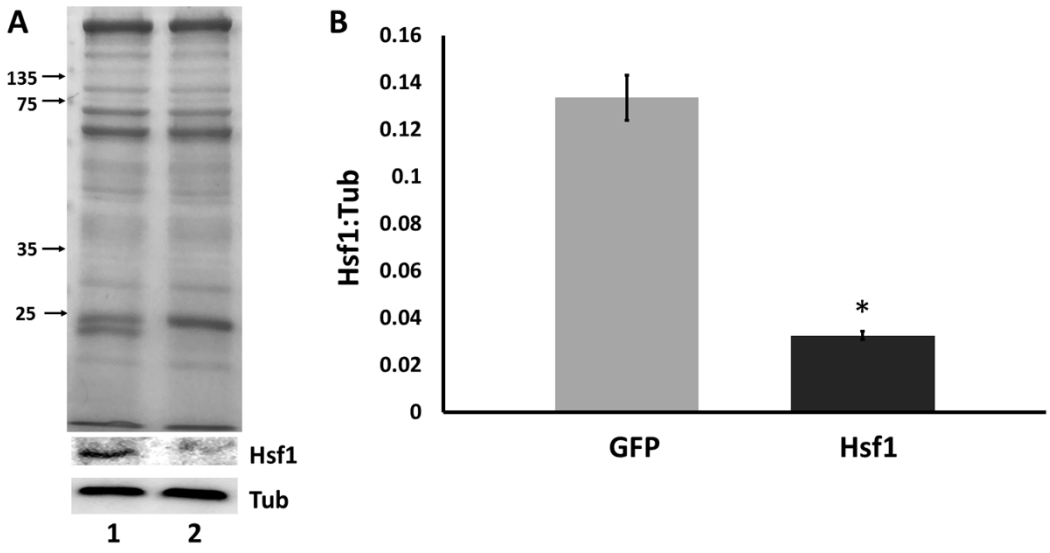

Fig.11. Hsf1 knockdown by RNAi in *A. franciscana* cysts. A. Protein extracts from 50 cysts released from females injected with either *GFP* dsRNA (1) or *hsf1* dsRNA (2) were resolved in SDS polyacrylamide gels and either stained with Coomassie blue (upper) or transferred to nitrocellulose and probed with antibody to Hsf1 (Hsf1) or tubulin (Tub). The experiment was repeated several times and a representative example is shown. B. The bands on blots were quantified with Image Studio Software and the ratio of Hsf1 to tyrosinated α-tubulin was determined. Experiments were done 3 times and error bars show standard deviation. The asterisks indicate that the amount of Hsf1 in cysts from females receiving *hsf1* dsRNA was statistically different ($p < 0.05$) from the amount of Hsf1 in cysts from females receiving *GFP* dsRNA.

Fig. 12. Knockdown of Hsf1 reduced the stress tolerance of *A. franciscana* cysts. A. Cysts released from females injected with either *GFP* or *hsf1* dsRNA were incubated in sea water for 7 days, desiccated, frozen and then incubated in sea water at room temperature to evaluate hatching. The experiment was done 3 times and error bars show standard deviation. The asterisk indicates that the survival of cysts from females receiving *hsf1* dsRNA was statistically different ($p < 0.05$) than the survival of cysts from females receiving *GFP* dsRNA. B. To determine if cysts were alive following knock down of Hsf1, 10 cysts obtained from females injected with either *hsf1* or *GFP* dsRNA as indicated in the figure were incubated in test solution and the change in absorbance was measured after 1 day at 553 nm and then on 4 consecutive days. The experiment was repeated 5 times and the standard error is shown.

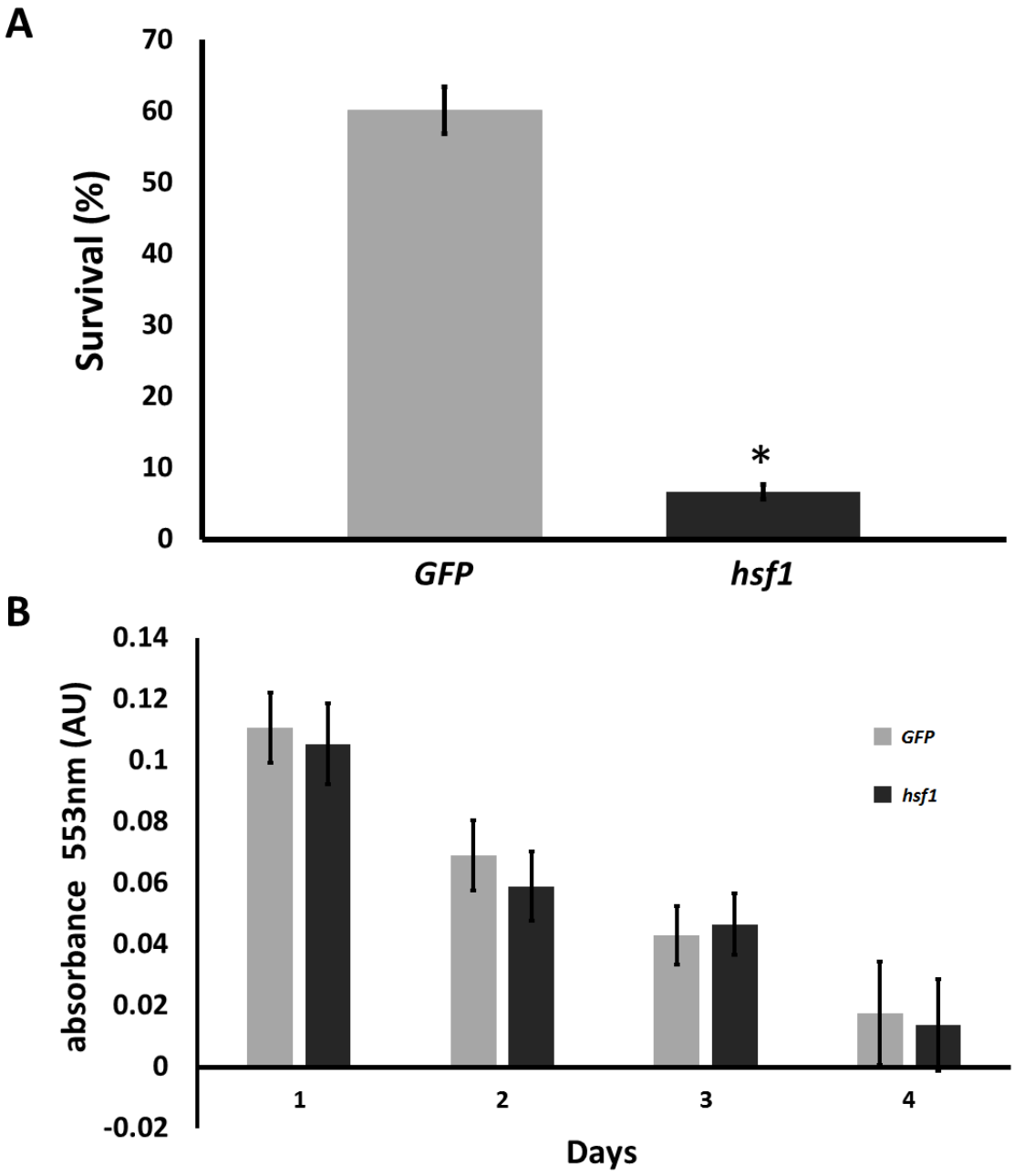
A
70
60
50
40
30
20
10
0
Survival (%)
*
GFP
hsf1
B
0.14
0.12
0.1
0.08
0.06
0.04
0.02
0
-0.02
absorbance 553nm (AU)
GFP
hsf1
1
2
3
4
Days

Because it is not possible to determine by visual inspection if cysts are viable the metabolic activities of cysts released from females injected with *GFP* and *hsf1* dsRNA were measured and found to be very similar to one another, indicating that cysts were viable. The metabolic activities of cysts from both groups declined to almost undetectable levels by 4 days after release (Fig. 12B).

3.4 Hsf1 knockdown reduced diapause-specific molecular chaperone mRNAs and proteins

3.4.1 *p26*, *ArHsp21*, *ArHsp22* and *artemin* mRNAs were reduced in cysts upon knockdown of Hsf1

qRT-PCR revealed that knockdown of Hsf1 respectively reduced the amount of mRNA encoding p26, ArHsp21, ArHsp22 and artemin in cysts by 65.3%, 73.7%, 35.0% and 80.4% (Fig. 13A-D).

3.4.2 Knockdown of Hsf1 reduced diapause-specific molecular chaperones in cysts

Immunoprobing of western blots demonstrated that *A. franciscana* cysts with reduced Hsf1 possessed diminished amounts of p26, ArHsp21, ArHsp22 and artemin (Fig. 14A-D). Although these chaperones were always reduced in Hsf1 knockdown cysts, the extent of knockdown varied from one experiment to another, ranging from 43% to 54% for p26, 31% to 34% for ArHsp21, 44% to 50% for ArHsp22, and 52% to 74% for artemin, as determined by the quantification of immune-reactive proteins on

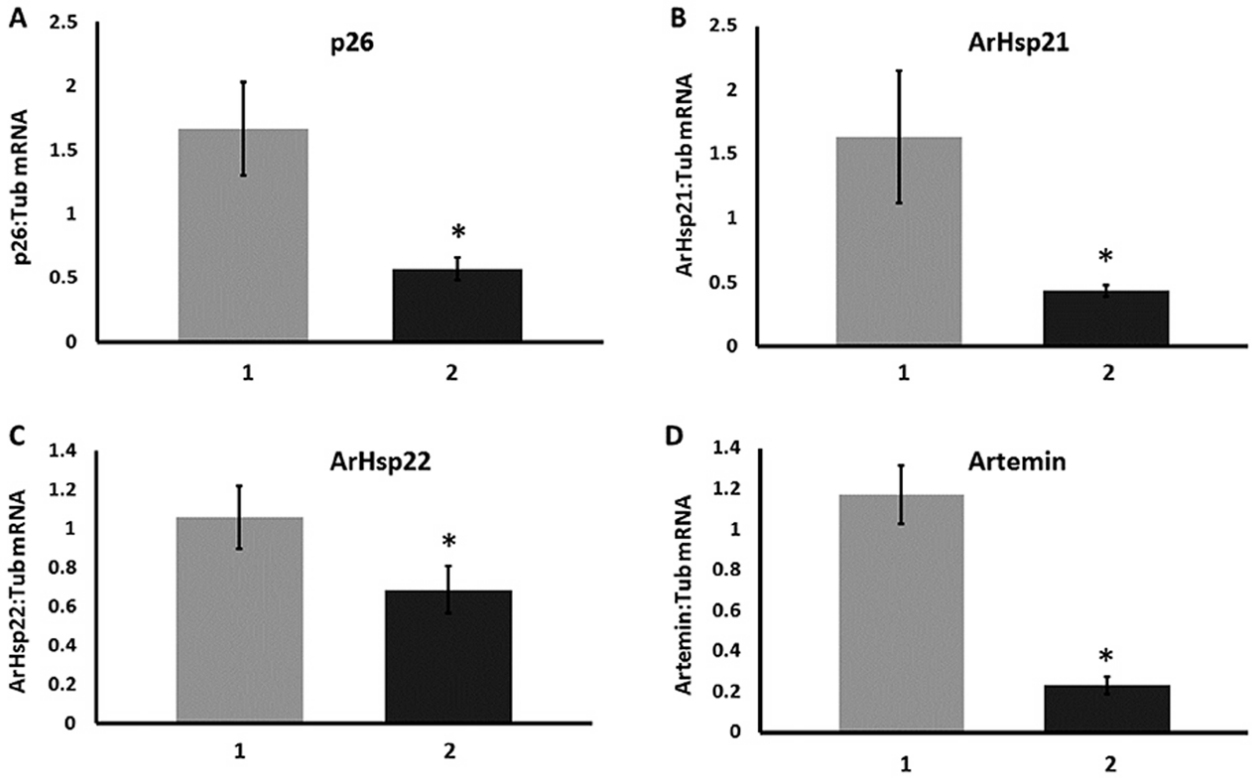

Fig.13. Knockdown of Hsf1 reduced mRNA encoding diapause-specific molecular chaperones in *A. franciscana* cysts. RNA was prepared from cysts released from *A. franciscana* females injected with either *GFP* (1) or *Hsf1* (2) dsRNA. mRNA for p26, ArHsp21, ArHsp22 and artemin, as indicated in the figure, was quantified by qRT-PCR using tyrosinated α-tubulin as internal standard. Experiments for each molecular chaperone were done 3 times and error bars show standard deviation. The asterisks indicate that the amount of molecular chaperone mRNA in cysts from females receiving *hsf1* dsRNA was statistically different ($p < 0.05$) from the amount of molecular chaperone mRNA in cysts from females receiving *GFP* dsRNA.

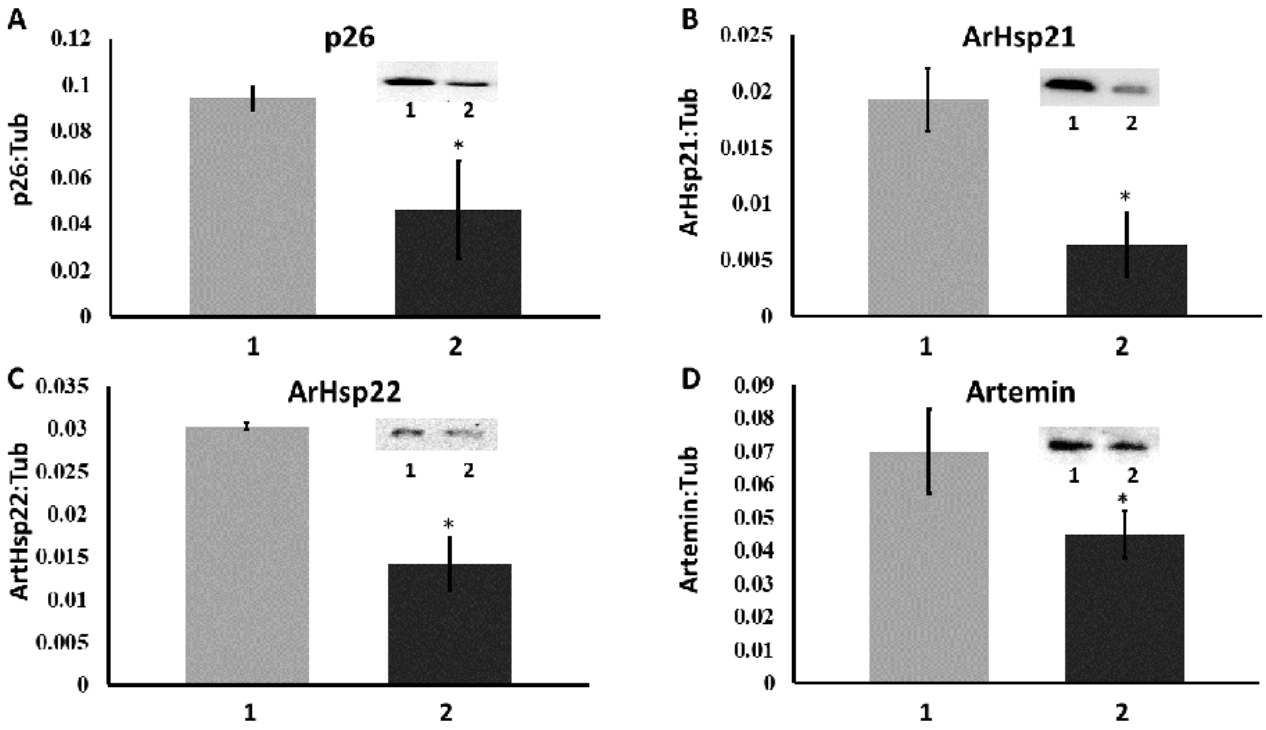

Fig.14. Knockdown of Hsf1 reduced diapause-specific molecular chaperones in *A. franciscana* cysts. Protein extracts from 50 cysts released from females injected with either *GFP* dsRNA (1) or *hsf1* dsRNA (2) were resolved in SDS polyacrylamide gels, blotted to nitrocellulose and reacted with antibodies to p26, ArHsp21, ArHsp22 and artemin, as indicated in the figure. Insets, representative examples of western blots probed with antibodies to p26, ArHsp21, ArHsp22, artemin. The bands on blots were quantified with Image Studio Software and the ratio of each molecular chaperone to tyrosinated α-tubulin was determined. Experiments for each molecular chaperone were done 2 times and error bars show standard deviation. The asterisks indicate that the amount of each molecular chaperone in cysts from females receiving *hsf1* dsRNA was statistically different ($p < 0.05$) from the amount of that molecular chaperone in cysts from females receiving *GFP* dsRNA.

western blots by using Image Studio Lite Ver 5.2 (LI-COR Biotechnology, Lincoln, NE, USA).

3.5 Injection of *A. franciscana* females with *hsf1* dsRNA reduced *hsf1* mRNA and Hsf1 in nauplii

RT-PCR revealed that nauplii released by *A. franciscana* females injected with *hsf1* dsRNA had less *hsf1* mRNA than did nauplii released by females receiving *GFP* dsRNA, but tubulin mRNA was similar in both types of nauplii (Fig.15A). As determined by qRT-PCR, the amount of *hsf1* mRNA in nauplii freshly released from *A. franciscana* females injected with *hsf1* dsRNA was reduced 56% as compared to nauplii from females receiving *GFP* dsRNA (Fig.15B).

As shown by the immunoprobing of western blots and the quantification of immune-reactive proteins by the using of Image Studio, there was a 67% decrease in the amount of Hsf1 in nauplii released by females receiving *hsf1* mRNA as compared to nauplii released from females receiving *GFP* mRNA ($p < 0.05$) (Fig. 16).

3.6 Loss of Hsf1 reduced the viability of nauplii

All nauplii released by females, whether injected with *GFP* or *hsf1* dsRNA were, as indicated by swimming behavior, viable. However, all of the nauplii with reduced Hsf1 died within 3 days of release from females whereas 44.1% of nauplii with normal amounts of Hsf1 survived (Fig. 17).

Fig.15. Knockdown of *hsf1* mRNA in *A. franciscana* nauplii. A. RNA samples were prepared from nauplii released from females injected with either *hsf1* dsRNA (F) or *GFP* dsRNA (G). cDNA was amplified by RT-PCR with Hsf1 and tubulin primers as indicated in the figure and resolved in agarose gels. M, DNA size marker. B. The amount of *hsf1* mRNA in *A. franciscana* nauplii released from females receiving *GFP* (1) and *hsf1* (2) dsRNA was determined by qRT-PCR using tyrosinated α-tubulin as internal standard. The experiment was done 3 times and error bars show standard deviation. The asterisk indicates that the amount of *hsf1* mRNA in nauplii from females receiving dsRNA for *hsf1* was statistically different ($p < 0.05$) from the amount of *hsf1* mRNA in nauplii from females receiving *GFP* dsRNA.

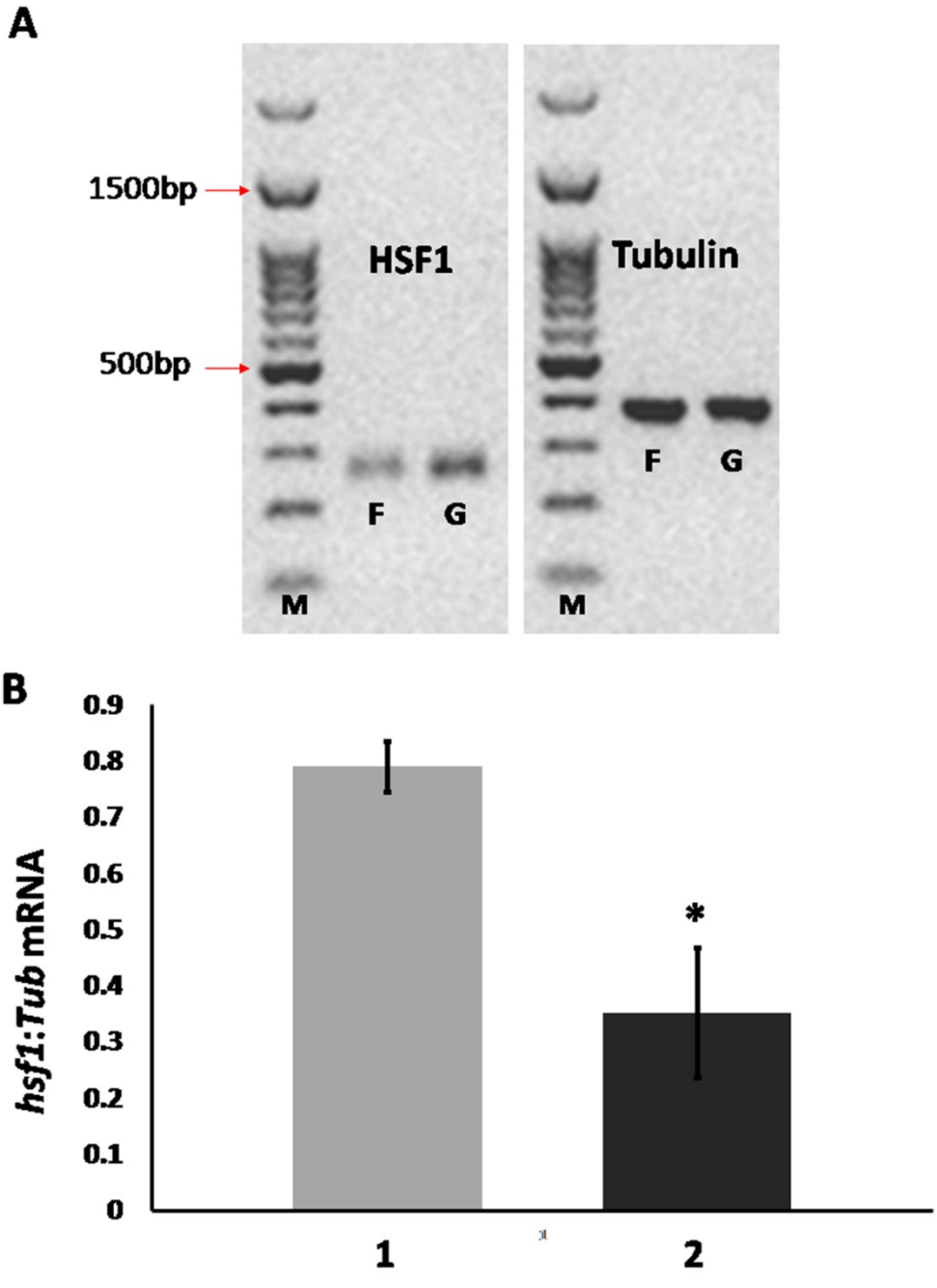
A
1500bp
500bp
HSF1
F
G
M
Tubulin
F
G
M
B
hsf1:Tub mRNA
0.9
0.8
0.7
0.6
0.5
0.4
0.3
0.2
0.1
0
*
1
2

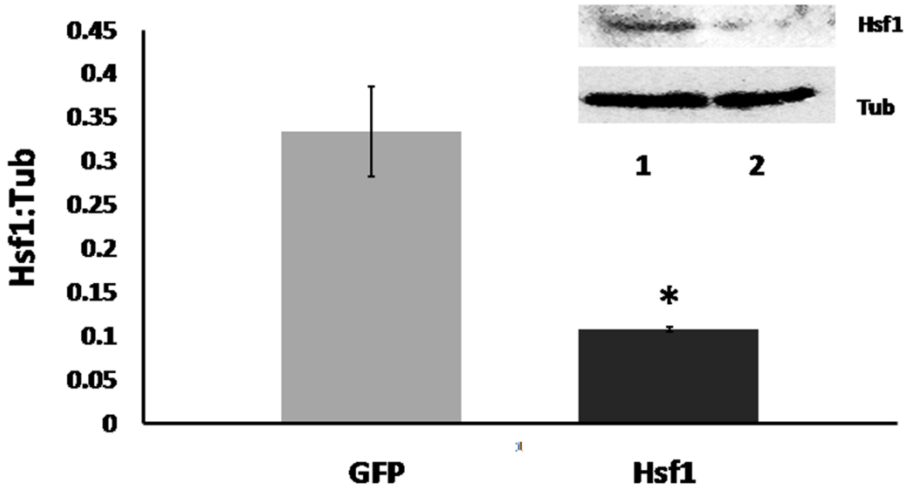

Fig. 16. Hsf1 knockdown by RNAi in *A. franciscana* nauplii. Protein extracts from 60 nauplii released from females injected with *GFP* dsRNA (1) and *hsf1* dsRNA (2) were resolved in SDS polyacrylamide gels, blotted to nitrocellulose and probed with antibodies to Hsf1 and tyrosinated α-tubulin. Inset, representative blot. The bands on blots were quantified with Image Studio Software and the ratio of Hsf1 to tyrosinated α-tubulin was determined. The experiments were done 3 times and error bars show standard deviation. The results are expressed as mean values ±S.D. The asterisks indicate that the amount of Hsf1 in nauplii from females receiving *hsf1* dsRNA was statistically different ($p < 0.05$) from the amount of Hsf1 in nauplii from females receiving *GFP* dsRNA.

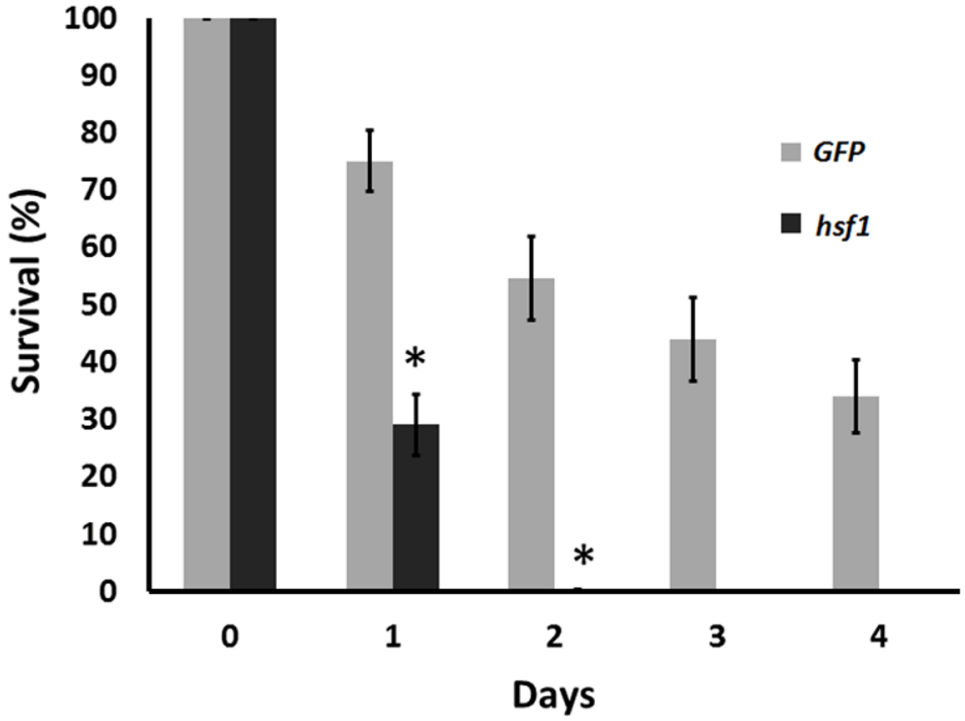

Fig. 17. *A. franciscana* nauplii with depleted Hsf1 die prematurely. Surviving (motile) nauplii released from females injected with either *GFP* or *hsf1* dsRNA were counted daily and compared to the number of viable nauplii upon release. The experiment was done 6 times and error bars show standard deviation. The asterisks on days 1 and 2 indicate that the survival of nauplii released from females receiving *hsf1* dsRNA was statistically different ($p < 0.05$) from the survival of nauplii released from females receiving *GFP* dsRNA.

3.7 Hsf1 knockdown did not change cysts and nauplii release time

The time from fertilization to release of cysts from females injected with either *hsf1* dsRNA or *GFP* dsRNA was approximately 5 days ($p > 0.05$) (Fig. 18). The time from fertilization to release of nauplii from females injected with either *hsf1* dsRNA or *GFP* dsRNA was approximately 5 days ($p > 0.05$) (Fig. 18).

3.8 *A. franciscana* females injected with *hsf1* dsRNA exhibited reduced longevity

Cyst producing adult females of *A. franciscana* injected with *GFP* dsRNA survived on average 29.5 days ($n = 13$) after injection whereas those injected with *hsf1* dsRNA survived 13.5 days ($n = 13$) (Fig. 19), a significant difference ($p < 0.05$).

Nauplius-producing *A. franciscana* females injected with *GFP* dsRNA survived on average 28.3 days ($n = 11$) after injection whereas those injected with *hsf1* dsRNA survived 15 days ($n = 11$) (Fig. 19), a significant difference ($p < 0.05$).

3.9 *hsf1* mRNA and Hsf1 in oocytes, embryos, cysts and nauplii of *A. franciscana*

3.9.1 *hsf1* mRNA during early development of *A. franciscana*

qRT-PCR using *α-tubulin* mRNA as an internal standard showed that *hsf1* mRNA increased significantly in oviparous (diapause-destined) embryos by two days after fertilization, and then decreased as development progressed (Fig. 20). In comparison, *hsf1* mRNA also appeared by day 2 in ovoviviparously developing embryos but in amounts much less than in oviparous embryos. *hsf1* mRNA increased until nauplii

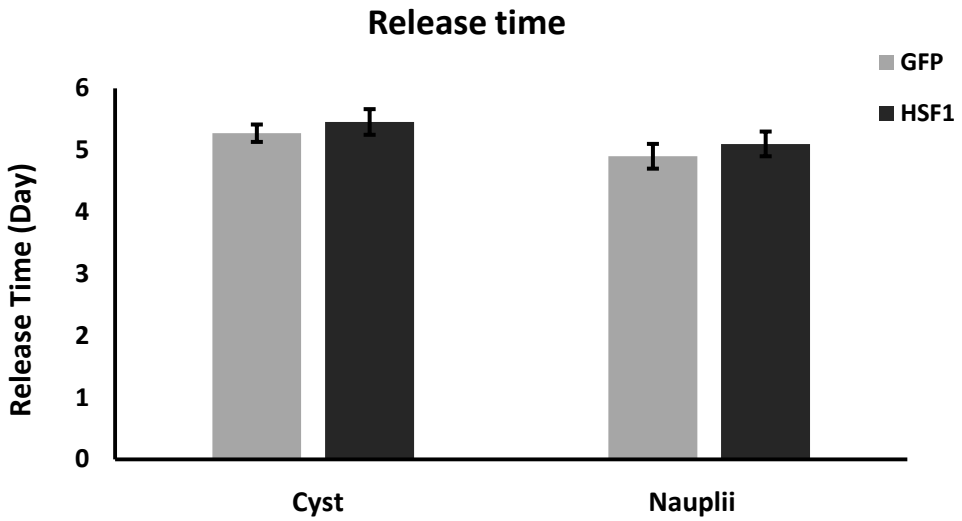

Fig. 18. Release time for *A. franciscana* cysts and nauplii. The time it takes from fertilization to the release of cysts and nauplii from females receiving either *GFP* dsRNA (n=13) or *hsf1* dsRNA (n=13) was recorded. Error bars show standard deviation. The difference in release time for both cysts and nauplii from females receiving *hsf1* versus *GFP* dsRNA was not significant ($p > 0.05$).

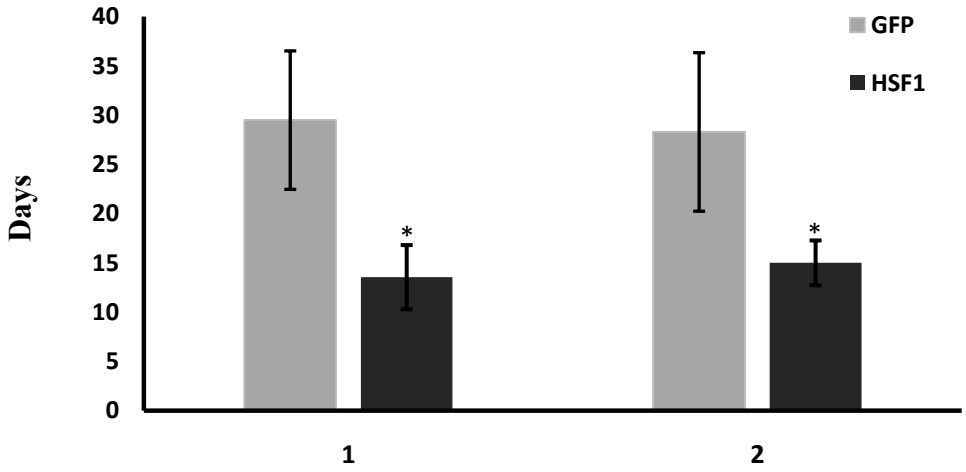

Fig.19. Injection of *hsf1* dsRNA reduced the longevity of *A. franciscana* females. The mean time from the day females were injected to the day they died was recorded. Females were injected with either *GFP* dsRNA or *hsf1* dsRNA. Cyst producing females (1); nauplii producing females (2). Asterisks indicate that the mean life span of females injected with *hsf1* dsRNA was significantly different ($p < 0.05$) than the life span of females injected with *GFP* dsRNA. Error bars represent standard deviation.

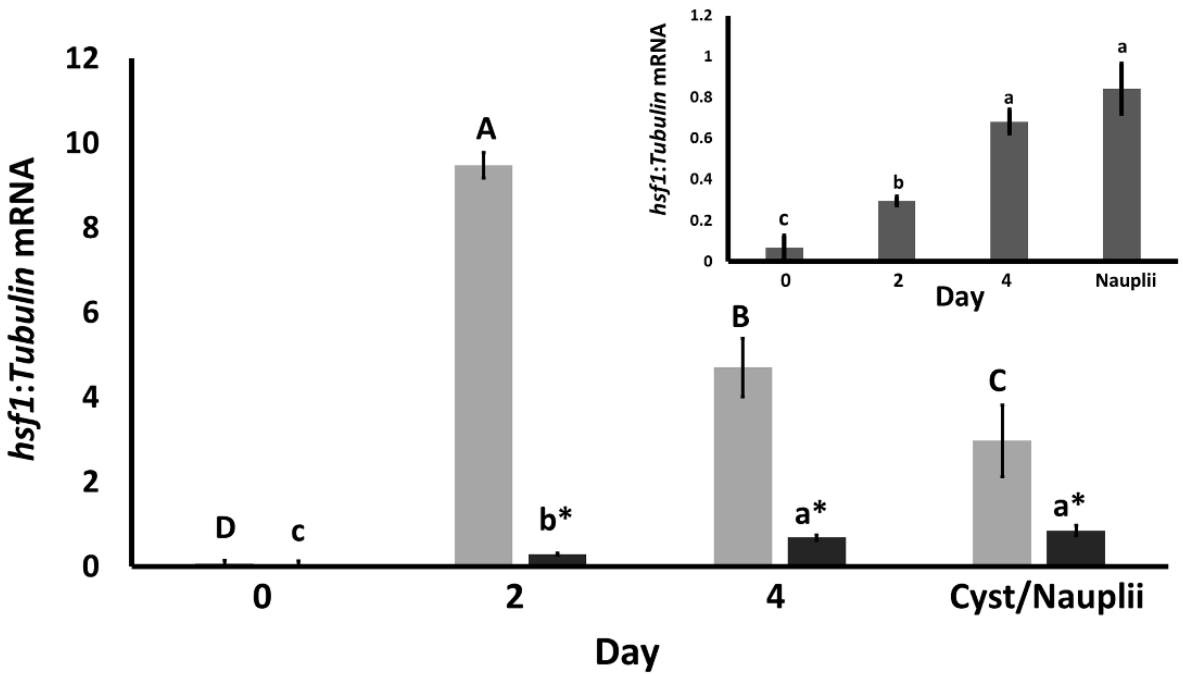

Fig. 20. *hsf1* mRNA quantification during oviparous and ovoviviparous development. RNA was prepared from oviparous (grey) and ovoviviparous (black) oocysts, embryos on days 2 and 4 after fertilization and from freshly released cysts (grey) and nauplii (black). *hsf1* mRNA was then quantified by qRT-PCR using tyrosinated α-tubulin as internal standard. Inset, enlarged view of *hsf1* mRNA in ovoviviparous oocytes, embryos and nauplii. The experiments were done in triplicate and error bars show standard deviation. The values represented by bars labeled with different letters are significantly different ($p < 0.05$) from one another. Asterisks indicate that the amount of mRNA was significantly different ($p < 0.05$) between samples from oviparous and ovoviviparous embryos on the day indicated.

were released but did not reach the level of *hsf1* mRNA in newly released cysts (Fig. 20).

3.9.2 Hsf1 during early development of *A. franciscana*

Immunoprobing of western blots using tyrosinated α-tubulin as internal standard showed that Hsf1 increased significantly by day 2 post-fertilization and then decreased until the release of cysts from females (Fig. 21A, C). By comparison, Hsf1 appeared at day 2 post-fertilization in ovoviviparously developing embryos but at a much lower level than in oviparous embryos (Fig. 21B, C). Hsf1 increased until nauplii were released reaching a slightly higher level than Hsf1 in newly released cysts (Fig. 21B, C).

3.10 Hsf1 localization in *A. franciscana* embryos.

Hsf1 antibody probes Hsf1 but no other protein as indicated by controls with no antibody or Hsf1 antibody pre-mixed with antigen (Fig. A5) (Appendix A). Examination by confocal microscope demonstrated that before fertilization there is no Hsf1 in the nuclei of oocytes that will develop either oviparously or ovoviviparously, however Hsf1 was observed in oviparous embryos at 2 days after fertilization and in cysts (Fig. 22A). A small amount of Hsf1 was localized in nuclei at 2 days post-fertilization, reaching a peak by 4 days and then declining in nuclei of cysts (Fig. 22A). Hsf1 was initially observed at day 4 post-fertilization in ovoviviparously

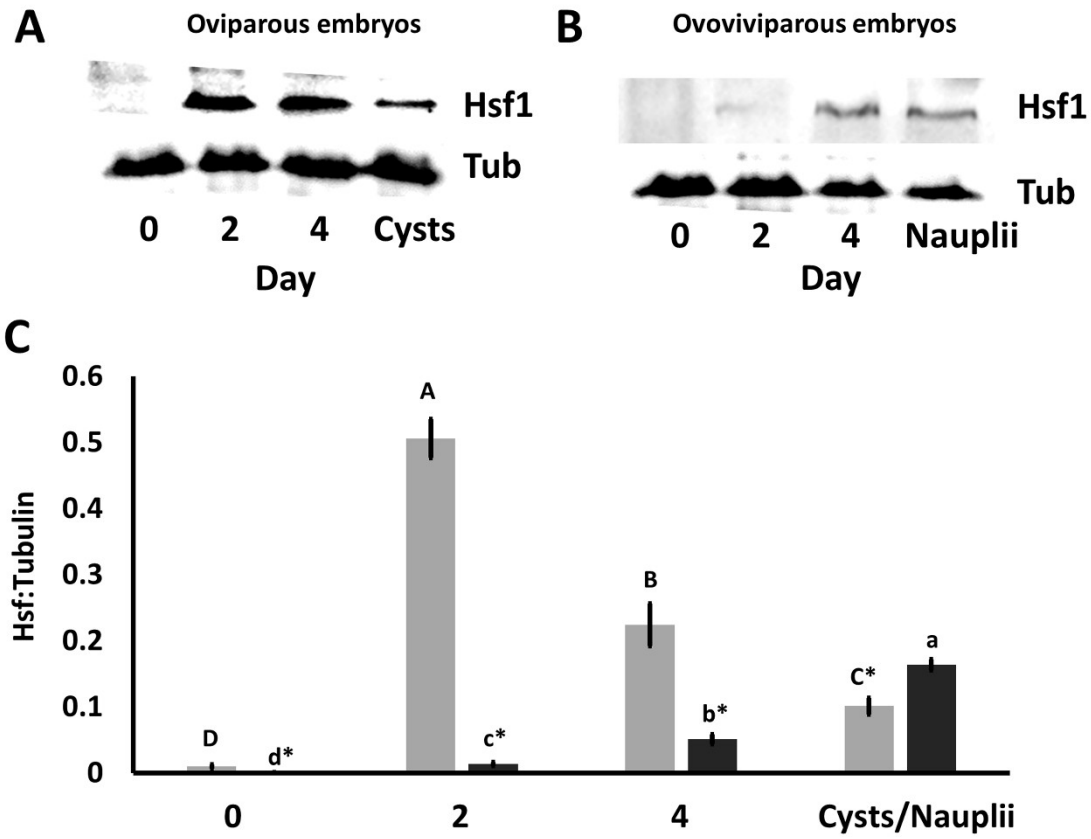

Fig. 21. Hsf1 quantification during oviparous and ovoviviparous *A. franciscana* development. Protein extracts from oviparous and ovoviviparous oocytes and embryos on days 2, 4 post-fertilization and freshly released cysts and nauplii were resolved in SDS polyacrylamide gels, blotted to nitrocellulose and reacted with antibodies to Hsf1 and tubulin. A, B, representative examples of western blots probed with antibody to Hsf1 and tubulin. C. Immunoreactive bands were quantified with Image Studio Software and the ratio of Hsf1 to tyrosinated α-tubulin was determined. Experiments were done in duplicate and error bars show standard deviation. Bars with different letters are significantly different ($p < 0.05$) from one another. Asterisks indicate that the amount of protein was significantly different ($p < 0.05$) between samples from oviparous and ovoviviparous embryos on the day indicated.

Fig. 22. Hsf1 localization in developing *A. franciscana*. Oviparous and ovoviviparous oocytes, embryos on 2 and 4 days after fertilization and freshly released cysts or nauplii were gently crushed to release nuclei and reacted with antibody that recognized Hsf1 followed by fluorescein isothiocyanate-conjugated goat anti-rabbit IgG. Samples were then stained with DAPI, mounted in mounting media and examined by confocal microscopy. A, oviparous embryos and cysts. B, ovoviviparous embryos and nauplii. DAPI, DAPI staining; FITC, antibody staining; M, merged picture. Scale bars, 10 μm.

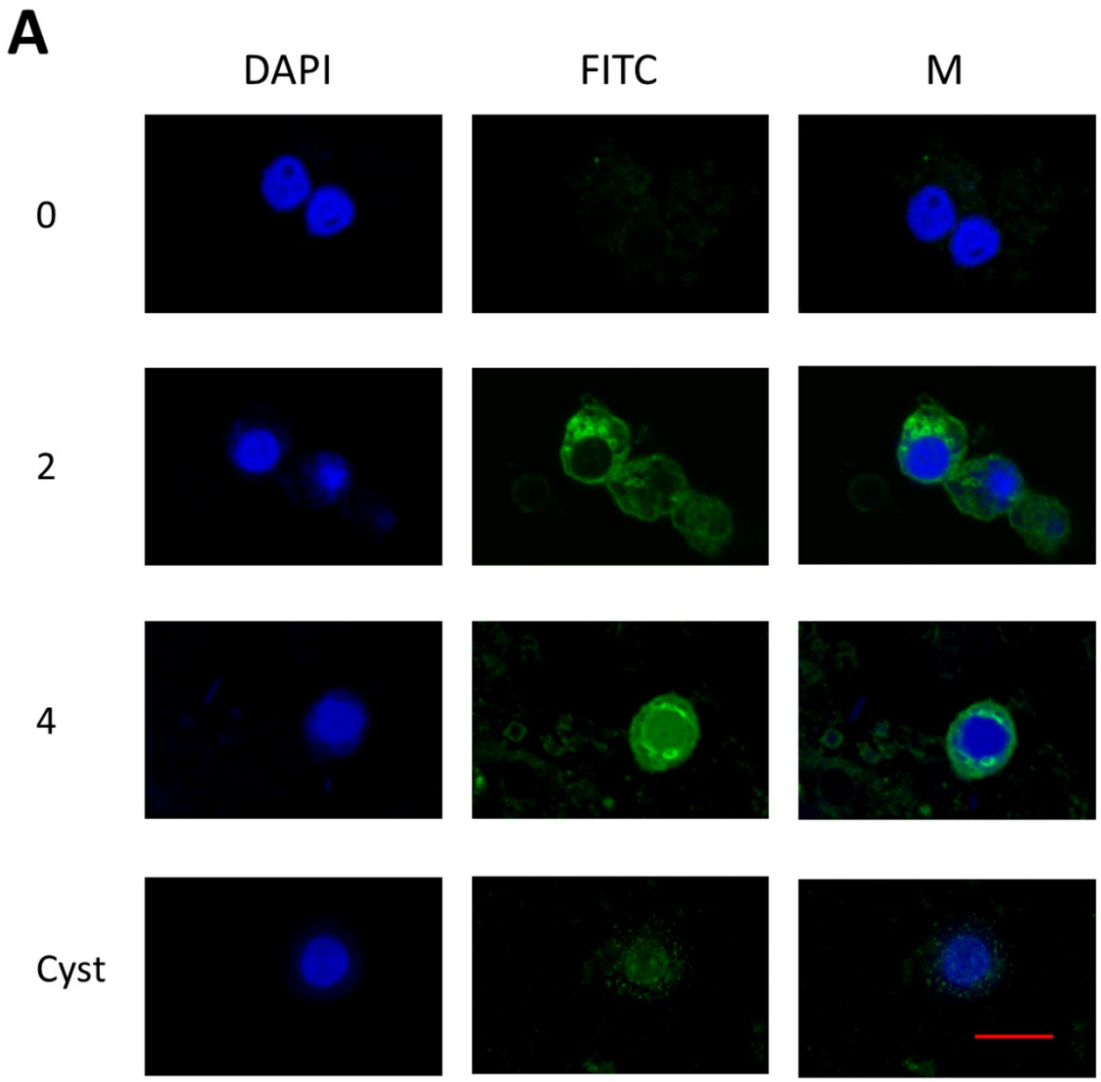
A
DAPI
FITC
M
0
2
4
Cyst

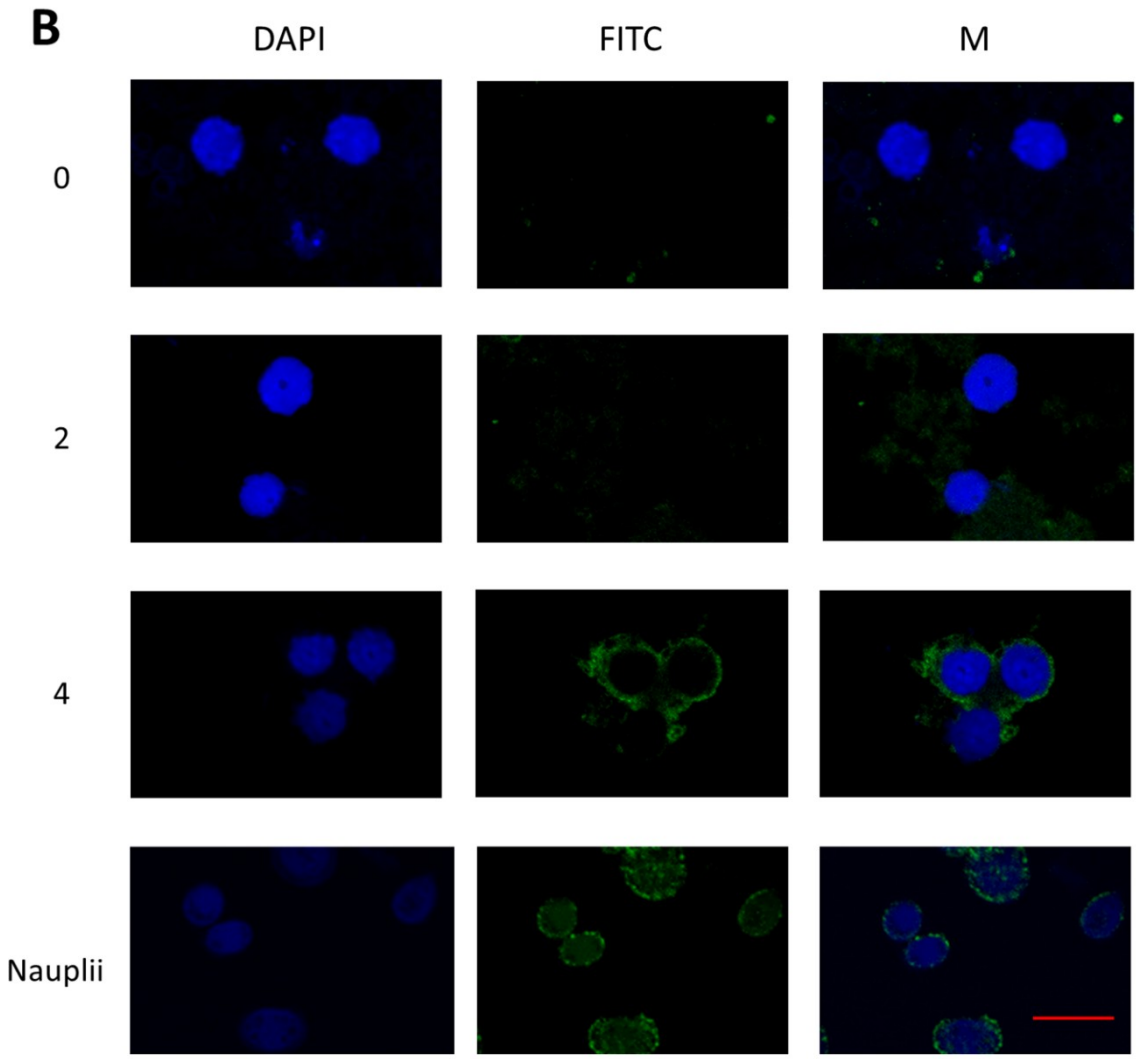
B
DAPI
FITC
M
0
2
4
Nauplii

developing embryos and persisted in freshly released nauplii where it first appeared to localize to nuclei (Fig. 22B). The localization of Hsf1 in the nuclei was confirmed by optical sectioning of the nuclei (Fig. 23).

Fig. 23. Optical sections of Hsf1 localization in developing *A. franciscana*. Developing *A. franciscana* were gently crushed to release nuclei and reacted with antibody that recognized Hsf1 followed by fluorescein isothiocyanate-conjugated goat anti-rabbit IgG. Samples were then stained with DAPI, mounted in mounting media and examined by confocal microscopy. A, oviparously developing embryos on day 2 post-fertilization. B, oviparously developing embryos on day 4 post-fertilization. C, freshly released cysts. D, ovoviviparously developing embryos on day 4 post-fertilization. E, freshly released nauplii. 1-8 continuous series of 0.79 μm optical sections. DAPI, DAPI staining; FITC, antibody staining. Scale bars, 10 μm.

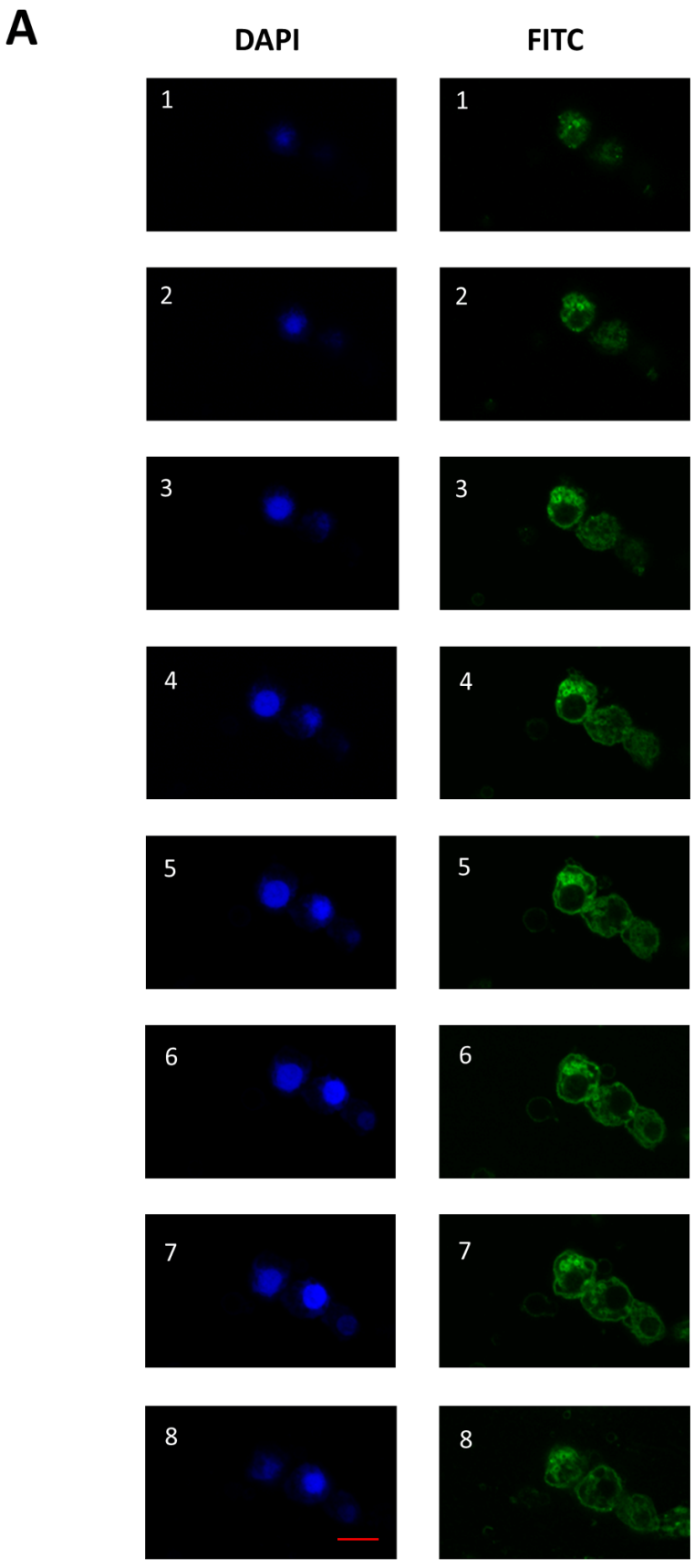
A
DAPI
FITC
1
2
3
4
5
6
7
8

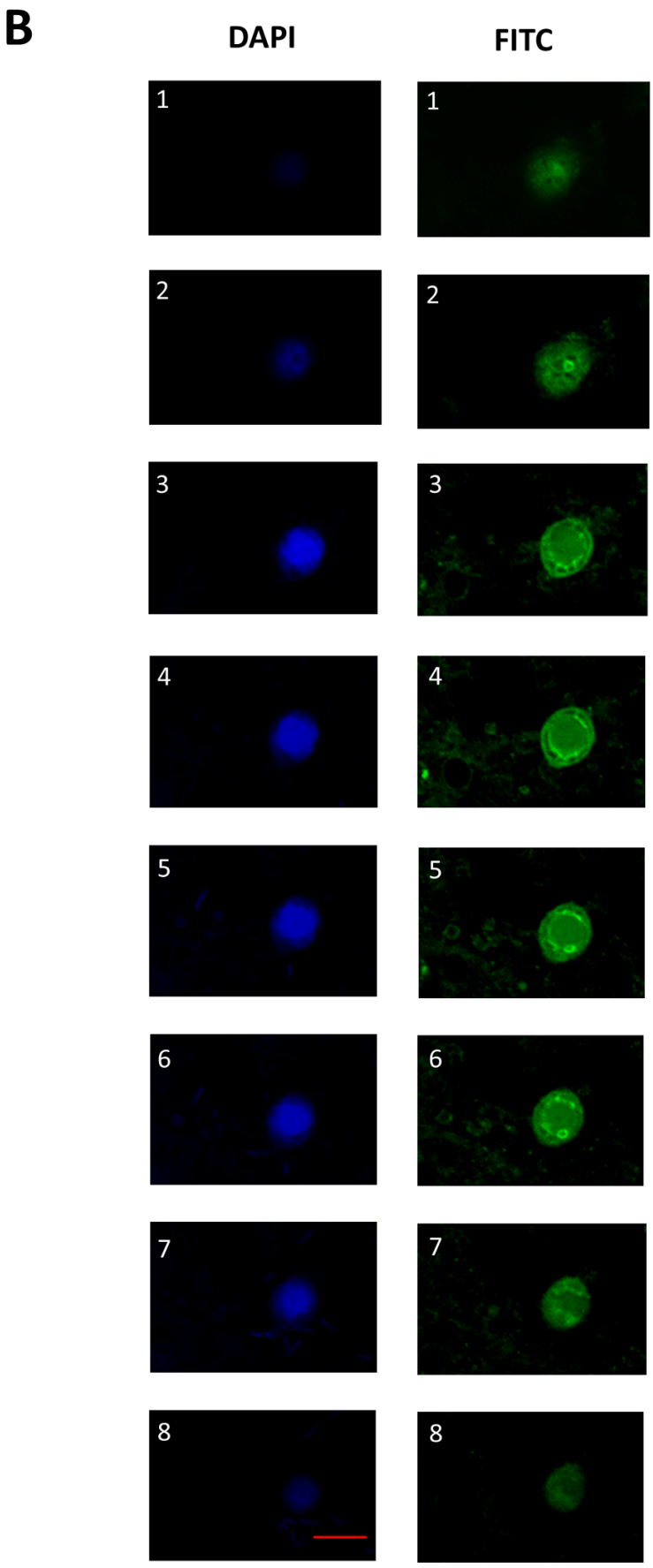
B
DAPI
FITC
1
1
2
2
3
3
4
4
5
5
6
6
7
7
8
8

C

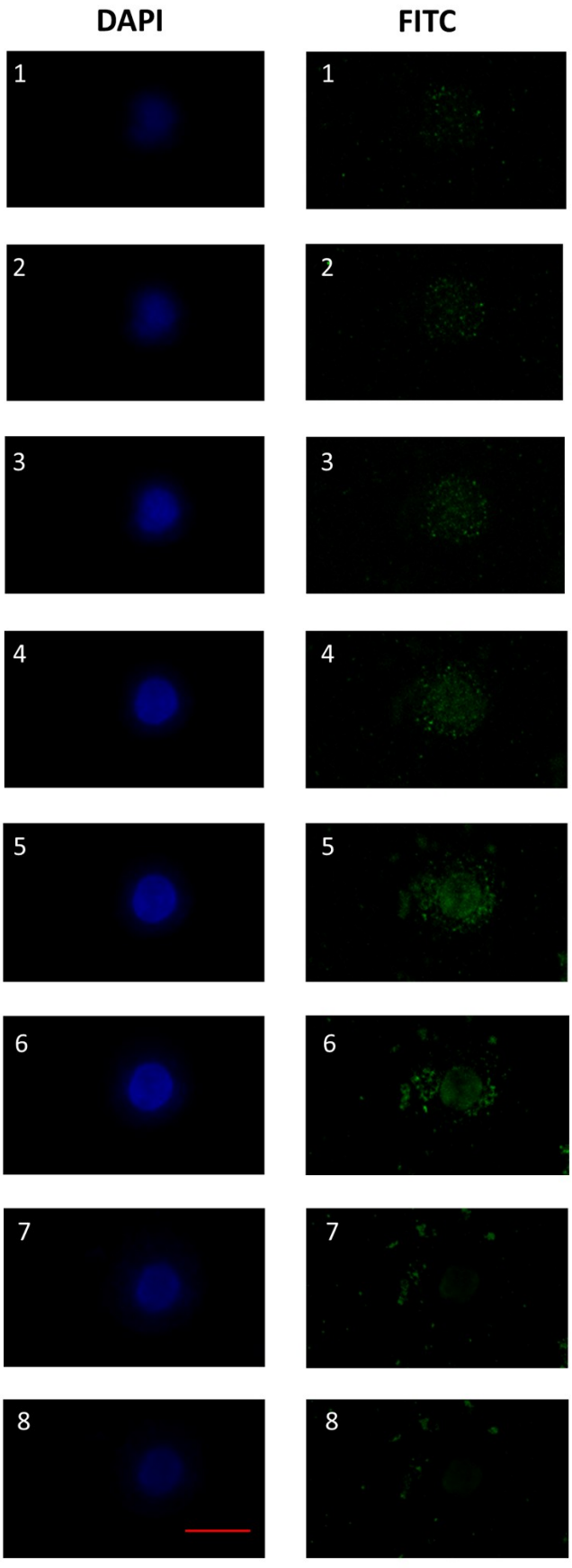

D

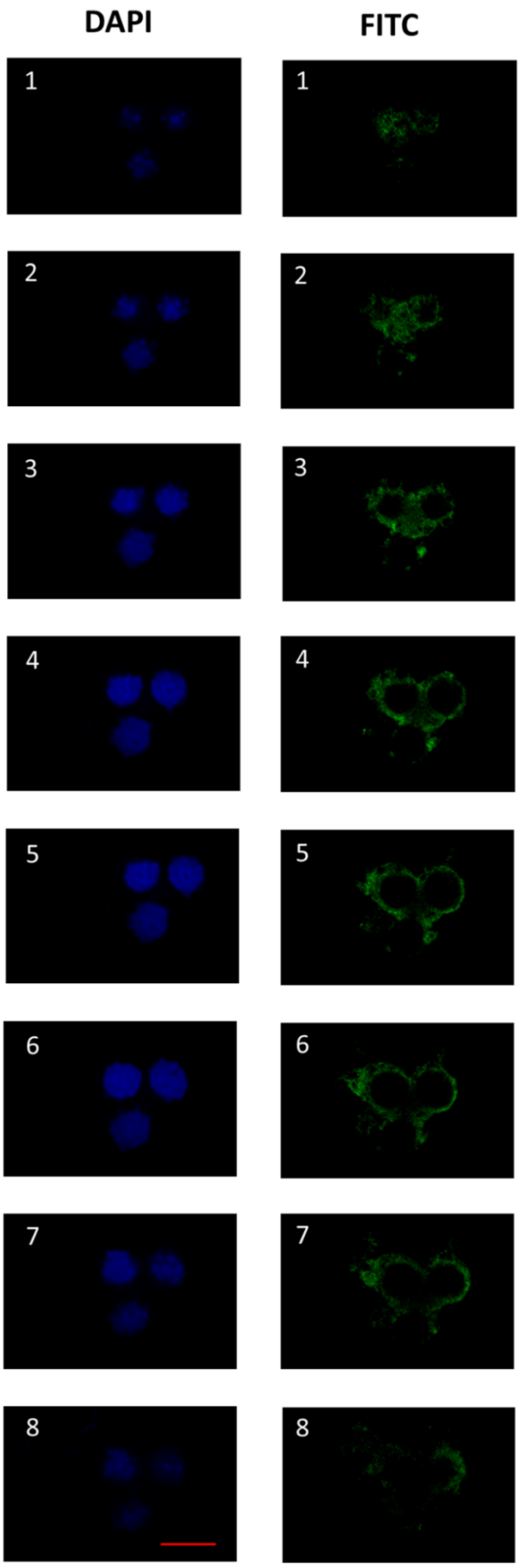

E

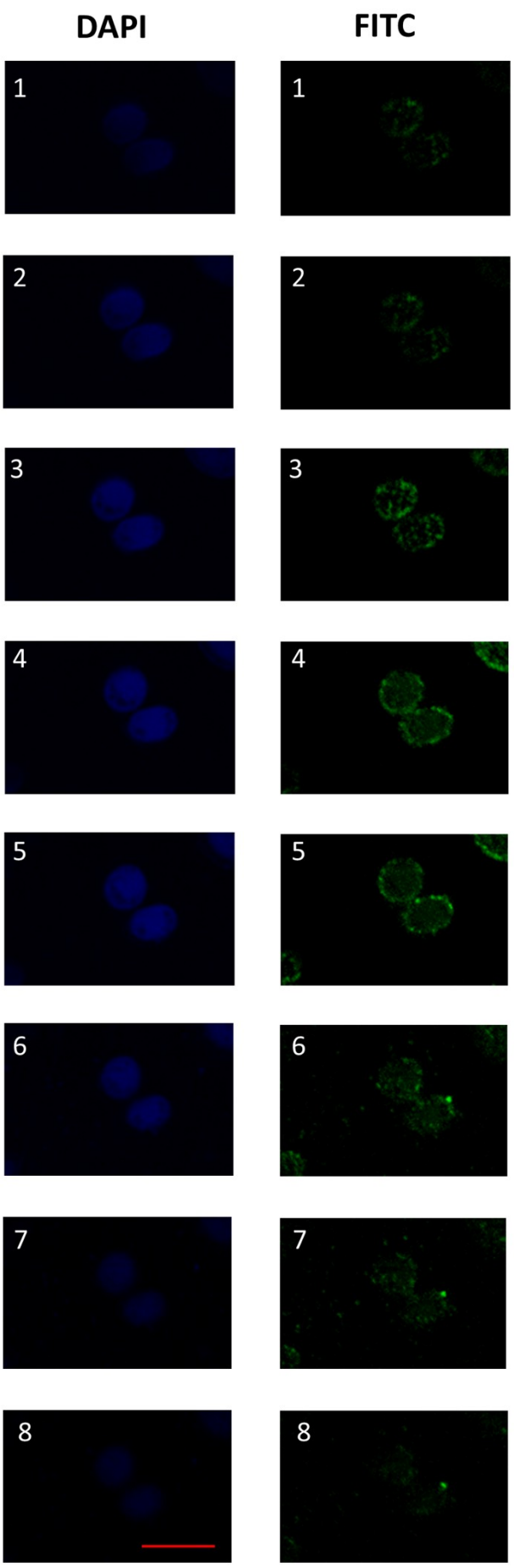

Chapter 4 Discussion

4.1 *A. franciscana* Hsf1 sequence analysis

Only one type of Hsf was cloned from *A. franciscana* even though amplification was done with several degenerate primer pairs. Generally, one HSF has been observed in each arthropod species examined (Åkerfelt et al., 2010; Yan et al., 2014; Huang et al., 2014). As in other species, *A. franciscana* Hsf1 has a typical DBD which is the hallmark of the HSF family. The *A. franciscana* DBD has a characteristic helix-turn-helix structure containing three helical bundles and antiparallel β-sheets (Nakai, 2016). The helical bundles, especially the third α-helix which interacts with the major groove of DNA, are critical to DNA binding and the regulation of gene expression by HSF1s (Nakai, 2016). The conserved HR-A & HR-B domain has typical hydrophobic heptad repeats, which consist of seven amino acids. Conservation of the DBD and HR-A & HR-B domains indicates that they are key components of Hsf1, with the DBD critical for binding to HSEs, and the HR-A &HR-B domain essential for Hsf1 trimer formation. HR-C is characterized by heptad repeats consisting of the hydrophobic amino acids leucine, isoleucine and valine, as is HR-A & HR-B. HR-C forms an intramolecular coiled coil with the HR-A & HR-B domain to prevent HSF trimerization. Although present in *A. franciscana* Hsf1, the HR-C domain is not found in HSFs of some other invertebrates such as *C. elegans*. The presence of HR-C indicates that *A. franciscana* Hsf1 exists as a monomer in cells which differs from mammalian HSF4 and yeast HSF which are always in the trimer

state. *A. franciscana* Hsf1 has an RD domain which is posttranslationally modified as part of the activation process and a TAD domain, important for interacting with chaperones and controlling Hsf1 activity. RD and TAD are not conserved among Hsfs from species in Table 3.

Hsf1 from *A. franciscana* is somewhat shorter than Hsfs from other species in Table 3, perhaps because *A. franciscana* evolved earlier than the insects and vertebrates listed there. Species evolving late in evolution tend to have more complicated HSFs (Nakai, 2016). The conserved DBD and HR-A & HR-B domains are about 1/3 of the length of Hsf1 and both domains, unlike the other domains, have many amino acid residues in common. This explains why the identity between Hsf1 from *A. franciscana* and other species is normally about 30% to 35%.

4.2 RNAi reduced *hsf1* mRNA in *A. franciscana* and led to the loss of Hsf1

RNAi, the technique employed to examine the function of Hsf1 in *A. franciscana*, has been applied to the study of ArHsp40, Hsp70, artemin and sHSPs in *A. franciscana*, where the levels of mRNA and protein knockdown vary (Jiang et al., 2016; Iryani et al., 2017; King et al., 2014; King and MacRae, 2012). The work described herein is, however, to my knowledge the first to study Hsf1 in crustaceans using RNAi.

dsRNA was used to knockdown Hsf1 in *A. franciscana* cysts and nauplii. Either *hsf1* or *GFP* dsRNA was injected into the egg sacs of *A. franciscana* females before fertilization with *GFP* dsRNA having no effect because *A. franciscana* does not have

a *GFP* gene (Zhao et al., 2012). On the other hand, injection of *hsf1* dsRNA reduced the amount of *hsf1* mRNA in *A. franciscana* cysts and nauplii and correspondingly cysts and nauplii from females injected with *hsf1* dsRNA had less Hsf1 than cysts and nauplii from females injected with *GFP* dsRNA. RNAi did not eliminate either *hsf1* mRNA or Hsf1 and normally the knockdown of target proteins by RNAi is not complete. As an example, knockdown of *hsf1* and Hsf1 in vascular smooth muscle cells was not complete with the use of small interference RNA (siRNA) (Chen and Currie, 2006). In another example, RNAi reduces *Arcad* mRNA in *A. franciscana* and leads to shortened abdomens in nauplii released from females although some nauplii exhibit normal body length (Nguyen et al., 2016).

4.3 Loss of Hsf1 reduced stress tolerance in diapausing cysts of *A. franciscana*

Before entering diapause, cysts from Hsf1 and GFP knockdown females had similar metabolic activity, shown by the emission of equal amounts of CO_2 as determined by measuring the absorbance of test solutions at 553nm, indicating that cysts were viable. However, only about 6% of cysts lacking Hsf1 hatched after desiccation and freezing to break diapause while approximately 60% of cysts from females receiving *GFP* dsRNA, and thus possessing Hsf1, hatched after diapause. A mutation to *Hsf1* that inhibits its activity reduces stress tolerance in *C. elegans* (Prahlad et al., 2008) and *hsf1*$^{-/-}$ double knockout mouse cells cannot develop thermotolerance (Åkerfelt et al., 2007; McMillan et al., 1998). Both examples support the idea that Hsf1 is important for stress tolerance during diapause.

Hsf1 is activated during stress, modulating the expression of a variable repertoire of genes including those encoding molecular chaperones (Brunquell et al., 2016; Mahat et al., 2016; Solis et al., 2016). Biochemical and physiological changes associated with the stress response are an integral aspect of diapause and they entail modification of gene expression in response to environmental cues received prior to stress exposure. For example, Hsps are up-regulated in diapausing cysts of *A. franciscana* (Liang and MacRae, 1999; Qiu and MacRae, 2008 a, b). The upregulation of HSP synthesis is seen not only in *A. franciscana* cysts during diapause, but also in organisms such as rotifers (Denekamp et al., 2009; Clark et al., 2012), copepods (Aruda et al., 2011) and insects (Li et al., 2007; Rinehart et al., 2007; Lu and Xu, 2010; Fan et al., 2013; Lü et al., 2014; King and MacRae, 2015; Popović et al., 2015) where they assist in maintaining protein homeostasis and stress tolerance.

4.3.1 Hsf1 is required for maximal synthesis of diapause-specific molecular chaperones

Knockdown of Hsf1 in *A. franciscana* cysts reduced p26, ArHsp21, ArHsp22 and artemin, all of which are up-regulated in cysts but not nauplii. Putative HSEs were identified in the upstream regions of the *A. franciscana* gene encoding p26 (Qiu et al., 2006), suggesting that Hsf1 regulates the transcription of the *p26* gene in *A. franciscana*. Reduced ArHsp21 and ArHsp22 due to the knockdown of Hsf1 indicates that Hsf1 regulates both sHSPs, although HSEs are yet to be identified in ArHsp21 and ArHsp22 promotors. Hsf1 also regulates artemin transcription given that

knockdown of Hsf1 reduced artemin mRNA.

The loss of p26 is undoubtedly one of the reasons why *A. franciscana* stress tolerance is impaired after Hsf1 knockdown. Knockdown of p26 decreases stress tolerance and reduces the hatching of cysts from 58% to 6% (King and MacRae, 2012). Cyst hatching after Hsf1 knockdown was similar to that obtained after p26 knockdown indicating that Hsf1 is a key protein in protecting encysted embryos against harsh environments because it is required for p26 gene expression. Apparently, cysts need a substantial amount of p26 to survive desiccation and freezing, and a reduction of about 50% in p26 protein has the same effect as the loss of almost all p26. p26 protects proteins from irreversible denaturation during diapause and may enhance stress tolerance by protecting microfilaments, intermediate filaments and microtubules (King and MacRae, 2013; Liang and MacRae, 1999).

p26 prevents spontaneous diapause termination in *A. franciscana* and the knockdown of p26 results in the termination of diapause (King and MacRae, 2012). The knockdown of Hsf1 did not trigger the end of diapause indicating that there is sufficient p26 in Hsf1 knockdown cysts to prevent spontaneous termination. p26 may counter the effects of reactive oxygen species (ROS) (Robbins et al., 2010; King et al., 2014), which often play a role in cell signaling and may be involved in diapause termination (Jovanović- Galović et al., 2004).

The similar time to release of cysts from females injected with *hsf1* and *GFP* dsRNA revealed that knockdown of Hsf1 does not slow the development of oviparous embryos however the loss of p26 slows the development of diapause-destined

embryos (King and MacRae, 2012). That the loss of p26 caused by Hsf1 knockdown did not alter the time for cyst release from females indicates that there is sufficient p26 remaining for the normal development of diapause-destined embryos.

ArHsp22, a heat inducible sHSP that appears two hours after heat shock of adults, is the only known heat inducible sHSP in *A. franciscana*. ArHsp22 localizes to cyst nuclei where it forms large oligomers and it acts as a molecular chaperone *in vitro* by protecting citrate synthase and insulin from denaturation (Qiu and MacRae, 2008b). ArHsp22 was reduced 53% due to Hsf1 knockdown which may contribute to the decreased stress tolerance of *A. franciscana*. Knockdown reveals that the loss of ArHsp22 is lethal to *A. franciscana* adult females (King et al., 2013), yet most females injected with *hsf1* dsRNA survived long enough to release cysts, indicating that there was enough ArHsp22 for the survival of *A. franciscana* females.

ArHsp21 may also protect encysted embryos during diapause. ArHsp21 is not heat inducible but it prevents the denaturation of insulin and heat-induced aggregation of citrate synthase *in vitro* (Qiu and MacRae, 2008a). ArHsp21 accounts for less than 2% of soluble protein in cysts and knockdown of ArHsp21 causes about 7% reduced hatch after desiccation and freezing (King et al., 2013), suggesting that ArHsp21 has a role in *A. franciscana* cysts stress tolerance. ArHsp21 knockdown did not slow oviparous embryo development or cause spontaneous hatching (King et al., 2013), so the loss of ArHsp21 due to Hsf1 knockdown was unlikely to affect the development *A. franciscana* embryos.

Artemin, a ferritin-like protein has chaperone activity *in vitro*, preventing

heat-induced denaturation of citrate synthase and transfected mammalian 293H kidney cells containing artemin exhibit increased tolerance to heat and oxidative stress (Chen et al., 2007). Artemin accounts for more than 6% of soluble protein in *A. franciscana* cysts and artemin is not ATP-dependent so it is potentially functional when metabolism is reduced (Chen et al., 2003). The knockdown of artemin reduced cyst hatching after desiccation and freezing (King et al., 2014), indicating a role for artemin in stress tolerance. Artemin was reduced 37% due to Hsf1 knockdown which may contribute to the decreased stress tolerance in *A. franciscana* cysts.

Artemin binds non-polyadenlated RNAs and may prevent them from interfering with the translation of proteins essential for oviparous embryo development (Warner et al., 2004), perhaps explaining why the knockdown of artemin extends the time for the complete release of a brood of cysts from a female (King et al., 2014). Release time for a brood of cysts did not increase upon Hsf1 knockdown indicating that there was sufficient artemin for this process to occur.

4.3.2 Hsf1 and molecular chaperones not specific to diapause

Knockdown of Hsf1 in *A. franciscana* reduces the amount of Hsp90 in cysts released from females (Shea and Doucet, unpublished data), showing that Hsf1 regulates Hsp90 and knockdown of Hsp90 in *A. franciscana* reduces hatching by 15% after desiccation and freezing of diapausing cysts (Fatani, 2017). Therefore, knockdown of Hsf1 may reduce stress tolerance in diapausing cysts because HSP90 is decreased. HSP90 is not the only HSP regulated by HSF1 during diapause. Two

Hsp70s and Hsp60 in the fresh fly *S. crassipalpis* are important during diapause (Rinehart et al., 2007) and Hsp70 and Hsp60 are regulated by Hsf1 during the recovery from hypoxia (Michaud et al., 2011). Knockdown of Hsf1 probably sabotages stress tolerance by down-regulating multiple HSPs during *A. franciscana* cyst diapause.

A. franciscana experiences cold and desiccation during diapause as do some other animals (King and MacRae, 2012; Aruda et al., 2011; Kihara et al., 2011; King and MacRae, 2015). HSPs are up-regulated to protect animals against cold environment and desiccation and their synthesis is probably regulated by Hsf1. For example, HSPs are induced in *Drosophila* upon cold stress accompanied by an increase in dHSFd, a spliced isoform of *Drosophila* HSF1 (Fujikake et al., 2005). Hsp70, which is probably regulated by Hsf1, is up-regulated to protect *S. crassipalpis* and the eutardigrade *Richtersius coronifer* during desiccation (Tammariello et al., 1999; Jonsson and Schill, 2007). Additionally, Hsf1 is required to protect the fresh fly *S. crassipalpis* because it promotes the synthesis of the sHsps, Hsp23 and Hsp27, during desiccation and rehydration (Hayward et al., 2003). These examples support the role of HSF1 in generating tolerance to desiccation and cold, stresses commonly encountered by *A. franciscana* during diapause.

4.4 Knockdown of Hsf1 decreases the longevity of *A. franciscana* adult females

A. franciscana females injected with *GFP* dsRNA tended to live longer than females receiving *hsf1* dsRNA, with females possessing Hsf1 usually producing 4

broods before death while those lacking Hsf1 usually producing 2 broods. Interestingly, some females injected with *GFP* dsRNA survived for a few months and one even lived for 11 months. Knockdown of Hsf1 reduced survival time equally for females producing either cysts or nauplii, showing that Hsf1 is important to their longevity regardless of the embryos they are carrying. Observations from other species support the importance of Hsf1 in longevity. For example, over-expression of Hsf1 increases the life span of *C. elegans* (Murshid et al., 2013; Zhao et al., 2005) whereas loss of Hsf1 reduces the life span because a calcium-binding protein, PAT-10 is lost. The loss of PAT-10 decreases actin filament stability and causes the collapse of the cytoskeleton (Baird et al., 2014). HSF1 regulates the expression of genes in human cancer cells required for metabolism, the cell cycle and translation (Mendillo et al., 2012) and knockdown in HeLa cells further reveals that HSF1 regulates genes related to protein folding, apoptosis, RNA splicing, and ubiquitination (Nakai, 2016; Page et al., 2006), all important processes in *A. franciscana* adults. Examination of an *hsf1* mutant of *S. cerevisiae* demonstrated that Hsf1 controls genes needed for the maintenance of cell wall integrity, energy metabolism, protein degradation and carbohydrate metabolism (Yamamoto et al., 2005). In other organisms, processes associated with development, reproduction, metabolism and virulence were shown to be influenced by HSF1 (Åkerfelt et al., 2010; Fujimoto and Nakai, 2010; Anckar and Sistønen, 2011 and Bruquell et al., 2016). The loss of Hsf1 undoubtly disturbs protein homeostasis, metabolism and cell integrity, which leads to a shortened life span and death of organisms including *A. franciscana*.

A decrease in Hsf1 DNA binding activity decreases HSP70 and life span in *Daphnia pulex* (Schumpert et al., 2014) and decreased Hsp70, which is regulated by Hsf1, reduces the life span of *Drosophila* (Sorensen and Loeschcke, 2002). Hsp70 suppresses apoptosis in mouse cells by interacting with apoptotic regulators such as p38 (Lee et al, 2001), suggesting a protective role for Hsp70. Hsp83, whose synthesis is regulated by Hsf1 (Salamanca et al., 2011), regulates gene expression and signal transduction thereby suppressing mutation-induced phenotypes which could be lethal to *Drosophila* (Lachowiec et al., 2013; Rutherford and Lindquist, 1998; Queitsch et al., 2002) and increasing *Drosophila* longevity (Chen and Wagner, 2012). Thus Hsf1 may maintain *A. franciscana* life span by regulating Hsps.

4.5 Hsf1 influences the survival of *A. franciscana* nauplii

A. franciscana nauplii lacking Hsf1 die before exiting the second instar stage, indicating that Hsf1 is critical to the development of nauplii after their release from females. The digestive system is not fully operational in early nauplii of *A. franciscana* and nauplii use yolk as their source of nutrients until later stages when algae are consumed (Lovett and Felder, 1989). Trypsin and chymotrypsin, the main proteinases responsible for protein digestion, increase during nauplii development and reach maximum levels after the larvae stage where they contribute to nutrient utilization (Hernandez-Cortes et al., 2017). Hsf1 may influence development of the early digestive system. As an example, HSP70, which is activated by HSF1 (Yuan et al., 2017), is augmented in the hepatopancreas as the stock density of the larvae of

white shrimp *Litopenaeus vannamei* increases, enhancing antioxidant ability and protecting hepatopancreas function (Gao et al., 2017). The knockdown of Hsf1 may have reduced Hsp activity and disturbed the digestive system of *A. franciscana* and thus leading to the death of nauplii.

Hsf1 is involved in the evolutionarily conserved insulin and insulin-like growth factor (IGF) signaling IIS pathway which plays a major role in longevity (Murshid et al., 2013) and works with two other transcription factors, Nrf2 and FoxO3 to maintain protein homeostasis in *C. elegans* (Murshid et al., 2013). IGF is essential for the proliferation of embryonic cells from the shrimp, *Penaeus chinensis* (Fan and Wang, 2002), indicating a role in crustacean development. Moreover, the IGF signaling pathway is important for metabolic control in larvae of the white shrimp *Penaeus vannamei* and it is required for muscle contraction in crustaceans (Gutierrez et al., 2007; Chuang and Wang, 1994). Knockdown of Hsf1 may disturb the IGF signaling pathway in *A. franciscana* nauplii and thereby reduce survivability.

4.6 Hsf1 synthesis and localization during the development of *A. franciscana*

4.6.1 Hsf1 during the development of diapause-destined *A. franciscana* embryos

hsf1 mRNA and Hsf1 were in very low amounts in oocytes before fertilization but increased significantly by day 2 post-fertilization in oviparously developing embryos before decreasing until cyst release. The appearance of Hsf1 precedes the synthesis of p26 mRNA in diapause-destined embryos which starts 2 days post fertilization followed on day 3 by p26 production (Liang and MacRae, 1999). The

same is true for *ArHsp21* mRNA which appears in diapause-destined embryos on day 2 post-fertilization and increases until cyst release (Qiu and MacRae, 2008a) and for ArHsp22 mRNA which appears in diapause-destined embryos on day 3 post-fertilization and increases until cyst release (Qiu and MacRae, 2008b). Thus the up-regulation of Hsf1 coincides with the initial production of sHsp mRNA. Hsf1 localized to nuclei at the time production of sHsps mRNA starts, showing that it is appropriately positioned in the cell to initiate transcription. Hsf1 is up-regulated before the production of *Hsp70a* and *Samui* mRNAs which are important for egg development and diapause in *B. mori* (Kihara et al., 2011). The up-regulation of *hsf1* mRNA occurs before *Hsps* mRNA is observed during the recovery of *S. crassipalpis* from hypoxia (Michaud et al., 2011). Hsf1 decreases as diapause-destined embryos develop suggesting that a large amount of Hsf1 is not needed once Hsps or other Hsf1 regulated proteins essential for diapause reach a threshold. Residual Hsf1 in cysts after release from females may be required for the synthesis of proteins such as the constitutively expressed Hsc70 before the cysts enter diapause.

4.6.2 Hsf1 during the development of ovoviviparous embryos

hsf1 mRNA increased in ovoviviparous embryos as did Hsf1 which was present in protein extracts from day 4 nauplius-destined embryos and newly released nauplii where it localized in nuclei, indicating that development from fertilized eggs to nauplii involved Hsf1. Hsf1 was less abundant in ovoviviparous as opposed to oviparous embryos and it localized to nuclei later during development of

ovoviviparous embryos, explaining in part why ovoviviparous embryos don't synthesize diapause-specific molecular chaperones, such as p26 and artemin. Nonetheless, Hsf1 was synthesized in ovoviviparous embryos, and increased as development processed, indicating that it has a different role in ovoviviparously developing embryos and nauplii.

The regulation of Hsps by Hsf1 during development occurs in other species. Increased HSF in *Drosophila* embryos and larvae is essential for the enhanced synthesis of HSP70 (Jedlicka et al., 1997) and the induced synthesis of HSP70 is tightly correlated with the localization of HSF to nuclei (Wang and Lindquist, 1998). Hsf1 regulates Hsp83, the Hsp which mediates posterior pole cell differentiation of *Drosophila* embryo where it may chaperone hormone receptors, tyrosine kinases, protein kinase C (PKC) and tubulin (Ding et al., 1993). Hsf1 regulates genes related to segmentation during late stage *Drosophila* development (Kuchar et al., 2017), and these genes are essential to the development of *A. franciscana* nauplii (Nguyen et al., 2016). Mutation of *hsf1* leading to its inactivation arrests development of *Drosophila* indicating it is required for the expression of genes necessary for cell growth during embryo development (Jedlicka et al., 1997). Hsf1 regulates *HasHsp70* and *HasHsp90* mRNA that appear at the cleavage stage and persist in swimming larvae of the vestigastropod *Haliotis asinine*. Both of these Hsps may recognize and bind unstable motifs of structurally divergent protein that arise during cleavage and later development stages (Gunter and Degnan, 2007). Thus, Hsps are likely to be required during development for the folding of nascent proteins in rapidly growing cells and to

assist in protein translocation through the membranes of developing organelles (Ciocca et al., 2013; Hartl et al., 2011), processes vital for development.

As a final possibility, Hsf1 interconnects the insulin/IGF-1 and TGF-β (transforming growth factor-beta) pathways to control development of *C. elegans* (Barna et al., 2012). The function of Hsf1 is achieved by regulating the expression of *daf-7* which encodes a TGF-β ligand to induce the TGF-β signaling axis promoting the development of young larvae (Barna et al., 2012). Hsf1 also interacts with and regulates DAF-16/FoXO in insulin/IGF-1 signaling and thereby maintains protein homeostasis and promotes development (Murshid et al., 2013; Barna et al., 2012).

4.7 Conclusions

A. franciscana Hsf1 is a transcription factor similar in sequence and domain structure to Hsf1s from other species. RNAi was used in this work to knock down Hsf1 in cysts and nauplii. Cysts with decreased Hsf1 entered diapause but exhibited reduced stress tolerance which undoubtedly due to the reduction in p26, ArHsp21, ArHsp22 and artemin. The viability of *A. franciscana* nauplii was reduced sharply due to Hsf1 knockdown, indicating a role for Hsf1 in nauplius growth and development. The life span of *A. franciscana* females decreased due to Hsf1 knockdown, demonstrating that Hsf1 influences *A. franciscana* survivability.

Hsf1 appeared in both oviparously and ovoviviparously developing *A. franciscana* embryos, but the spatial and temporal distribution patterns were different. Hsf1 was more abundant in oviparously developing embryos than in ovoviviparously

developing embryos and Hsf1 located to nuclei earlier in the former than in the latter. Additionally, Hsf1 decreased in oviparous embryos after day 2 post-fertilization whereas it increased in ovoviviparous embryos. These data indicate that Hsf1 has different roles in oviparously versus ovoviviparously developing embryos, especially in the synthesis of sHsps but also in general growth and development of the organism.

The work described in this study constitutes, to the best of my knowledge, the first *in vivo* demonstration that Hsf1 has an important role in rendering diapause and quiescent cysts of *A. franciscana* stress tolerant and that the influence of Hsf1 resides, at least in part, in its ability to regulate the synthesis of molecular chaperones. Novel developmental effects of Hsf1 on nauplii were revealed suggesting the importance of Hsf1 during developmental processes other than diapause. Overall, this research contributes to our understanding of the role of Hsf1 in diapause and development in *A. franciscana*, a novel model crustacean. *A. franciscana* is also an important feed source for aquaculture and crustaceans are becoming more valuable as a source of food. The research thus has the potential to be applied to aquaculture.

APPENDIX A Supplemental data

A

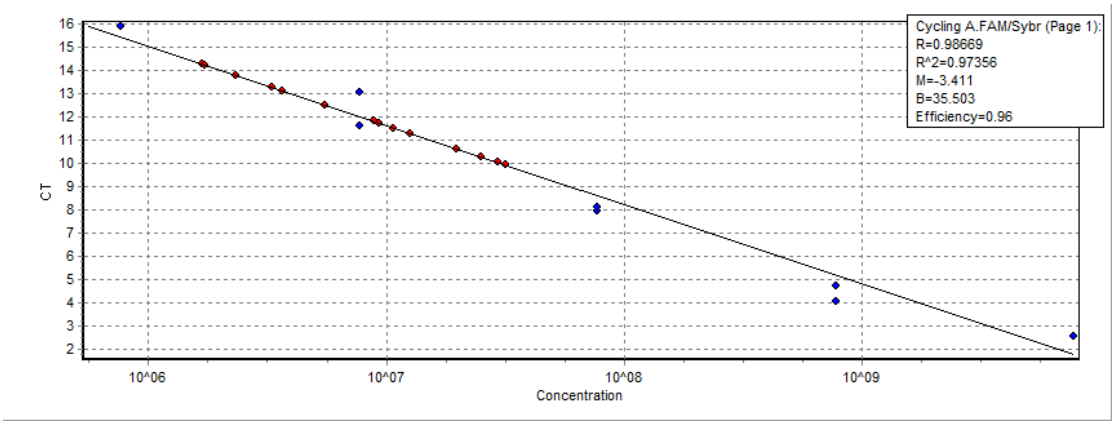

B

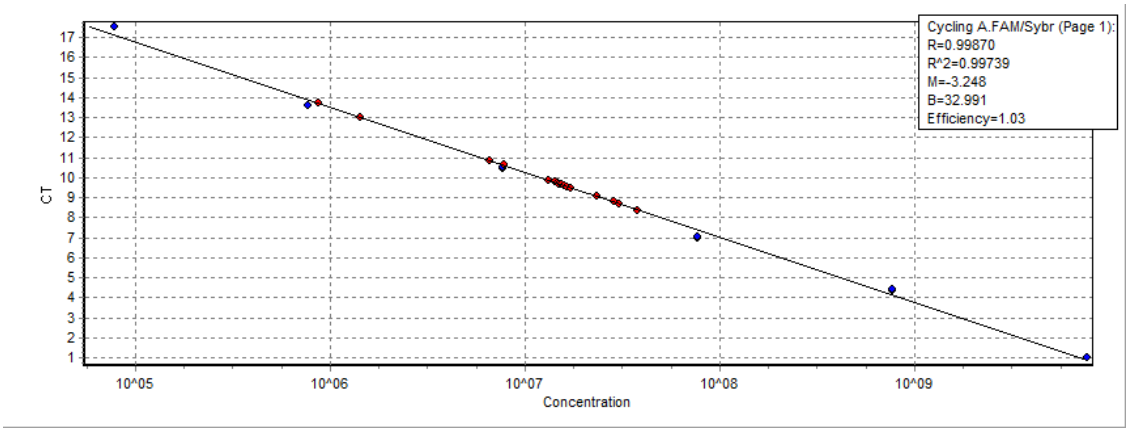

C

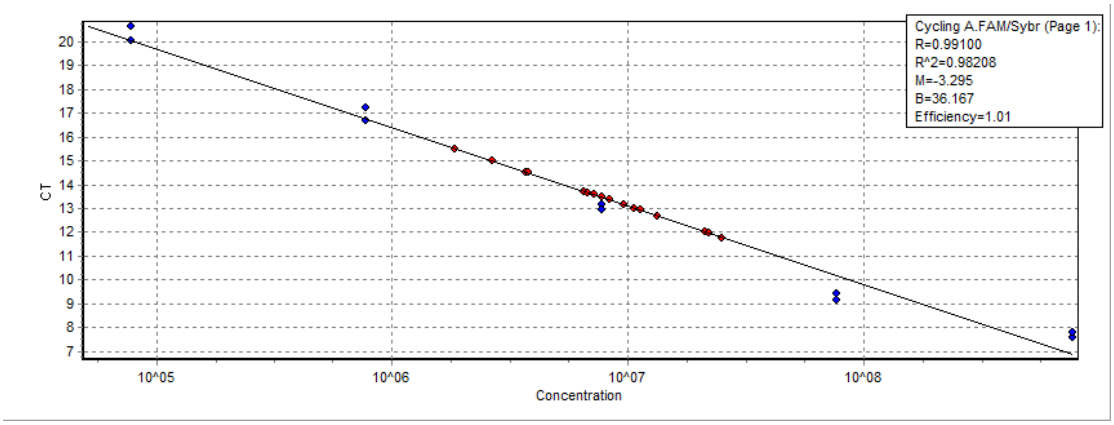

D

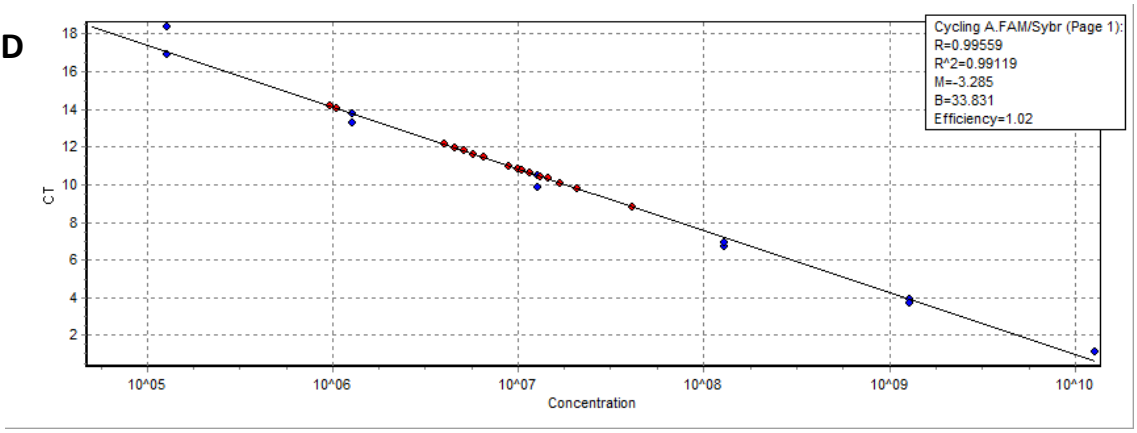
Cycling A.FAM/Sybr (Page 1):
R=0.99559
R^2=0.99119
M=-3.285
B=33.831
Efficiency=1.02
CT
Concentration
10^05
10^06
10^07
10^08
10^09
10^10

E

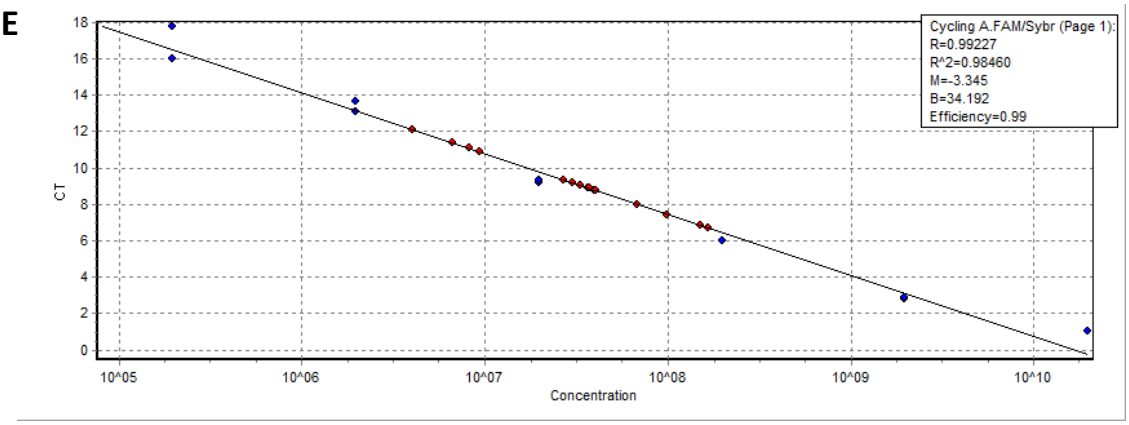
Cycling A.FAM/Sybr (Page 1):
R=0.99227
R^2=0.98460
M=-3.345
B=34.192
Efficiency=0.99
CT
Concentration
10^05
10^06
10^07
10^08
10^09
10^10

F

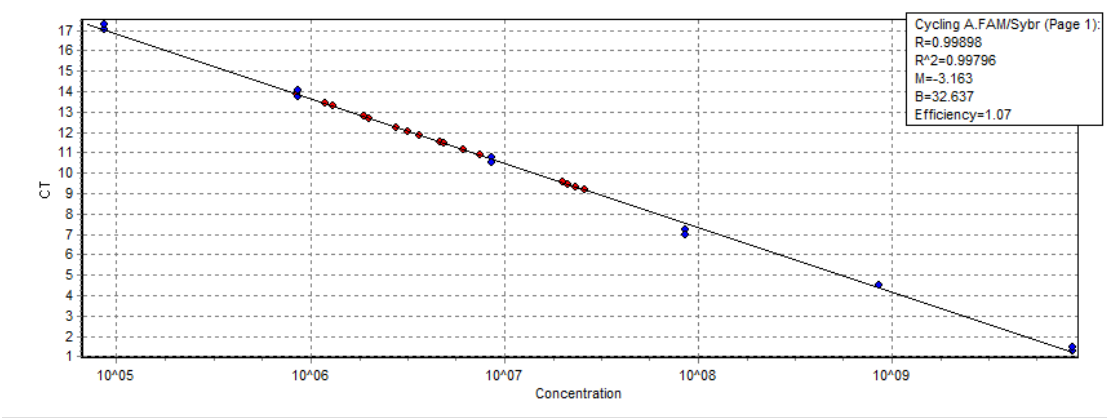
Cycling A.FAM/Sybr (Page 1):
R=0.99898
R^2=0.99796
M=-3.163
B=32.637
Efficiency=1.07
CT
Concentration
10^05
10^06
10^07
10^08
10^09

G

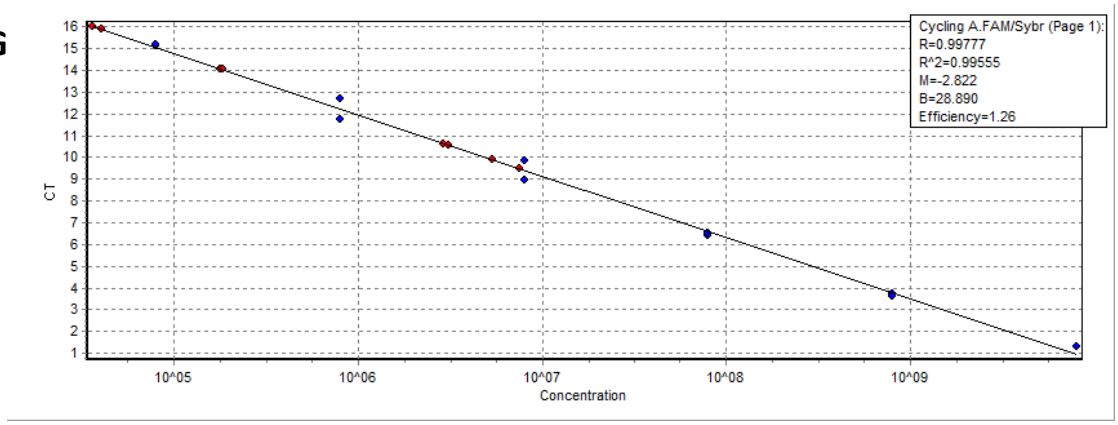
Cycling A.FAM/Sybr (Page 1):
R=0.99777
R^2=0.99555
M=-2.822
B=28.890
Efficiency=1.26
CT
Concentration
10^05
10^06
10^07
10^08
10^09

H

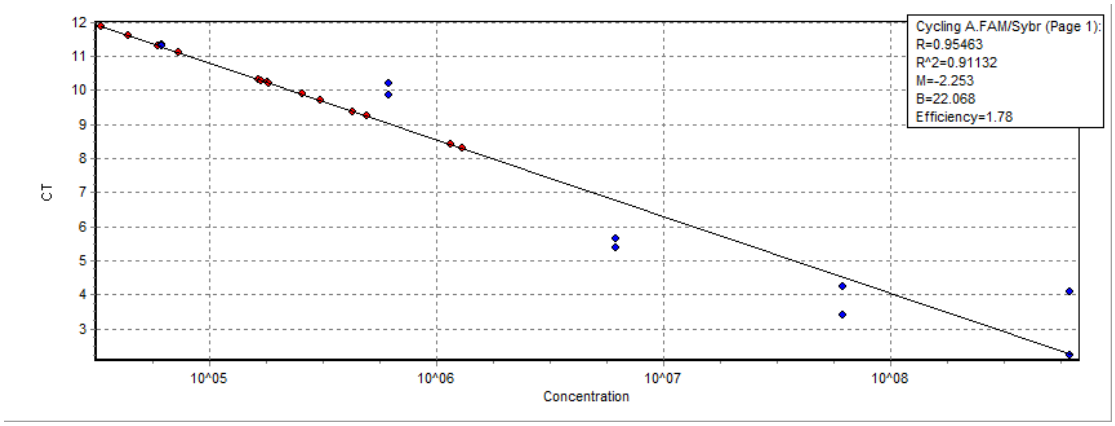
Cycling A.FAM/Sybr (Page 1):
R=0.95463
R^2=0.91132
M=-2.253
B=22.068
Efficiency=1.78
CT
Concentration
10^05
10^06
10^07
10^08

I

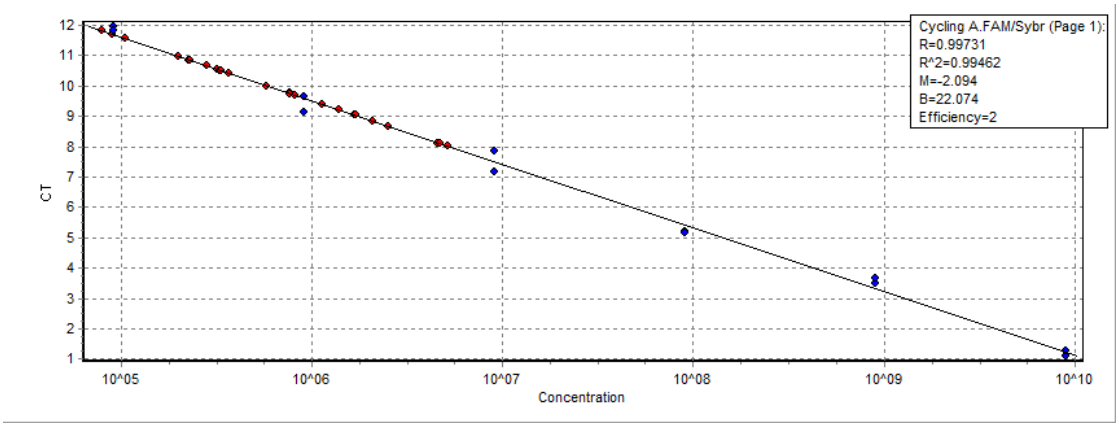
Cycling A.FAM/Sybr (Page 1):
R=0.99731
R^2=0.99462
M=-2.094
B=22.074
Efficiency=2
CT
Concentration
10^05
10^06
10^07
10^08
10^09
10^10

J

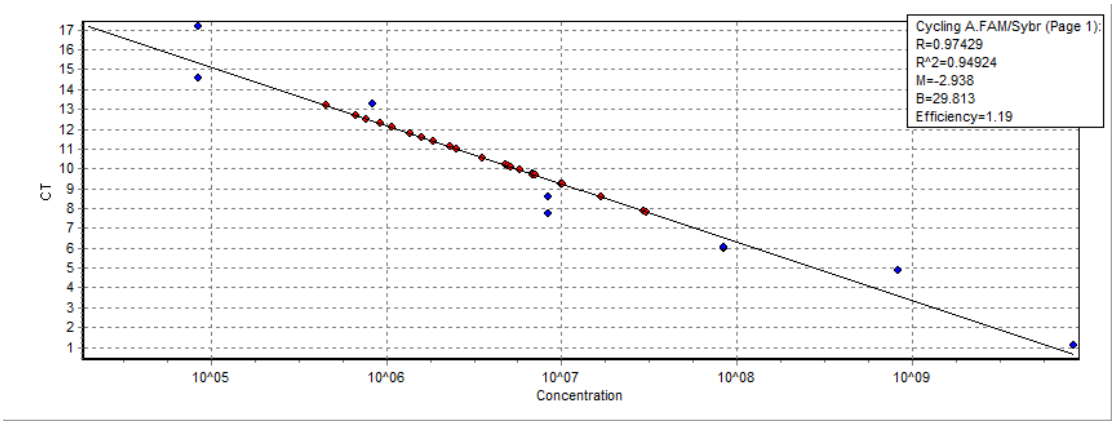
Cycling A.FAM/Sybr (Page 1):
R=0.97429
R^2=0.94924
M=-2.938
B=29.813
Efficiency=1.19
CT
Concentration
10^05
10^06
10^07
10^08
10^09

K

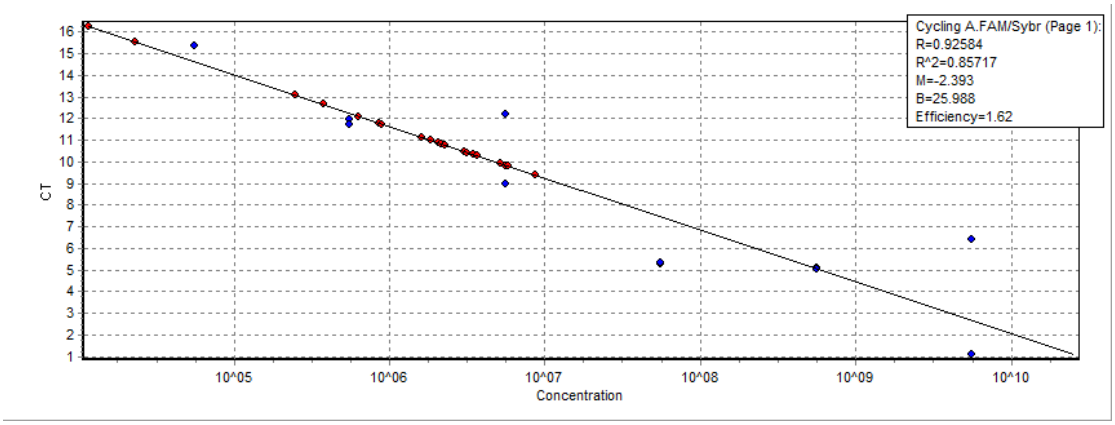
Cycling A.FAM/Sybr (Page 1):
R=0.92584
R^2=0.85717
M=-2.393
B=25.988
Efficiency=1.62
CT
Concentration
10^05
10^06
10^07
10^08
10^09
10^10

L

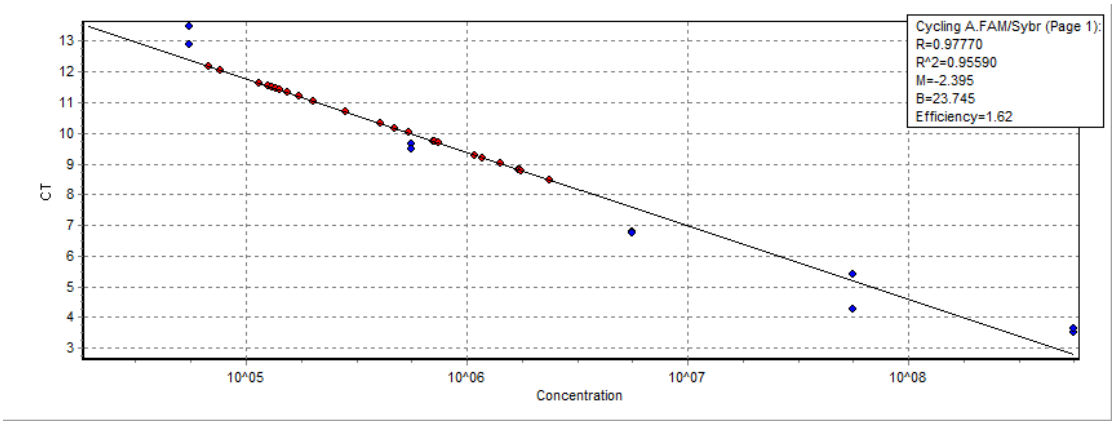
Cycling A.FAM/Sybr (Page 1):
R=0.97770
R^2=0.95590
M=-2.395
B=23.745
Efficiency=1.62
CT
Concentration
10^05
10^06
10^07
10^08

Fig A1. Standard curves for copy numbers of the transcripts of different genes generated by qPCR. qPCR was performed with templates (blue dots) of known concentration (copy number per μl) to generate curves based on cycle threshold values for different transcripts. A, *α-tubulin* of knockdown cysts; B, *hsf1* of knockdown cysts; C, *p26* of knockdown cysts; D, *ArHsp21* of knockdown cysts; E, *ArHsp22* of knockdown cysts; F, *Artemin* of knockdown cysts; G, *α-tubulin* of knockdown nauplii; H, *hsf1* of knockdown nauplii; I, *α-tubulin* of oviparous oocytes, embryos on 2 and 4 days after fertilization and freshly released cysts; J, *hsf1* of oviparous oocytes, embryos on 2 and 4 days after fertilization and freshly released cysts; K, *α-tubulin* of ovoviviparous oocytes, embryos on 2 and 4 days after fertilization and freshly released nauplii; L, *hsf1* of ovoviviparous oocytes, embryos on 2 and 4 days after fertilization and freshly released nauplii.

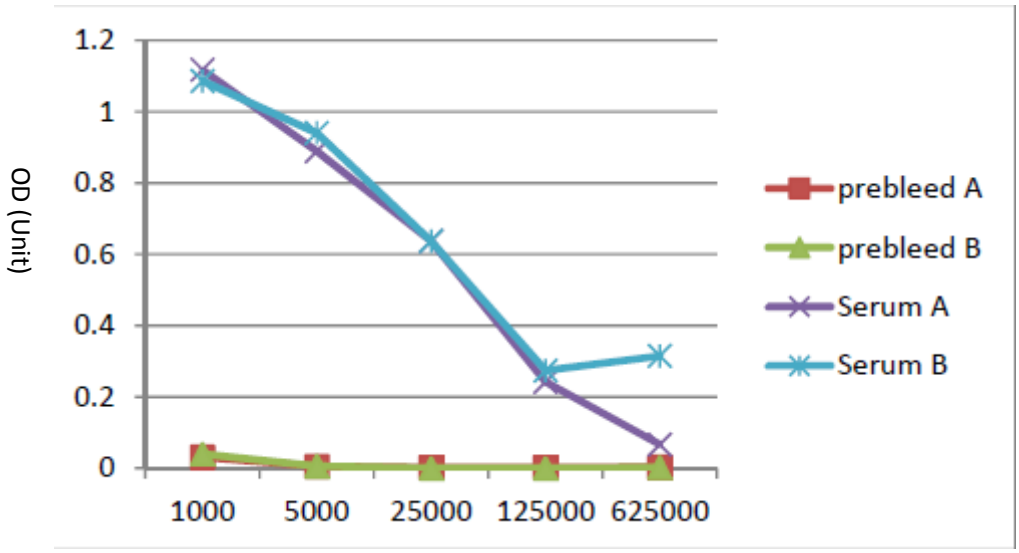

Fig A2. Titration for prebleed and first bleed serum from rabbit A and B, both of which were injected with antigen as mentioned in material and method. Figure was provided by Abbiotec.

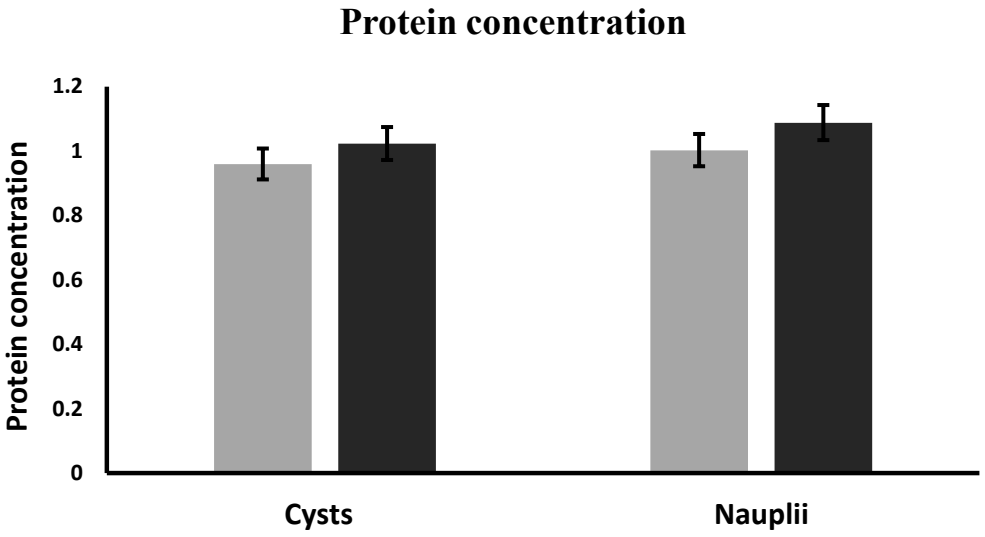

Figure A3. Proteins prepared from 50 cysts and 60 nauplii were measured with SPECTRAmax PLUS384 (Molecular Device, Sunnyvale, CA, USA) and compared with a protein standard made with BSA (ThermoFisher Scientific). Four individual samples were prepared and measured for GFP (Grey) and Hsf1 (Black) knockdown cysts and nauplii. Error bars show standard deviation.

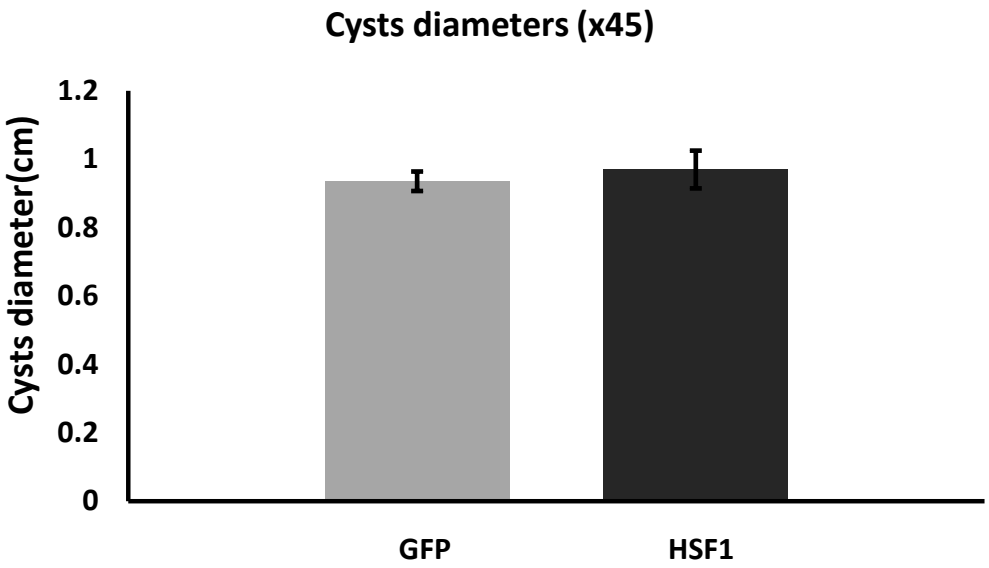

Fig. A4. Cysts diameters and protein containing. The diameters of cysts released from females receiving *GFP* and *hsf1* dsRNA were measured with an eyepiece micrometer under Olympus SZ61 stereomicroscope (Olympus).at 45x magnification. 50 cysts were used in each of 4 individual experiments. Error bars show standard deviation.

Fig A5. Antibody specificity for fluorescence probing. Embryos on 2 days after fertilization were gently crushed to release nuclei and reacted with PBSAT without Hsf1 antibody, Hsf1 antibody pre-mixed with antigen and Hsf1 antibody separately, and followed by fluorescein isothiocyanate-conjugated goat anti-rabbit IgG. Samples were then stained with DAPI, mounted in mounting media and examined by confocal microscopy.

APPENDIX B Micropipette preparation

Setting for pulling micropipettes used in microinjection of *A. francsicana* females.

Heat: 950

Pull: 12

Velocity: 100

Time: 150

Pressure: 500

APPENDIX C Solutions and recipes

Arranged by the order in which they appear in the Materials and Methods

Solutions for agarose gels

5 x TBE (diluted 10-fold for electrophoresis)

54 g Tris

27.5 g boric acid

20 ml 0.5 M EDTA, pH 8.0

dH_2O to 1 litre

stored in plastic bottle in room temperature

Solutions for bacteria growth and protein expression

LB broth

12.5 g LB broth miller

dH_2O to 500 ml and autoclave

LB petri dish with Amp

7.5 g LB broth miller

4.5 g agarose

dH_2O to 300 ml and autoclave

add 0.3 ml 50 mg/ml Amp, mix and add 20 ml to each petri dish

SOC media

0.4 g Tryptone

0.1 g yeast extracts

0.05 g NaCl

0.2 ml 250 mM KCl

add dH_2O to total volume 20ml, use NaOH adjust pH to 7.0, autoclave

After cooling to room temperature Add autoclaved 0.2 ml 2 M $MgCl_2$ and 0.2 ml 2 M glucose sterilized with 0.22 μm filter membrane.

IPTG solution (200 mg/ml)

1 g IPTG

dH_2O to 5 ml and filter through 0.22 µl membrane

Ampicillin solution (50 mg/ml)

0.1 g Ampicillin

dH_2O to 2 ml

X-Gal (20 mg/ml)

0.1 g X-Gal

dH_2O to 5 ml

Solutions for SDS-Polyacrylamide Gel Electrophoresis

PIPES buffer: 100 mM Pipes, 1 mM $MgCl_2$ 1 mM EGTA

30.24 g Pipes

0.31 g $MgCl_2$

0.38 g EGTA

dH_2O to 1 L

pH 6.5

1A: acylamide/bis-acrylamide, 37.5:1 in dH_2O storage in 4℃

1B: 1.5 M Tris (pH 8.8) with 0.5% (w/v) SDS

18.3 g Tris

2.5 ml 20% (w/v) SDS

dH_2O to 100 ml

pH 8.8

1C: 0.2% (v/v) TEMED

100 µl TEMED

dH_2O to 50 ml

1D: 5% (w/v) ammonium persulfate

50 mg ammonium persulfate

dH_2O to 10 ml

2B: 0.5 M Tris (pH 6.8) with 0.5% (w/v) SDS

6.0 g Tris

2.5 ml 20% (w/v) SDS

dH_2O to 100 ml

pH 6.8

2C: 2% (v/v) TEMED

100 µl TEMED

dH_2O to 5 ml

12.5% SDS Polyacrylamide Running Gel

1A (acrylamide/bis-acrylamide, 37.5:1 in deionized H_2O) 5.0 ml, 1B 4.0 ml, 1C 2.0 ml, dH_2O 3.0 ml, 1D 2.0 ml

SDS Polyacrylamide Stacking Gel

1A 1.0 ml, 2B 2.5 ml, 2C 1.25 ml, dH_2O 4.0 ml, 1D 1.25 ml

2 x Treatment Buffer (diluted four-fold for electrophoresis): 125 mM Tris, 140 mM SDS, 20% (v/v) glycerol, 10% (v/v) β-mercaptoethanol, 0.1% (w/v) bromophenol blue, pH 6.8

0.6 g Tris

1.6 g SDS

8 ml glycerol

4 ml β-mercaptoethanol

0.04 g bromophenol blue

dH_2O to 40 ml

pH 6.8

Running Buffer: 25 mM Tris, 200 mM glycine with 0.04% (w/v) SDS

12.0 g Tris

57.6 g glycine

8.0 ml 20% (w/v) SDS

dH_2O to 4 L

Solutions for Western Blotting

Transfer Buffer: 25 mM Tris, 200 mM glycine in 20% (v/v) methanol

800 mL methanol

12.0 g Tris

57.6 g glycine

dH_2O to 4 L

TBS: 10 mM Tris, 140 mM NaCl, pH 7.4

1.21 g Tris

8.18 g NaCl

dH_2O to 1 L

pH 7.4

TBS-T: 10 mM Tris, 140 mM NaCl and 0.1% Tween-20, pH 7.4

1.21 g Tris

8.18 g NaCl

1 mL Tween-20

dH_2O to 1 L

pH 7.4

HST: 10 mM Tris, 1 M NaCl, 0.5% (v/v) Tween-20, pH 7.4

1.21 g Tris

58.4 g NaCl

5 ml Tween-20

dH_2O to 1 L

pH 7.4

2% ponceau S solution (0.1% (w/v) ponceau S, 5% (v/v) acetic acid)

2.0 g ponceau S

30.0 g Trichloroacetic acid (TCA)

Add dH_2O to 1L

Solutions for immunofluoresence

PBS: 137 mM NaCl, 2.7 mM KCl, 10 mM Na_2HPO_4, 1.8 mM KH_2PO_4

8.0 g NaCl

2.7 g KCl

1.42 g Na_2HPO_4

0.24 g KH_2PO_4

pH 7.4

dH_2O to 1 L and autoclave

PBSAT: 0.5% BSA (w/v), 0.75% Triton X-100 (w/v) in PBS

0.25 g BSA

0.376 g Triton X-100

Add PBS buffer to 50 ml

References

Abane, R. and Mezger, V. (2010) Roles of heat shock factors in gametogenesis and development. *Febs J*. 277(20): 4150-4172.

Åkerfelt, M., Morimoto, R. I. and Sistønen, L. (2010) Heat shock factors: Integrators of cell stress, development and lifespan. *Nat. Rev. Mol. Cell Biol*. 11(8): 545-555.

Åkerfelt, M., Trouillet, D., Mezger, V. and Sistønen, L. (2007) Heat shock factors at a crossroad between stress and development. *Ann. NY Acad. Sci*. 1113: 15-27.

Anckar, J. and Sistønen, L. (2011) Regulation of HSF1 function in the heat stress response: Implications in aging and disease. *Annu. Rev. Biochem*. 80: 1089-1115.

Anckar, J. and Sistønen, L (2007) Heat shock factor 1 as a coordinator of stress and developmental pathways. *Adv. Exp. Med. Biol.* 594: 78-88.

Aruda, A. M., Baumgartner, M. F., Reitzel, A. M. and Tarrant, A. M. (2011) Heat shock protein expression during stress and diapause in the marine copepod *calanus finmarchicus. J. Insect Physiol*. 57(5): 665-675.

Baird, N. A., Douglas, P. M., Simic, M. S., Grant, A. R., Moresco, J. J., Wolff, S. C., Yates, John R., III., Manning, G. and Dillin, A. (2014) HSF-1-mediated cytoskeletal integrity determines thermotolerance and life span. *Science*. 346(6207): 360-363.

Bakthisaran, R., Tangirala, R. and Rao, C. M. (2015) Small heat shock proteins: Role in cellular functions and pathology. *BBA-Proteins Proteomics* 1854(4): 291-319.

Baringou, S., Rouault, J., Koken, M., Hardivillier, Y., Hurtado, L. and Leignel, V. (2016) Diversity of cytosolic HSP70 heat shock protein from decapods and their phylogenetic placement within arthropoda. *Gene* 591(1): 97-107.

Barna, J., Princz, A., Kosztelnik, M., Hargitai, B., Takacs-Vellai, K. and Vellai, T. (2012) Heat shock factor-1 intertwines insulin/IGF-1, TGF-beta and cGMP signaling to control

development and aging. *BMC Dev. Biol*. 12: 32.

Birch-Machin, I., Gao, S., Huen, D., McGirr, R., White, R. and Russell, S. (2005) Genomic analysis of heat-shock factor targets in *drosophila*. *Genome Biol*. 6(7): R63.

Brunquell, J., Morris, S., Lu, Y., Cheng, F. and Westerheide, S. D. (2016) The genome-wide role of HSF-1 in the regulation of gene expression in *caenorhabditis elegans*. *BMC Genomics*. 17: 559.

Bu, L., Jin, Y., Shi, Y., Chu, R., Ban, A., Eiberg, H., Andres, L., Jiang, H., Zheng, G., Qian, M., Cui, B., Xia, Y., Liu, J., Hu, L., Zhao, G., Hayden, M. and Kong, X. (2002) Mutant DNA-binding domain of HSF4 is associated with autosomal dominant lamellar and marner cataract. *Nat. Genet*. 31(3): 276-278.

Carra, S., Alberti, S., Arrigo, P. A., Benesch, J. L., Benjamin, I. J., Boelens, W., Bartelt-Kirbach, B., Brundel, B. J. J. M., Buchner, J., Bukau, B., Carver, J. A., Ecroyd, H., Emanuelsson, C., Finet, S., Golenhofen, N., Goloubinoff, P., Gusev, N., Haslbeck, M., Hightower, L. E., Kampinga, H. H., Klevit, R. E., Liberek, K., Mchaourab, H. S., McMenimen, K. A., Poletti, A., Quinlan, R., Strelkov, S. V., Toth, M. E., Vierling, E. and Tanguay, R. M. (2017) The growing world of small heat shock proteins: From structure to functions. *Cell Stress Chaperones*. 22(4): 601-611.

Chang, Y., Ostling, P., Åkerfelt, M., Trouillet, D., Rallu, M., Gitton, Y., El Fatilmy, R., Fardeau, V., Le Crom, S., Morange, M., Sistønen, L. and Mezger, V. (2006) Role of heat-shock factor 2 in cerebral cortex formation and as a regulator of p35 expression. *Genes Dev*. 20(7): 836-847.

Chen, B. and Wagner, A. (2012) Hsp90 is important for fecundity, longevity, and buffering of cryptic deleterious variation in wild fly populations. *BMC Evol. Biol*. 12: 25.

Chen, T., Amons, R., Clegg, J., Warner, A. and MacRae, T. (2003) Molecular characterization of artemin and ferritin from *Artemia franciscana*. *Eur. J. Biochem*. 270(1): 137-145.

Chen, T., Villeneuve, T. S., Garant, K. A., Amons, R. and MacRae, T. H. (2007) Functional

characterization of artemin, a ferritin homolog synthesized in *Artemia* embryos during encystment and diapause. *Febs J*. 274(4): 1093-1101.

Chen, Y. and Currie, R. (2006) Small interfering RNA knocks down heat shock factor-1 (HSF-1) and exacerbates pro-inflammatory activation of NF-kappa B and AP-1 in vascular smooth muscle cells. *Cardiovasc. Res*. 69(1): 66-75.

Chuang, N. and Wang, P. (1994) Characterization of Insulin-Receptor from the Muscle of the Shrimp *Penaeus-Japonicus* (Crustacea, Decapoda). *Comp. Biochem. Physiol. C-Pharmacol. Toxicol. Endocrinol*. 108: 289-297.

Ciocca, D. R., Arrigo, A. P. and Calderwood, S. K. (2013) Heat shock proteins and heat shock factor 1 in carcinogenesis and tumor development: An update. *Arch. Toxicol*. 87(1): 19-48.

Clark, M. S., Denekamp, N. Y., Thorne, M. A. S., Reinhardt, R., Drungowski, M., Albrecht, M. W., Klages, S., Beck, A., Kube, M. and Lubzens, E. (2012) Long-term survival of hydrated resting eggs from *Brachionus plicatilis*. *PLoS One*. 7(1): e29365.

Clegg, J. S. (2011) Stress-related proteins compared in diapause and in activated, anoxic encysted embryos of the animal extremophile, *Artemia franciscana*. *J. Insect Physiol*. 57(5): 660-664.

Clegg, J. S. (2005) Desiccation tolerance in encysted embryos of the animal extremophile, *Artemia. Integr. Comp. Biol*. 45(5): 715-724.

Clegg, J. S. (1997) Embryos of *Artemia franciscana* survive four years of continuous anoxia: The case for complete metabolic rate depression. *J. Exp. Biol*. 200(3): 467-475.

Clegg, J. S. (1967) Metabolic studies of cryptobiosis in encysted embryos of *Artemia salina*. *Comp. Biochem. Physiol*. 20(3): 801-&.

Clegg, J. S. and Evans, D. (1962) Free glycerol in dormant cysts of the brine shrimp, *Artemia salina*. *Am. Zool*. 2(3): 399-399.

Clegg, J., Drinkwater, L. and Sorgeloos, P. (1996) The metabolic status of diapause embryos of

Artemia franciscana (SFB). *Physiol. Zool*. 69(1): 49-66.

Clos, J., Westwood, J., Becker, P., Wilson, S., Lambert, K. and Wu, C. (1990) Molecular-cloning and expression of a hexameric *Drosophila* heat-shock factor subject to negative regulation. *Cell*. 63(5): 1085-1097.

Colinet, H., Lee, S. F. and Hoffmann, A. (2010) Temporal expression of heat shock genes during cold stress and recovery from chill coma in adult *Drosophila melanogaster*. *Febs J*. 277(1): 174-185.

Craig, E. A. (2018) Hsp70 at the membrane: Driving protein translocation. *BMC Biol*. 16: 11.

Dai, L., Chen, D., Liu, Y., Zhao, Y., Yang, F., Yang, J. and Yang, W. (2011) Extracellular matrix peptides of *Artemia* cyst shell participate in protecting encysted embryos from extreme environments. *PLoS One* 6(6): e20187.

Denekamp, N. Y., Thorne, M. A. S., Clark, M. S., Kube, M., Reinhardt, R. and Lubzens, E. (2009) Discovering genes associated with dormancy in the monogonont rotifer *Brachionus plicatilis*. *BMC Genomics* 10: 108.

Ding, D., Parkhurst, S. M., Halsell, S. R. and Lipshitz, H. D. (1993) Dynamic Hsp83 RNA localization during *Drosophila* oogenesis and embryogenesis. *Mol. Cell. Biol*. 13(6): 3773-3781.

Duarte, F. M., Fuda, N. J., Mahat, D. B., Core, L. J., Guertin, M. J. and Lis, J. T. (2016) Transcription factors GAF and HSF act at distinct regulatory steps to modulate stress-induced gene activation. *Genes Dev*. 30(15): 1731-1746.

Edelmann, W., Cohen, P., Kneitz, B., Winand, N., Lia, M., Heyer, J., Kolodner, R., Pollard, J. and Kucherlapati, R. (1999) Mammalian *MutS* homologue 5 is required for chromosome pairing in meiosis. *Nat. Genet*. 21(1): 123-127.

Eriksson, M., Jokinen, E., Sistønen, L. and Leppa, S. (2000) Heat shock factor 2 is activated during mouse heart development. *Int. J. Dev. Biol*. 44(5): 471-477.

Fan, L., Lin, J., Zhong, Y. and Liu, J. (2013) Shotgun proteomic analysis on the diapause and non-diapause eggs of domesticated silkworm *Bombyx mori*. *PLoS One*. 8(4): e60386.

Fan, T. and Wang, X. (2002) In vitro culture of embryonic cells from the shrimp, *Penaeus chinensis*. *J. Exp. Mar. Biol. Ecol*. 267: 175-184.

Fargeas, C., Florek, M., Huttner, W. and Corbeil, D. (2003) Characterization of prominin-2, a new member of the prominin family of pentaspan membrane glycoproteins. *J. Biol. Chem*. 278(10): 8586-8596.

Fatani. A. (2017) Hsp90 in *Artemia franciscana* During Development and Diapause. Master's thesis., Dalhousie University. http://hdl.handle.net/10222/73003.

Fire, A., Xu, S., Montgomery, M., Kostas, S., Driver, S. and Mello, C. (1998) Potent and specific genetic interference by double-stranded RNA in *Caenorhabditis elegans*. *Nature* 391(6669): 806-811.

Fremdt, H., Amendt, J. and Zehner, R. (2014) Diapause-specific gene expression in *Calliphora vicina* (Diptera: Calliphoridae)-a useful diagnostic tool for forensic entomology. *Int. J. Legal Med*. 128: 1001-1011.

Friedrich, K., Giese, K., Buan, N. and Vierling, E. (2004) Interactions between small heat shock protein subunits and substrate in small heat shock protein-substrate complexes. *J. Biol. Chem*. 279(2): 1080-1089.

Fujikake, N., Nagai, Y., Popiel, H., Kano, H., Yamaguchi, M. and Toda, T. (2005) Alternative splicing regulates the transcriptional activity of *Drosophila* heat shock transcription factor in response to heat/cold stress. *FEBS Lett*. 579: 3842-3848.

Fujimoto, M. and Nakai, A. (2010) The heat shock factor family and adaptation to proteotoxic stress. *Febs J*. 277(20): 4112-4125.

Fujimoto, M., Hayashida, N., Katoh, T., Oshima, K., Shinkawa, T., Prakasam, R., Tan, K., Inouye, S., Takii, R. and Nakai, A. (2010) A novel mouse HSF3 has the potential to activate

nonclassical heat-shock genes during heat shock. *Mol. Biol. Cell.* 21(1): 106-116.

Gao, Y., He, Z., Vector, H., Zhao, B., Li, Z., He, J., Lee, J. and Chu, Z. (2017) Effect of stocking density on growth, oxidative stress and HSP 70 of pacific white shrimp *Litopenaeus vannamei*. *Turk. J. Fish. Quat. Sci*. 17(5): 877-884.

Ghildiyal, M. and Zamore, P. D. (2009) Small silencing RNAs: An expanding universe. *Nat. Rev. Genet*. 10(2): 94-108.

Gkouvitsas, T., Kontogiannatos, D. and Kourti, A. (2008) Differential expression of two small Hsps during diapause in the corn stalk borer *Sesamia nonagrioides* (Lef.). *J. Insect Physiol*. 54: 1503-1510.

Gomez-Pastor, R., Burchfiel, E. T. and Thiele, D. J. (2018) Regulation of heat shock transcription factors and their roles in physiology and disease. *Nat. Rev. Mol. Cell Biol*. 19(1): 4-19.

Gonsalves, S. E., Moses, A. M., Razak, Z., Robert, F. and Westwood, J. T. (2011) Whole-genome analysis reveals that active heat shock factor binding sites are mostly associated with non-heat shock genes in *Drosophila melanogaster*. *PLoS One* 6(1): e15934.

Goto, S. and Kimura, M. (2004) Heat-shock-responsive genes are not involved in the adult diapause of *Drosophila triauraria*. *Gene.* 326: 117-122.

Gunter, H. M. and Degnan, B. M. (2007) Developmental expression of Hsp90, Hsp70 and HSF during morphogenesis in the vetigastropod *Haliotis asinina*. *Dev. Genes Evol*. 217(8): 603-612.

Gutierrez, A., Nieto, J., Pozo, F., Stern, S. and Schoofs, L. (2007) Effect of insulin/IGF-I like peptides on glucose metabolism in the white shrimp *Penaeus vannamei*. *Gen. Comp. Endocrinol*. 153: 170-175.

Hartl, F. U., Bracher, A. and Hayer-Hartl, M. (2011) Molecular chaperones in protein folding and proteostasis. *Nature*. 475(7356): 324-332.

Hashikawa, N., Yamamoto, N. and Sakurai, H. (2007) Different mechanisms are involved in the transcriptional activation by yeast heat shock transcription factor through two different types of heat shock elements. *J. Biol. Chem*. 282: 10333-10340.

Hayward, S., Rinehart, J. and Denlinger, D. (2004) Desiccation and rehydration elicit distinct heat shock protein transcript responses in flesh fly pupae. *J. Exp. Biol*. 207: 963-971.

Hernandez-Cortes, P., Rivera-Perez, C., Garcia-Carreno, F., Martinez-Alarcon, D. (2017) Proteinases during early development of the pacific white leg shrimp *penaeus vannamei*. *Biol. Bull*. 232(1): 2-11.

Hietakangas, V., Ahlskog, J., Jakobsson, A., Hellesuo, M., Sahlberg, N., Holmberg, C., Mikhailov, A., Palvimo, J., Pirkkala, L. and Sistønen, L. (2003) Phosphorylation of serine 303 is a prerequisite for the stress-inducible SUMO modification of heat shock factor 1. *Mol. Cell. Biol*. 23(8): 2953-2968.

Huang, Y., Cai, X., Zou, Z., Wang, S., Wang, G., Wang, Y. and Zhang Z. (2014) Molecular cloning, characterization and expression analysis of three heat shock responsive genes from *Haliotis diversicolor*. *Fish. Shellfish. Immunol*. 36(2):590-9.

Ipsaro, J. J. and Joshua-Tor, L. (2015) From guide to target: Molecular insights into eukaryotic RNA-interference machinery. *Nat. Struct. Mol. Biol*. 22(1): 20-28.

Iryani, M. T. M., MacRae, T. H., Panchakshari, S., Tan, J., Bossier, P., Abd Wahid, M. E. and Sung, Y. Y. (2017) Knockdown of heat shock protein 70 (Hsp70) by RNAi reduces the tolerance of *Artemia franciscana* nauplii to heat and bacterial infection. *J. Exp. Mar. Biol. Ecol*. 487: 106-112.

Jaeger, A. M., Makley, L. N., Gestwicki, J. E. and Thiele, D. J. (2014) Genomic Heat Shock Element Sequences Drive Cooperative Human Heat Shock Factor 1 DNA Binding and Selectivity. *J. Biol. Chem*. 289: 30459-30469.

Jedlicka, P., Mortin, M. and Wu, C. (1997) Multiple functions of drosophila heat shock transcription

factor in vivo. *Embo j*. 16(9): 2452-2462.

Jiang, G., Rowarth, N. M., Panchakshari, S. and MacRae, T. H. (2016) ArHsp40, a type 1 J-domain protein, is developmentally regulated and stress inducible in post-diapause *Artemia franciscana*. *Cell Stress Chaperones*. 21(6): 1077-1088.

Jonsson, K. I. and Schill, R. O. (2007) Induction of Hsp70 by desiccation, ionising radiation and heat-shock in the eutardigrade *Richtersius coronifer*. *Comp. Biochem. Physiol. B-Biochem. Mol. Biol*. 146: 456-460.

Jovanović-Galović, A., Blagojević, D. P., Grubor-Lajsić, G., Worland, R. and Spasić, M. B. (2004) Role of antioxidant defense during different stages of preadult life cycle in european corn borer (*ostrinia nubilalis, hubn*.): Diapause and metamorphosis. *Arch. Insect Biochem. Physiol*. 55(2): 79-89.

Kichine, E., Roze, V., Di Cristofaro, J., Taulier, D., Navarro, A., Streichemberger, E., Decarpentrie, F., Metzler-Guillemain, C., Levy, N., Chiaroni, J., Paquis-Flucklinger, V., Fellmann, F. and Mitchell, M. J. (2012) HSFY genes and the P4 palindrome in the AZFb interval of the human Y chromosome are not required for spermatocyte maturation. *Hum. Reprod*. 27(2): 615-624.

Kihara, F., Niimi, T., Yamashita, O. and Yaginuma, T. (2011) Heat shock factor binds to heat shock elements upstream of heat shock protein 70a and *samui* genes to confer transcriptional activity in *Bombyx mori* diapause eggs exposed to 5 degrees C. *Insect Biochem. Mol. Biol*. 41(11): 843-851.

King, A. M. and MacRae, T. H. (2015) Insect heat shock proteins during stress and diapause. *Annu. Rev. Entomol*. 60: 59-75.

King, A. M. and MacRae, T. H. (2012) The small heat shock protein p26 aids development of encysting *Artemia* embryos, prevents spontaneous diapause termination and protects against stress. *PLoS One* 7(8): e43723.

King, A. M., Toxopeus, J. and MacRae, T. H. (2014) Artemin, a diapause-specific chaperone,

contributes to the stress tolerance of *Artemia franciscana* cysts and influences their release from females. *J. Exp. Biol.* 217(10): 1719-1724.

King, A. M., Toxopeus, J. and MacRae, T. H. (2013) Functional differentiation of small heat shock proteins in diapause-destined *Artemia* embryos. *Febs J*. 280(19): 4761-4772.

Kline, M. and Morimoto, R. (1997) Repression of the heat shock factor 1 transcriptional activation domain is modulated by constitutive phosphorylation. *Mol. Cell. Biol*. 17(4): 2107-2115.

Koštál, V. (2006) Eco-physiological phases of insect diapause. *J. Insect Physiol*. 52(2): 113-127.

Koštál, V., Shimada, K. and Hayakawa, Y. (2000) Induction and development of winter larval diapause in a drosophilid fly, *Chymomyza costata*. *J. Insect Physiol*. 46(4): 417-428.

Kuchar, J., McDonough, C. and Sackerson C. (2007) Heat shock factor controls expression of a non-heat shockprotein gene in *Drosophila* embryos. *Bios*. 78(2): 62-68.

Kus-Liskiewicz, M., Polanska, J., Korfanty, J., Olbryt, M., Vydra, N., Toma, A. and Widlak, W. (2013) Impact of heat shock transcription factor 1 on global gene expression profiles in cells which induce either cytoprotective or pro-apoptotic response following hyperthermia. *BMC Genomics* 14: 456.

Lachowiec, J., Lemus, T., Thomas, J. H., Murphy, P. J. M., Nemhauser, J. L. and Queitsch, C. (2013) The protein chaperone HSP90 can facilitate the divergence of gene duplicates. *Genetics.* 193(4): 1269-+.

Lee, S., Choi, S., Lee, K., Chung, H., Kim, T., Cho, C. and Lee, Y. (2001) Role of inducible heat shock protein 70 in radiation-induced cell death. *Cell Stress and Chaperones*. 6: 273-281.

Li, A. Q., Popova-Butler, A., Dean, D. H. and Denlinger, D. L. (2007) Proteomics of the flesh fly brain reveals an abundance of upregulated heat shock proteins during pupal diapause. *J. Insect Physiol*. 53(4): 385-391.

Li, F., Luan, W., Zhang, C., Zhang, J., Wang, B., Xie, Y., Li, S. and Xiang, J. (2009) Cloning of

cytoplasmic heat shock protein 90 (FcHSP90) from *Fenneropenaeus chinensis* and its expression response to heat shock and hypoxia. *Cell Stress Chaperones* 14(2): 161-172.

Li, J., Han, J., Chen, P., Chang, Z., He, Y., Liu, P., Wang, Q. and Li, J. (2012) Cloning of a heat shock protein 90 (HSP90) gene and expression analysis in the ridgetail white prawn *Exopalaemon carinicauda*. *Fish Shellfish Immunol*. 32(6): 1191-1197.

Li, J., Wei, G., Wang, L., Qian, C., Li, K., Zhang, C., Dai, L., Sun, Y., Liu, D., Zhu, B. and Liu, C. (2016) KPNA3-knockdown eliminates the second heat shock protein peak associated with the heat shock response of male silkworm pupae (*Bombyx mori*) by reducing heat shock factor transport into the nucleus. *Gene* 575(2): 452-457.

Liang, P. and MacRae, T. H. (1999) The synthesis of a small heat shock/alpha-crystallin protein in *Artemia* and its relationship to stress tolerance during development. *Dev. Biol*. 207(2): 445-456.

Lin, J. and Lis, J. (1999) Glycogen synthase phosphatase interacts with heat shock factor to activate *CUP1* gene transcription in *Saccharomyces cerevisiae*. *Mol. Cell. Biol*. 19(5): 3237-3245.

Lovett, D. and Felder, D. (1989) Ontogeny of gut morphology in the white shrimp *Penaeus-setiferus* (decapoda, penaeidae). *J. Morphol*. 201(3): 253-272.

Lu, M., Hua, J., Cui, Y. and Du, Y. (2014) Five small heat shock protein genes from *Chilo suppressalis*: Characteristics of gene, genomic organization, structural analysis, and transcription profiles. *Cell Stress Chaperones*. 19(1): 91-104.

Lu, Y. and Xu, W. (2010) Proteomic and phosphoproteomic analysis at diapause initiation in the cotton bollworm, *Helicoverpa armigera*. *J. Proteome Res*. 9(10): 5053-5064.

Lü, Z. C., Wang, L. H., Zhang, G. F., Wan, F. H., Guo, J. Y., Yu, H. and Wang, J. B. (2014) Three heat shock protein genes from bactrocera (tetradacus) *Minax enderlein*: Gene cloning, characterization, and association with diapause. *Neotropical Entomology.* 43(4): 362-372.

Luo, W., Sun, W., Taldone, T., Rodina, A. and Chiosis, G. (2010) Heat shock protein 90 in

neurodegenerative diseases. *Mol. Neurodegener*. 5: 24.

Ma, W., Li, H., Dai, Z., Yang, J., Yang, F. and Yang, W. (2013) Chitin-binding proteins of *Artemia* diapause cysts participate in formation of the embryonic cuticle layer of cyst shells. *Biochem. J*. 449: 285-294.

MacRae, T. H. (2000) Structure and function of small heat shock/alpha-crystallin proteins: Established concepts and emerging ideas. *Cell Mol. Life Sci*. 57(6): 899-913.

MacRae, T. H. (2005) Diapause: diverse states of development and metabolic arrest. *J.Biol. Res.* 3, 3-14.

MacRae, T. H. (2016) Stress tolerance during diapause and quiescence of the brine shrimp, *Artemia*. *Cell Stress Chaperones.* 21(1): 9-18.

MacRae, T. H. (2010) Gene expression, metabolic regulation and stress tolerance during diapause. *Cell Mol. Life Sci*. 67(14): 2405-2424.

Mahat, D. B., Salamanca, H. H., Duarte, F. M., Danko, C. G. and Lis, J. T. (2016) Mammalian heat shock response and mechanisms underlying its genome-wide transcriptional regulation. *Mol Cell*. 62: 63-78.

McMillan, D., Xiao, X., Shao, L., Graves, K. and Benjamin, I. (1998) Targeted disruption of heat shock transcription factor 1 abolishes thermotolerance and protection against heat-inducible apoptosis. *J. Biol. Chem*. 273(13): 7523-7528.

Mendillo, M. L., Santagata, S., Koeva, M., Bell, G. W., Hu, R., Tamimi, R. M., Fraenkel, E., Ince, T. A., Whitesell, L. and Lindquist, S. (2012) HSF1 drives a transcriptional program distinct from heat shock to support highly malignant human cancers. *Cell*. 150(3): 549-562.

Michaud, M. R., Teets, N. M., Peyton, J. T., Blobner, B. M. and Denlinger, D. L. (2011) Heat shock response to hypoxia and its attenuation during recovery in the flesh fly, *Sarcophaga crassipalpis*. *J. Insect Physiol*. 57: 203-210.

Miozzo, F., Saberan-Djoneidi, D. and Mezger, V. (2015) HSFs, stress sensors and sculptors of transcription compartments and epigenetic landscapes. *J. Mol. Biol*. 427(24): 3793-3816.

Moore, D. S., Hansen, R. and Hand, S. C. (2016) Liposomes with diverse compositions are protected during desiccation by LEA proteins from *Artemia franciscana* and trehalose. *Biochim. Biophys. Acta-Biomembr*. 1858(1): 104-115.

Murshid, A., Eguchi, T. and Calderwood, S. K. (2013) Stress proteins in aging and life span. *Int. J. Hyperthermia*. 29(5): 442-447.

Nakai A (Ed). (2016) Heat Shock Factor. Springer Japan. Print.

Neudegger, T., Verghese, J., Hayer-Hartl, M., Hartl, F. U. and Bracher, A. (2016) Structure of human heat-shock transcription factor 1 in complex with DNA. *Nat. Struct. Mol. Biol*. 23(2): 140-+.

Nguyen, D. V., Christiaens, O., Bossier, P. and Smagghe, G. (2016) RNA interference in shrimp and potential applications in aquaculture. *Rev in Aquacul*. 0, 1-12.

Nilsson, B., Jepsen, P. M., Rewitz, K. and Hansen, B. W. (2014) Expression of hsp70 and ferritin in embryos of the copepod *Acartia tonsa* (dana) during transition between subitaneous and quiescent state. *J. Plankton Res*. 36(2): 513-522.

Page, T. J., Sikder, D., Yang, L., Pluta, L., Wolfinger, R. D., Kodadek, T. and Thomas, R. S. (2006) Genome-wide analysis of human HSF1 signaling reveals a transcriptional program linked to cellular adaptation and survival. *Mol. Biosyst*. 2(12): 627-639.

Perkins, L., Doctor, J., Zhang, K., Stinson, L., Perrimon, N. and Craig, E. (1990) Molecular and developmental characterization of the heat-shock cognate-4 gene of *Drosophila melanogaster*. *Mol. Cell. Biol*. 10(6): 3232-3238.

Pirkkala, L., Nykanen, P. and Sistønen, L. (2001) Roles of the heat shock transcription factors in regulation of the heat shock response and beyond. *Faseb j*. 15(7): 1118-1131.

Pisa, V., Cozzolino, M., Gargiulo, S., Ottone, C., Piccioni, F., Monti, M., Gigliotti, S., Talamo, F., Graziani, F., Pucci, P. and Verrotti, A. C. (2009) The molecular chaperone Hsp90 is a component of the cap-binding complex and interacts with the translational repressor cup during *Drosophila* oogenesis. *Gene.* 432(1-2): 67-74.

Popovic, Z. D., Subotic, A., Nikolic, T. V., Radojicic, R., Blagojevic, D. P., Grubor-Lajsic, G. and Koštál, V. (2015) Expression of stress-related genes in diapause of european corn borer (*Ostrinia nubilalis hbn*.). *Comp. Biochem. Physiol. B-Biochem. Mol. Biol*. 186: 1-7.

Prahlad, V., Cornelius, T. and Morimoto, R. I. (2008) Regulation of the cellular heat shock response in *Caenorhabditis elegans* by thermosensory neurons. *Science* 320(5877): 811-814.

Qiu, Z., Bossier, P., Wang, X., Bojikova-Fournier, S. and MacRae, T. H. (2006) Diversity, structure, and expression of the gene for p26, a small heat shock protein from *Artemia*. *Genomics*. 88(2): 230-240.

Qiu, Z. and MacRae, T. H. (2008) ArHsp21, a developmentally regulated small heat-shock protein synthesized in diapausing embryos of *Artemia franciscana*. *Biochem. J*. 411: 605-611.

Qiu, Z. and MacRae, T. H. (2008) ArHsp22, a developmentally regulated small heat shock protein produced in diapause-destined *Artemia* embryos, is stress inducible in adults. *Febs J*. 275(14): 3556-3566.

Queitsch, C., Sangster, T. A. and Lindquist, S. (2002) Hsp90 as a capacitor of phenotypic variation. *Nature*. 417(6889): 618-624.

Raychaudhuri, S., Loew, C., Koerner, R., Pinkert, S., Theis, M., Hayer-Hartl, M., Buchholz, F. and Hartl, F. U. (2014) Interplay of acetyltransferase EP300 and the proteasome system in regulating heat shock transcription factor 1. *Cell*. 156(5): 975-985.

Reznik, S. Y. and Voinovich, N. D. (2016) Diapause induction in *Trichogramma telengai*: The dynamics of maternal thermosensitivity. *Physiol. Entomol*. 41(4): 335-343.

Rinehart, J. P., Robich, R. M. and Denlinger, D. L. (2006) Enhanced cold and desiccation tolerance

in diapausing adults of *Culex pipiens*, and a role for hsp70 in response to cold shock but not as a component of the diapause program. *J. Med. Entomol*. 43(4): 713-722.

Rinehart, J. P., Li, A., Yocum, G. D., Robich, R. M., Hayward, S. A. L. and Denlinger, D. L. (2007) Up-regulation of heat shock proteins is essentail for cold survival during insect diapause. *Proc. Natl. Acad. Sci.* U. S. A. 104(27): 11130-11137.

Rinehart, J. and Denlinger, D. (2000) Heat-shock protein 90 is down-regulated during pupal diapause in the flesh fly, *Sarcophaga crassipalpis*, but remains responsive to thermal stress. *Insect Mol. Biol*. 9(6): 641-645.

Robbins, H. M., Van Stappen, G., Sorgeloos, P., Sung, Y. Y., MacRae, T. H. and Bossier, P. (2010) Diapause termination and development of encysted *Artemia* embryos: Roles for nitric oxide and hydrogen peroxide. *J. Exp. Biol*. 213(9): 1464-1470.

Rowarth, N. (2017) Developmentally regulated HSP40s mediate diapause and stress tolerance of *Artemia franciscana*. Master's thesis., Dalhousie University, December 2017. http://hdl.handle.net/10222/73503.

Ruckova, E., Muller, P., Nenutil, R. and Vojtesek, B. (2012) Alterations of the Hsp70/Hsp90 chaperone and the HOP/CHIP co-chaperone system in cancer. *Cell. Mol. Biol. Lett*. 17(3): 446-458.

Rungrassamee, W., Leelatanawit, R., Jiravanichpaisal, P., Klinbunga, S. and Karoonuthaisiri, N. (2010) Expression and distribution of three heat shock protein genes under heat shock stress and under exposure to vibrio harvey in *Penaeus monodon*. *Dev. Comp. Immunol*. 34(10): 1082-1089.

Rutherford, S. L. and Lindquist, S. (1998) Hsp90 as a capacitor for morphological evolution. *Nature*. 396(6709): 336-342.

Sakano, D., Li, B., Xia, Q., Yamamoto, K., Fujii, H. and Aso, Y. (2006) Genes encoding small heat shock proteins of the silkworm, *Bombyx mori*. *Biosci. Biotechnol. Biochem*. 70(10):

2443-2450.

Sakurai, H. and Enoki, Y. (2010) Novel aspects of heat shock factors: DNA recognition, chromatin modulation and gene expression. *Febs J*. 277(20): 4140-4149.

Salamanca, H. H., Fuda, N., Shi, H. and Lis, J. T. (2011) An RNA aptamer perturbs heat shock transcription factor activity in *Drosophila melanogaster*. *Nucleic Acids Res*. 39: 6729-6740.

Sasibhushan, S., Ponnuvel, K. M. and Vijayaprakash, N. B. (2012) Diapause specific gene expression in the eggs of multivoltine silkworm *Bombyx mori*, identified by suppressive subtractive hybridization. *Comp. Biochem. Physiol. Biochem. Mol. Biol*. 161(4): 371-379.

Saunders, D., Henrich, V. and Gilbert, L. (1989) Induction of diapause in *Drosophila-melanogaster* photoperiodic regulation and the impact of arrhythmic clock mutations on time measurement. *Proc. Natl. Acad. Sci*. U. S. A. 86(10): 3748-3752.

Scharf, K., Berberich, T., Ebersberger, I. and Nover, L. (2012) The plant heat stress transcription factor (hsf) family: Structure, function and evolution. *Biochimica Et Biophysica Acta-Gene Regulatory Mechanisms*. 1819(2, Sp. Iss. SI): 104-119.

Schopf, F. H., Biebl, M. M. and Buchner, J. (2017) The HSP90 chaperone machinery. *Nat. Rev. Mol. Cell Biol*. 18: 345-360.

Schumpert, C., Handy, I., Dudycha, J. L. and Patel, R. C. (2014) Relationship between heat shock protein 70 expression and life span in *Daphnia*. *Mech. Ageing Dev*. 139: 1-10.

Sharon, M. A., Kozarova, A., Clegg, J. S., Vacratsis, P. O. and Warner, A. H. (2009) Characterization of a group 1 late embryogenesis abundant protein in encysted embryos of the brine shrimp *Artemia franciscana*. *Biochem. Cell Biol*. 87(2): 415-430.

Shi, X., Cui, B., Wang, Z., Weng, L., Xu, Z., Ma, J., Xu, G., Kong, X. and Hu, L. (2009) Removal of Hsf4 leads to cataract development in mice through down-regulation of gamma S-crystallin and bfsp expression. *BMC Mol. Biol*. 10: 10.

Shinka, T., Sato, Y., Chen, G., Naroda, T., Kinoshita, K., Unemi, Y., Tsuji, K., Toida, K., Iwamoto, T. and Nakahori, Y. (2004) Molecular characterization of heat shock-like factor encoded on the human Y chromosome, and implications for male infertility. *Biol. Reprod*. 71(1): 297-306.

Siomi, H. and Siomi, M. C. (2009) On the road to reading the RNA-interference code. *Nature*. 457(7228): 396-404.

Solis, E. J., Pandey, J. P., Zheng, X., Jin, D. X., Gupta, P. B. and Airoidi, E. M. (2016) Defining the essential function of yeast Hsf1 reveals a compact transcriptional program for maintaining eukaryotic proteostasis. *Mol Cell*. 63: 60-71.

Sorensen, J. and Loeschcke, V. (2002) Decreased heat-shock resistance and down-regulation of Hsp70 expression with increasing age in adult *Drosophila melanogaster*. *Funct. Ecol*. 16(3): 379-384.

Sorger, P. and Pelham, H. (1988) Yeast heat-shock factor is an essential dna-binding protein that exhibits temperature-dependent phosphorylation. *Cell*. 54(6): 855-864.

Stahl, P. J., Mielnik, A., Schlegel, P. N. and Paduch, D. A. (2011) Heat shock factor Y chromosome (HSFY) mRNA level predicts the presence of retrievable testicular sperm in men with nonobstructive azoospermia. *Fertil. Steril*. 96(2): 303-308.

Stanley, K. and Fenton, B. (2000) A member of the Hsp60 gene family from the peach potato aphid, *Myzus persicae* (Sulzer.). *Insect Mol. Biol*. 9: 211-215.

Sun, Y. and MacRae, T. (2005) Small heat shock proteins: Molecular structure and chaperone function. *Cell Mol. Life Sci*. 62(21): 2460-2476.

Tammariello, S. P., Rinehart, J. P. and Denlinger, D. L. (1999) Desiccation elicits heat shock protein transcription in the flesh fly, *Sarcophaga crassipalpis*, but does not enhance tolerance to high or low temperatures. *J. Insect Physiol*. 45: 933-938.

Tanabe, M., Kawazoe, Y., Takeda, S., Morimoto, R., Nagata, K. and Nakai, A. (1998) Disruption of the HSF3 gene results in the severe reduction of heat shock gene expression and loss of

thermotolerance. *Embo j*. 17(6): 1750-1758.

Tanguay, J. A., Reyes, R. C. and Clegg, J. S. (2004) Habitat diversity and adaptation to environmental stress in encysted embryos of the crustacean *Artemia*. *J. Biosci*. 29(4): 489-501.

Tarrant, A. M., Baumgartner, M. F., Verslycke, T. and Johnson, C. L. (2008) Differential gene expression in diapausing and active *Calanus finmarchicus* (copepoda). *Mar. Ecol. Prog. Ser*. 355: 193-207.

Toxopeus, J., Warner, A. H. and MacRae, T. H. (2014) Group 1 LEA proteins contribute to the desiccation and freeze tolerance of *Artemia franciscana* embryos during diapause. *Cell Stress Chaperones.* 19(6): 939-948.

Triantaphyllidis, G., Abatzopoulos, T. and Sorgeloos, P. (1998) Review of the biogeography of the genus *Artemia* (crustacea, anostraca). *J. Biogeogr*. 25(2): 213-226.

van Montfort, R., Basha, E., Friedrich, K., Slingsby, C. and Vierling, E. (2001) Crystal structure and assembly of a eukaryotic small heat shock protein. *Nat. Struct. Biol*. 8(12): 1025-1030.

Vasquez, M. C., Murillo, A., Brockmann, H. J. and Julian, D. (2015) Multiple-stressor interactions influence embryo development rate in the american horseshoe crab, *Limulus polyphemus*. *J. Exp. Biol*. 218(15): 2355-2364.

Veeramani, S. and Baskaralingam, V. (2011) Shell-bound iron dependant nitric oxide synthesis in encysted *Artemia* parthenogenetica embryos during hydrogen peroxide exposure. *Biometals.* 24: 1035-1044.

Voellmy, R. (2004) On mechanisms that control heat shock transcription factor activity in metazoan cells. *Cell Stress Chaperones.* 9(2): 122-133.

Wang, H., Wang, X., Zhou, C., Huang, L., Zhang, S., Guo, W. and Kang, L. (2007) cDNA cloning of heat shock proteins and their expression in the two phases of the migratory locust. *Insect Mol. Biol*. 16(2): 207-219.

Wang, Z. and Lindquist, S. (1998) Developmentally regulated nuclear transport of transcription factors in *Drosophila* embryos enable the heat shock response. *Development.* 125: 4841-4850.

Warner, A., Brunet, R., MacRae, T. H. and Clegg, J. S. (2004) Artemin is an RNA-binding protein with high thermal stability and potential RNA chaperone activity. *Arch. Biochem. Biophys*. 424: 189-200.

Warner, A. H., Miroshnychenko, O., Kozarova, A., Vacratsis, P. O., MacRae, T. H., Kim, J. and Clegg, J. S. (2010) Evidence for multiple group 1 late embryogenesis abundant proteins in encysted embryos of *Artemia* and their organelles. *J. Biochem*. 148(5): 581-592.

Westerheide, S. D., Anckar, J., Stevens, S. M., Jr., Sistønen, L. and Morimoto, R. I. (2009) Stress-inducible regulation of heat shock factor 1 by the deacetylase SIRT1. *Science*. 323(5917): 1063-1066.

Wilson, R. C. and Doudna, J. A. (2013) Molecular mechanisms of RNA interference. *Annu. Rev. Biophys*. 42: 217-239.

Xin, N., Sun, J., Zhang, B., Triantaphyllidis, G. V., Van Stappen, G. and Sorgeloos, P. (1994) International study on *Artemia* resources in the People's Republic of China. *Int. J. Salt Lake Res.* 3, 105-112.

Yamamoto, A., Mizukami, Y. and Sakurai, H. (2005) Identification of a novel class of target genes and a novel type of binding sequence of heat shock transcription factor in *Saccharomyces cerevisiae*. *J. Biol. Chem*. 280(12): 11911-11919.

Yamamoto, S., Subedi, G. P., Hanashima, S., Satoh, T., Otaka, M., Wakui, H., Sawada, K., Yokota, S., Yamaguchi, Y., Kubota, H. and Itoh, H. (2014) ATPase activity and ATP-dependent conformational change in the co-chaperone HSP70/HSP90-organizing protein (HOP)*. *J. Biol. Chem*. 289(14): 9880-9886.

Yamamoto, N., Takemori, Y., Sakurai, M., Sugiyama, K. and Sakurai, H. (2009) Differential

recognition of heat shock elements by members of the heat shock transcription factor family. *Febs J*. 276(7): 1962-1974.

Yan, H., Zhang, S., Li, X., Yuan, F., Qiu, W., Chen, Y., Weng, S., He, J. and Chen, Y. (2014) Identification and functional characterization of heat shock transcription factor1 in *Litopenaeus vannamei*. *Fish Shellfish Immunol*. 37(1): 184-192.

Yuan, K., Yuan, F., He, H., Bi, H., Weng, S., He, J. and Chen, Y. (2017) Heat shock 70 kDa protein cognate 5 involved in WSSV toleration of *Litopenaeus vannamei*. *Dev. Comp. Immunol*. 72: 9-20.

Zhao, Y., Ding, X., Ye, X., Dai, Z., Yang, J. and Yang, W. (2012) Involvement of Cyclin K Posttranscriptional Regulation in the Formation of *Artemia* Diapause Cysts. *PLoS One*. 7: e32129.

Zhao, Y., Sun, H., Lu, J., Li, X., Chen, X., Tao, D., Huang, W. and Huang, B. (2005) Lifespan extension and elevated hsp gene expression in *Drosophila* caused by histone deacetylase inhibitors. *J. Exp. Biol*. 208: 697-705.

Zou, J., Guo, Y., Guettouche, T., Smith, D. and Voellmy, R. (1998) Repression of heat shock transcription factor HSF1 activation by HSP90 (HSP90 complex) that forms a stress-sensitive complex with HSF1. *Cell.* 94(4): 471-480.

Zuehlke, A. D., Moses, M. A. and Neckers, L. (2018) Heat shock protein 90: Its inhibition and function. *Philos. Trans. R. Soc. B-Biol. Sci*. 372(1738): 20160527.